

Jagiellonian University Medical College, Faculty of Pharmacy  
Department of Technology and Biotechnology of Drugs

# **PhD DISSERTATION**

**ANNA MATYS**

THE SEARCH FOR COMPOUNDS ACTIVE AGAINST  
EFFLUX PUMPS OF BACTERIA AND TUMOR CELLS

**Supervisor**

Professor Katarzyna Kieć-Kononowicz, PhD

**Auxiliary supervisor**

Professor Jadwiga Handzlik, PhD

CRACOW 2019

## **ACKNOWLEDGEMENTS**

I would like to express my gratitude to all people without whom this PhD dissertation would have never been written. I would like to thank: my supervisor Professor Katarzyna Kieć-Kononowicz, Professor Leonard Amaral, Professor Isabel Couto, Professor Joseph Molnar, Professor Alicja Budak, Dr. Ana Armada, Dr. Ana Martins, Dr. Gabriella Spengler, Dr. Gniewomir Latacz and Dr. Karolina Witek.

I am also particularly grateful to Professor Jadwiga Handzlik who made our collaboration a real pleasure and Dr. Sabina Smusz and Dr. Jagna Witek for their willingness to share their knowledge and time I spent in exceptionally friendly atmosphere.

Last, but not least, I would like to give special thanks to my family: my husband, my parents and my mother-in-law who devoted their time to look after my daughter so that I could write this PhD dissertation.

*This work was partly supported by:  
COST Action BM0701:  
Antibiotic transport and efflux: new strategies to combat bacterial resistance  
and Preludium contest of the National Science Centre in Poland  
(2013/09/N/NZ7/02085 programme).*

# Abstract

---

This PhD dissertation presents literature review of the mechanisms of bacterial antibiotic resistance and resistance of cancer cells to antineoplastic treatment. It focuses especially on one of these mechanisms i.e. extrusion of drugs from the cell by means of efflux pumps.

Since hydantoin derivatives have many properties interesting from the pharmacological point of view, my research aimed to test hydantoin derivatives synthesized in the Department of Technology and Biotechnology of Drugs of the Jagiellonian University Medical College in terms of their efficacy against bacteria and cancer cells.

As far as bacteria are concerned, my research aimed to:

- determine direct antibacterial activity of 4 groups of hydantoin derivatives (2-piperazine derivatives of 5-arylideneimidazolone, amine derivatives of 5-arylidenehydantoin, amine derivatives of 5-naphthalen-5-methylhydantoin, N-1 arylpiperazine derivatives of 5-phenylhydantoin) against *S. aureus* and *E. coli* strains using minimum inhibitory concentration method
- determine ability of the compounds to increase/restore efficacy of selected antibiotics

For the active compounds, the research aimed to:

- determine their mechanism of action by means of molecular modeling
- check their toxicity using an online tool Molecular Property Explorer and *in-vitro* proliferation assay against HEK-293 cells.

BM36 ((Z)-5-(naphthalen-2-ylmethylene)-2-(piperazin-1-yl)-3H-imidazol-4(5H)-one hydrochloride) turned out to be the most active compound. It has been experimentally proven to decrease the MIC of oxacillin and cloxacillin against *S. aureus* MRSA HEMSA 5 strain, 128-fold and 256-fold, respectively. Based on the molecular modeling studies conducted later, it may be suggested that this compound prevents the antibiotic from binding to the active site of the MecR1 protein and thus prevents expression of a modified penicillin binding protein (PBP2a) whose presence makes *S. aureus* resistant to  $\beta$ -lactam antibiotics.

As far as cancer cells are concerned, my research aimed to test ability of four groups of hydantoin derivatives (arylidene hydantoin derivatives (N-unsubstituted), arylidene hydantoin derivatives (N-substituted), arylidene hydantoin derivatives (N-unsubstituted), arylidene hydantoin derivatives (N-substituted))

(N-3 phenylpiperazine derivatives), dimethylhydantoins (N-1 phenylpiperazine derivatives) and other hydantoin derivatives) to inhibit an efflux pump, P-glycoprotein, in mouse lymphoma cells transfected with human *P-pg* gene using ethidium bromide accumulation assay.

The most active compounds were arylidene hydantoins, especially phenylpiperazine derivatives. Among dimethylhydantoins (N-1 phenylpiperazine derivatives), the most active were derivatives containing methoxy group in the ortho position of the benzene ring (PI2A) and 3 fluorine atoms in the benzene ring and benzyl substituent (PI7A).

# Abstract in Polish

---

W rozprawie doktorskiej przedstawiono przegląd literaturowy mechanizmów oporności bakterii na antybiotyki i oporności komórek nowotworowych na leczenie przeciwnowotworowe. Niniejszy przegląd skupia się szczególnie na jednym z tych mechanizmów, tj. usuwaniu leków z komórki za pomocą pomp wyrzutu leków.

Ponieważ hydantoiny posiadają wiele właściwości interesujących z farmakologicznego punktu widzenia, celem moich badań było sprawdzenie czy pochodne hydantoiny zsyntetyzowane w Katedrze Technologii i Biotechnologii Leków CMUJ mają działanie antibakteryjne i antynowotworowe.

W przypadku bakterii celem moich badań było:

- określenie bezpośredniej aktywności przeciwbakteryjnej czterech grup pochodnych hydantoiny (2-piperazynowych pochodnych 5-arylidenoimidazolonu, aminowych pochodnych 5-arylidenohydantoiny, aminowych pochodnych 5-naftaleno-5-metylohydantoiny, N-1 arylopiperazynowych pochodnych 5-fenylohydantoiny) względem szczepów *S. aureus* i *E. coli* za pomocą metody minimalnych stężeń hamujących
- określenie zdolności tychże związków do zwiększania / przywracania skuteczności wybranych antybiotyków

W przypadku związków, które okazały się aktywne, celem badań było:

- określenie ich mechanizmu działania za pomocą modelowania molekularnego
- sprawdzenie ich toksyczności za pomocą internetowego narzędzia Molecular Property Explorer i testu proliferacji *in vitro* na komórkach HEK-293.

Najbardziej aktywnym związkiem okazał się BM36 (chlorowodorek (Z)-5-(naftaleno-2-ylometyleno)-2-(piperazyno-1-ylo)-3H-imidazolo-4(5H)-onu). Udowodniono eksperymentalnie, że zmniejsza on MIC oksacyliny i kloksacyliny względem szczepu *S. aureus* MRSA HEMSA 5 odpowiednio 128-krotnie i 256-krotnie. Na podstawie przeprowadzonych później badań modelowania molekularnego można zasugerować, że związek ten zapobiega wiązaniu antybiotyków do miejsca aktywnego białka MecR1, a zatem zapobiega ekspresji zmodyfikowanego białka wiążącego penicylinę (PBP2a), którego obecność powoduje, że *S. aureus* jest oporny na antybiotyki  $\beta$ -laktamowe.

W przypadku komórek nowotworowych, moje badania miały na celu sprawdzenie za pomocą testu akumulacji bromku etydyny zdolności czterech grup pochodnych hydantoiny (arylidenohydantoin (N-niepodstawionych), arylidenohydantoin (pochodnych N-3 fenylopiperazynowych), dimetylohydantoin (pochodnych N-1 fenylopiperazynowych) i innych pochodnych hydantoiny) do hamowania pompy wyrzutu leków, glikoproteiny P, w mysich komórkach chłoniaka transfekowanych ludzkim genem dla *P-gp*.

Najbardziej aktywnymi związkami okazały się arylidenohydantoiny, w szczególności pochodne fenylopiperazyny. Wśród dimetylohydantoin (pochodne fenylopiperazyny) najbardziej aktywne były pochodne zawierające grupę metoksyłową w pozycji orto pierścienia benzenowego (PI2A) i 3 atomy fluoru w pierścieniu benzenowym oraz podstawnik benzyłowy (PI7A).

# List of abbreviations

---

EB – ethidium bromide

EPI – efflux pump inhibitor

MD – molecular dynamics

MDR – multi-drug resistance

MecI – Methicillin resistance regulatory protein MecI

MecR1 – Methicillin resistance mecR1 protein

MRSA – methicillin-resistant *Staphylococcus aureus*

PBP2a – penicillin binding protein 2a

TMD – transmembrane domain

## TABLE of CONTENTS

Abstract in Polish

Abstract

List of abbreviations

1. Introduction .....	1
1.1 BACTERIAL ANTIBIOTIC RESISTANCE .....	1
1.1.1 Mechanisms of bacterial resistance .....	1
1.1.2 Bacterial efflux pumps .....	3
1.1.2.1 Physiological role of efflux pumps .....	3
1.1.2.2. Mechanism of active transport .....	4
1.1.2.3 Families of transporters .....	4
1.1.3 The AcrAB-TolC efflux pump .....	7
1.1.3.1 Substrates of the AcrAB-TolC efflux pump .....	8
1.1.3.2 Structure of the AcrAB-TolC efflux pump .....	8
1.1.3.2.1 The AcrA protein .....	8
1.1.3.2.2 The AcrB protein.....	9
1.1.3.2.3 The TolC protein .....	10
1.1.3.3 Mechanism of action of the AcrAB-TolC efflux pump .....	10
1.1.4 Strategies to circumvent efflux mechanism .....	10
1.1.5 Efflux pumps inhibitors.....	11
1.1.5.1 Peptidomimetics .....	11
1.1.5.2 Quinolines and quinazolines .....	12
1.1.5.3 Arylpiperidines and arylpiperazines.....	12
1.1.5.4 Phenothiazines.....	13
1.1.6 Resistance of methicillin-resistant <i>S. aureus</i> to $\beta$ -lactam antibiotics.....	13
1.2 CANCER DRUG RESISTANCE .....	16
1.2.1 Mechanisms of cancer drug resistance.....	16
1.2.1.1 Heterogeneity of tumor cells before treatment.....	16
1.2.1.2 Alteration of drug targets .....	16
1.2.1.3 Drug activation or inactivation.....	17
1.2.1.4 Reduced susceptibility to apoptosis .....	18
1.2.1.5 DNA damage repair.....	19
1.2.1.6 Steric hindrance.....	19
1.2.1.7 Extracellular vesicles.....	19
1.2.1.8 MicroRNAs (miRNAs) .....	20
1.2.1.9 Efflux pumps .....	20

1.2.2 Expression of efflux pumps in tumors .....	21
1.2.3 P-glycoprotein .....	24
1.2.3.1 Expression of P-gp in healthy tissues.....	24
1.2.3.2 Substrates of P-gp.....	24
1.2.3.3 Association between P-gp expression and cancer drug resistance.....	25
1.2.3.4 Structure of P-gp .....	26
1.2.3.5 Mechanism of action of P-gp .....	27
1.2.4 P-gp inhibitors .....	28
1.2.4.1 First-generation P-gp inhibitors .....	28
1.2.4.2 Second-generation P-gp inhibitors .....	29
1.2.4.3 Third-generation P-gp inhibitors .....	31
2. Purpose and scope of the research.....	34
2.1 Hydantoin derivatives against bacteria .....	34
2.2 Hydantoin derivatives against cancer .....	39
Experimental part .....	44
3. Materials and Methods .....	44
3.1. Cancer assays: assessment of the inhibition of P-glycoprotein.....	44
3.1.1. Cell line .....	44
3.1.2. Method of assessment of the inhibition of P-glycoprotein .....	44
3.1.3. Tested compounds.....	46
3. 2. Bacterial assays: assessment of restoration of antibiotic efficacy.....	50
3.2.1. Bacterial strains .....	50
3.2.2. Method of assessment of direct antibacterial activity of the compounds .....	53
3.2.3. Method of assessment of the compounds' ability to restore antibiotic efficacy ....	54
3.2.4. Tested compounds.....	55
3.3. Determination of the mechanism of action of the most active compounds against bacteria by molecular modeling .....	57
3.4. Toxicity assays .....	58
3.4.1. <i>In-silico</i> toxicity prediction .....	58
3.4.2. Proliferation assay .....	59
4. Results .....	61
4.1. Cancer assays: assessment of the inhibition of P-glycoprotein.....	61
4. 2. Bacterial assays: assessment of restoration of antibiotic efficacy.....	66
4.2.1. Restoration of ciprofloxacin efficacy.....	66
4.2.1.1. <i>E. coli</i> HEMEC 10 .....	67
4.2.1.2. <i>E. coli</i> ATCC 25923.....	70
4.2.2. Restoration of oxacillin efficacy .....	72

4.2.2.1. <i>S. aureus</i> MRSA HEMSA 5.....	73
4.2.2.2. <i>S. aureus</i> ATCC 25923 .....	76
4.2.3. Restoration of cloxacillin efficacy .....	79
4.2.3.1. <i>S. aureus</i> MRSA HEMSA 5.....	80
4.2.3.2. <i>S. aureus</i> ATCC 25923 .....	81
4.2.4. Restoration of ampicillin + sulbactam efficacy.....	82
4.2.4.1. <i>S. aureus</i> MRSA HEMSA 5.....	83
4.2.4.2. <i>S. aureus</i> ATCC 25923 .....	84
4.2.5. Restoration of ciprofloxacin efficacy.....	85
4.2.5.1. <i>S. aureus</i> MRSA HEMSA 5.....	86
4.2.5.2. <i>S. aureus</i> ATCC 25923 .....	87
4.2.6. Restoration of neomycin efficacy .....	88
4.2.6.1. <i>S. aureus</i> MRSA HEMSA 5.....	88
4.2.6.2. <i>S. aureus</i> ATCC 25923 .....	89
4.3. Determination of the mechanism of action of the most active compounds by molecular modeling.....	91
4.3.1. Docking results.....	91
4.3.2 Molecular Dynamics simulation .....	95
4.4. Toxicity assays .....	99
4.4.1. <i>In-silico</i> toxicity prediction .....	99
4.4.2. Proliferation assay .....	102
4.4.2.1 Anti-proliferative properties of 2-piperazine derivatives of 5-arylideneimidazolone .....	102
4.4.2.2. Anti-proliferative properties of N-1 arylpiperazine derivatives of 5-phenylhydantoin .....	106
5. Structure activity relationship — summary.....	108
References .....	114
6. Annex 1. Equipment and reagents.....	130
Annex 2. Scientific papers published as part of this PhD .....	133

# 1. Introduction

---

As a consequence of intense fight against infections and cancer, bacteria and cancer cells have developed numerous defense strategies to neutralize toxic effects of drugs what rendered these drugs ineffective. The capability of cancer cells to develop resistance to antineoplastic drugs is a leading cause of cancer metastases and relapse. Despite the emergence of multi-drug resistant bacteria such as e.g. methicillin-resistant *Staphylococcus aureus* (MRSA), no major antibiotic classes have been discovered for the last 25 years [1][2]. The prevalence of MRSA in Europe is presented in Fig. 1 [1]. Thus, the problem of multidrug resistance remains a topical issue that needs to be addressed urgently.

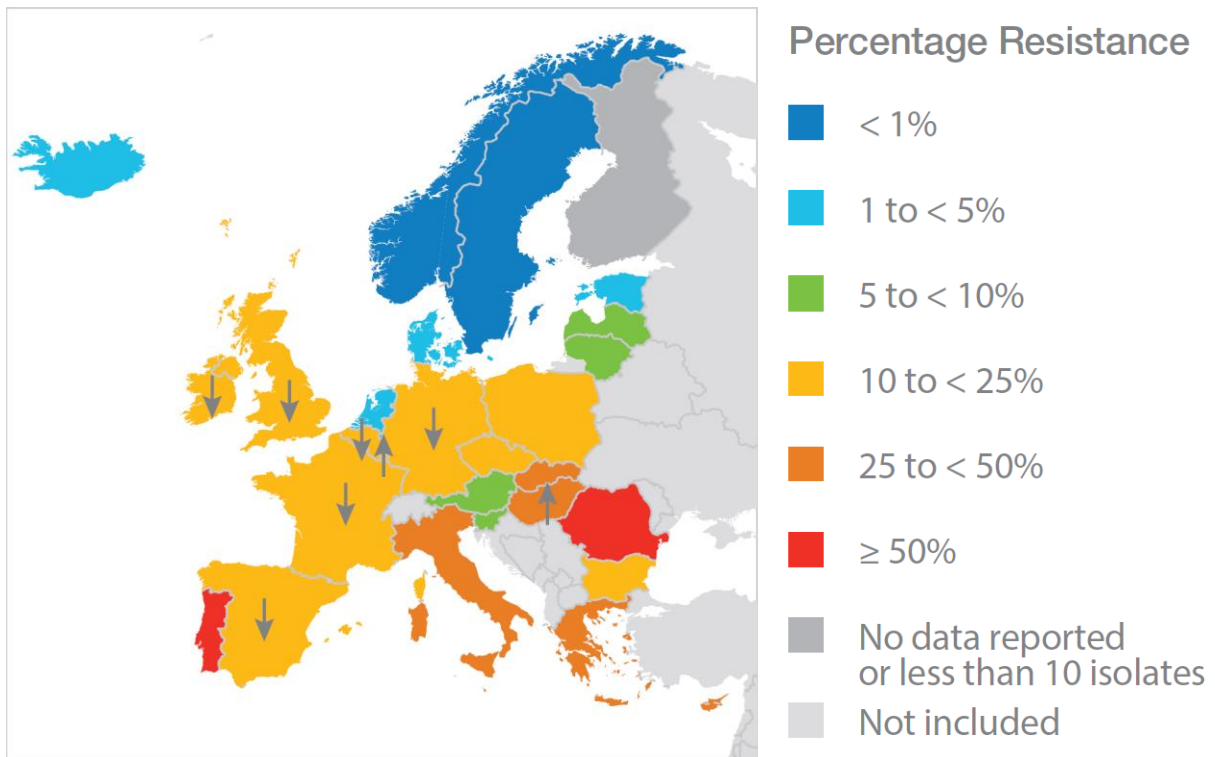


Fig. 1 Resistance to methicillin of *Staphylococcus aureus* (MRSA) in 2011  
Arrows indicate a significant increasing or decreasing trend for the period 2008-2011.

## 1.1 BACTERIAL ANTIBIOTIC RESISTANCE

### 1.1.1 Mechanisms of bacterial resistance

As a consequence of the intense fight against infections, bacteria developed numerous defense mechanisms against antimicrobial agents. These are:

### 1. modification of the drug target(s)

Bacteria modify their drug targets in order to weaken antibiotic binding. For example, fluoroquinolone resistance in *S. aureus* is mainly attributed to mutations occurring in the cellular targets GrlA/GrlB (topoisomerase IV, encoded by genes *grlA/grlB*) and GyrA/GyrB (DNA gyrase, encoded by genes *gyrA/gyrB*) which decrease drug affinity to the target, conferring high-level fluoroquinolone resistance [3]. Gram-positive bacteria in turn, change the structure of peptidoglycan which is the target of vancomycin. Vancomycin prevents cross-linking of peptidoglycan by binding to D-Ala-D-Ala dipeptide of the muramyl peptide. Gram-positive bacteria develop vancomycin resistance by replacing D-Ala-D-Ala with D-Ala-D-lactate which results in alteration of vancomycin binding [4].

### 2. enzymatic inactivation of antibiotics

Enzymatic inactivation renders antibiotics ineffective. Antibiotics may be modified by hydrolysis, group transfer and redox mechanism [5].  $\beta$ -lactamases hydrolyze the  $\beta$ -lactam ring in  $\beta$ -lactam antibiotics [6]. Also, the most common mechanism of aminoglycoside resistance is chemical modification by aminoglycoside-modifying enzymes (AMEs) [7].

### 3. reduction of intracellular drug concentration by changes in membrane permeability

Reduction of intracellular drug concentration may be achieved by the down-regulation of the expression of porins. Porins are channels used by hydrophilic antibiotics ( $\beta$ -lactams, fluoroquinolones) to enter the outer membrane of the Gram-negative bacteria [8].

### 4. reduction of intracellular drug concentration by active expel of antibiotics by efflux pumps

Recent studies suggest that efflux pumps may be used by the cell as a first-line defense mechanism, avoiding the drug to reach lethal concentrations, until a stable, more efficient alteration occurs, that allows survival in the presence of that agent [3][9]. Efflux pumps are a promising target for overcoming antibiotic resistance.

Since efflux pumps are a subject of this PhD dissertation, they will be described in more detail.

### **1.1.2 Bacterial efflux pumps**

Efflux pumps are membrane proteins found both in Gram-positive and Gram-negative bacteria. Research on membrane proteins is not an easy task due to their high hydrophobicity and low level of expression: they account for less than 0.1% of the mass fraction of all cellular proteins. In living cells, the percentage of membrane proteins amounts to 30% of all proteins, while their share in structures deposited in the Protein Data Bank is less than 5% [8].

#### ***1.1.2.1 Physiological role of efflux pumps***

Efflux pumps recognize harmful substances that entered the periplasm or cytoplasm, and extrude them before they make harm to the organism [10]. Furthermore, efflux pumps also excrete toxic products of metabolism [11].

Efflux pumps become useful in different situations. For example, the habitat of intestinal bacteria found in the digestion system of mammals and birds is rich in bile and bile salts. These substances have antimicrobial activity, thus the natural intestinal microflora must have defense mechanisms that protect against these substances [12]. Buckley *et al.* showed that *S. typhimurium* mutants where either *acrB* or *tolC* genes of the AcrAB-TolC efflux pump were knocked out colonized poorly and were not able to persist in the chicken gut [13].

Efflux pumps also secrete metabolites involved in quorum-sensing which is a mechanisms of cell-to-cell communication [14]. Quorum sensing controls many cellular functions, including biosynthesis of antimicrobial peptides, metabolic switch, motility, activation of many virulence factors and biofilm formation which makes bacteria much more difficult to eradicate [15]. Inhibition of efflux activity by efflux pump inhibitors was found to markedly reduce biofilm formation in both *E. coli* and *Klebsiella* strains [16]. The same phenomenon was observed in case of *Salmonella enterica* serovar *Typhimurium* when any efflux pump was inactivated by means of genetic engineering [17].

Efflux pumps are also suggested to play a direct role in bacterial pathogenesis by transporting virulence factors. Studies demonstrated that *Klebsiella pneumoniae* lacking AcrB and *Enterobacter cloacae* deficient in either AcrA or TolC showed reduced ability to cause infection in a mouse model, indicating that AcrAB-TolC is essential for the virulence of these strains [15][18][19]. These conclusions are in line with the results of similar studies on *Pseudomonas aeruginosa* [20].

### 1.1.2.2. Mechanism of active transport

Efflux pumps characterized in this PhD dissertation are systems based on active transport. Active transport is the movement of molecules across a membrane from a region of their lower concentration to a region of their higher concentration. Thus, it undergoes against the electrochemical gradient and requires supply of energy. The energy for active transport may be derived either from:

- hydrolysis of ATP (primary active transport)  
or
- conjugation of the transport with the transport of another molecule (usually  $\text{Na}^+$  or  $\text{H}^+$ ) that is moving along its electrochemical gradient (secondary active transport) [21]

### 1.1.2.3 Families of transporters

Bacterial efflux pumps belong to five unrelated families (Fig. 1, Table 1): MFS (Major Facilitator Superfamily), SMR (Small Multidrug Resistance), RND (Resistance Nodulation Division), ABC (ATP-binding cassette) and MATE (Multidrug And Toxic Compound Extrusion) [22].

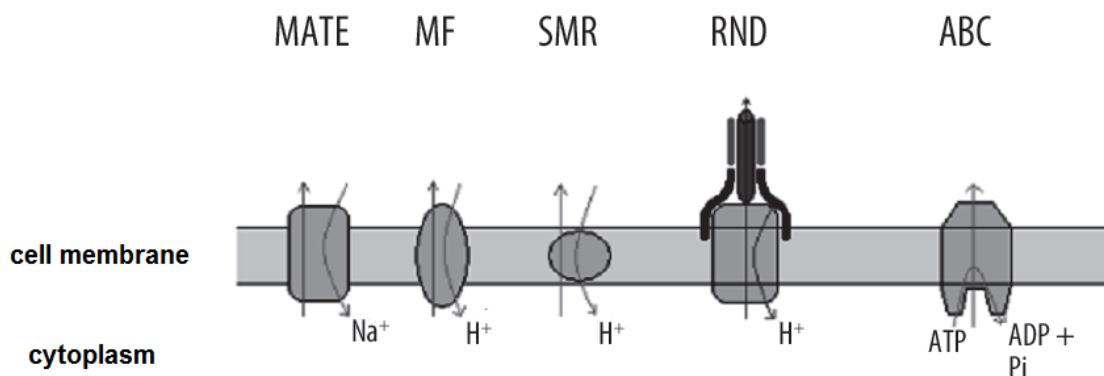


Fig. 1. Structure and principle of operation of membrane drug transporters [12]

**MFS transporters** are typically composed of approx. 400 amino acids that are arranged into 12, 14 or 24 membrane-spanning helices, with a large cytoplasmic loop between helices six and seven [23][24][25].

**SMR transporters** consist of approx. 110 amino acids and contain four transmembrane helices. Owing to the small sizes of the proteins that belong to this family, they probably function as oligomeric complexes [26].

**MATE transporters** consist of 400–700 amino acids that form 12 transmembrane helices. All proteins of the MATE family exhibit almost 40% identity of their amino acid sequence.

All genes that encode MATE proteins are derived from the same gene which was subsequently duplicated [27].

**RND transporters** were once believed to be unique to Gram-negative bacteria, but today it is known that they are also found in Gram-positive bacteria [28][29][30]. Since RND transporters cooperate with proteins in the periplasm and the outer membrane, such whole system of drug extrusion consists of a tripartite complex. One of the most thoroughly characterized RND efflux pump is AcrAB-TolC which will be described in chapter 1.1.3 [31].

MFS, SMR, MATE and RND transporters use a transmembrane proton gradient as the driving force for transport [32].

The minimal structural organization of **ABC transporters** includes the presence of four domains, *i.e.*, two nucleotide binding domains (NBDs) and two transmembrane permease domains (TMDs). The TMDs usually consist of six transmembrane  $\alpha$ -helices and form homo or heterodimers. Two NBDs bind ATP in the cytoplasmic side and cooperate with transmembrane domains [33]. The feature which distinguishes ABC transporters from the remaining families is the energy source for active extrusion of drugs, as it comes from the hydrolysis of ATP. Binding and hydrolysis of ATP triggers conformational changes in the transporter's structure, which enable export of substrates [34][35].

Substrates of MFS, SMR, MATE, RND and ABC transporters are given in Table 1.

Examples of efflux pumps in *S. aureus* and *E. coli* are given in Table 2.

Table 1. Comparison of bacterial transporter families [12]

Family of transporters	Protein structure	Substrates	Energy source
MFS	approx. 400 amino acids, 12 or 14 TMS, composed of one unit	tetracyclines, fluoroquinolones, chloramphenicol, macrolides, lincosamides, streptogramins	pH gradient
SMR	approx. 110 amino acids, 4 TMS, tetramers	chloramphenicol, streptomycin, tetracyclines	pH gradient
MATE	approx. 450 amino acids, 12 TMS	aminoglycosides, fluoroquinolones	Na <sup>+</sup> gradient
RND	approx. 1000 amino acids, 12 TMS, collaborate with outer membrane protein (OMP) and membrane fusion protein (MFP)	β-lactams, fluoroquinolones, chloramphenicol, tetracyclines, macrolides, sulfonamides, aminoglycosides, erythromycin	pH gradient
ABC	multi-unit complex	tetracyclines, fluoroquinolones, chloramphenicol, macrolides, lincosamides, aminoglycosides, rifampicin	ATP hydrolysis

Table 2. Representative efflux pumps in *S. aureus* and *E. coli*

Family of transporters	Representative efflux pumps in <i>S. aureus</i>	Representative efflux pumps in <i>E. coli</i>
MFS	NorA, QacA [3]	MdfA [36]
SMR	QacG [3]	YnfA [37]
MATE	MepA [3]	NorM [38]
RND	SecDF [28]	AcrAB-TolC [39]
ABC	AbcA [3]	CydDC [40]

### 1.1.3 The AcrAB-TolC efflux pump

AcrAB-TolC is a RND-based tripartite efflux pump which consists of the outer membrane protein TolC, the periplasmic membrane fusion protein AcrA, and the inner membrane transporter AcrB (Fig. 2) [41]. A small peptide, AcrZ, that binds to AcrB has also been identified. It is suggested to affect drug sensitivity of AcrB [39][42]. The maps of the crystallized full pump at 3.6 Å resolution can be segmented into a TolC trimer, an AcrA hexamer, and an AcrB trimer. Efficient extrusion of drugs requires all three components of the AcrAB-TolC pump [43].

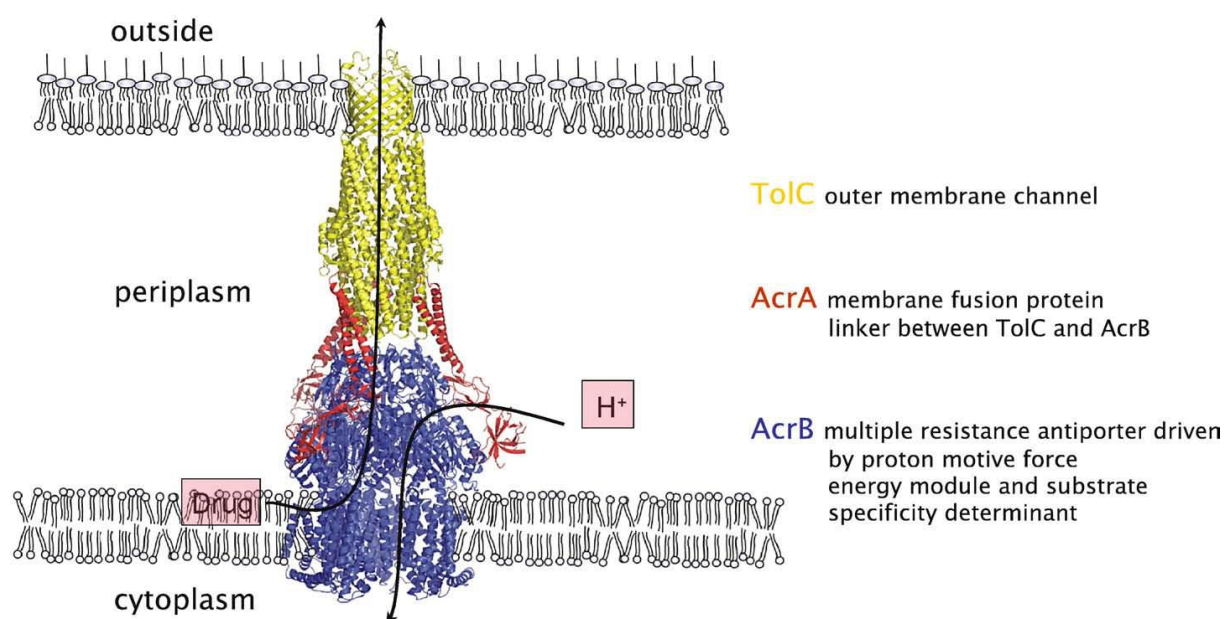


Fig 2. Schematic drawing of the AcrAB-TolC efflux pump [44]

### 1.1.3.1 Substrates of the AcrAB-TolC efflux pump

AcrAB-TolC exports a wide variety of toxic compounds including anionic, cationic, zwitterionic and neutral compounds [45]. Substrates of AcrAB-TolC include:

- antibiotics (ciprofloxacin, oxacillin, erythromycin, nalidixic acid, nitrocefin, novobiocin, minocycline, doxycycline and rifampicin)
- dyes (ethidium bromide, berberine, rhodamine 6G, acriflavine)
- detergents (triton X-100, sodium dodecyl sulfate)
- simple solvents (hexane, octane, cyclohexane, DMSO) [46][44][47].

### 1.1.3.2 Structure of the AcrAB-TolC efflux pump

#### 1.1.3.2.1 The AcrA protein

The crystallographic structure of the AcrA protein derived from *E. coli* was solved with a 2.71 Å resolution. AcrA is the linker between the two remaining proteins AcrB, and TolC. It consists of three domains: an  $\alpha$ -helical hairpin structure with a length of 105 Å involved in interaction with TolC, a lipophilic area, and a  $\beta$ -barrel structure (Fig. 3).. It is attached to the inner membrane by means of a lipid anchor which guarantees high flexibility of the protein [44][48].

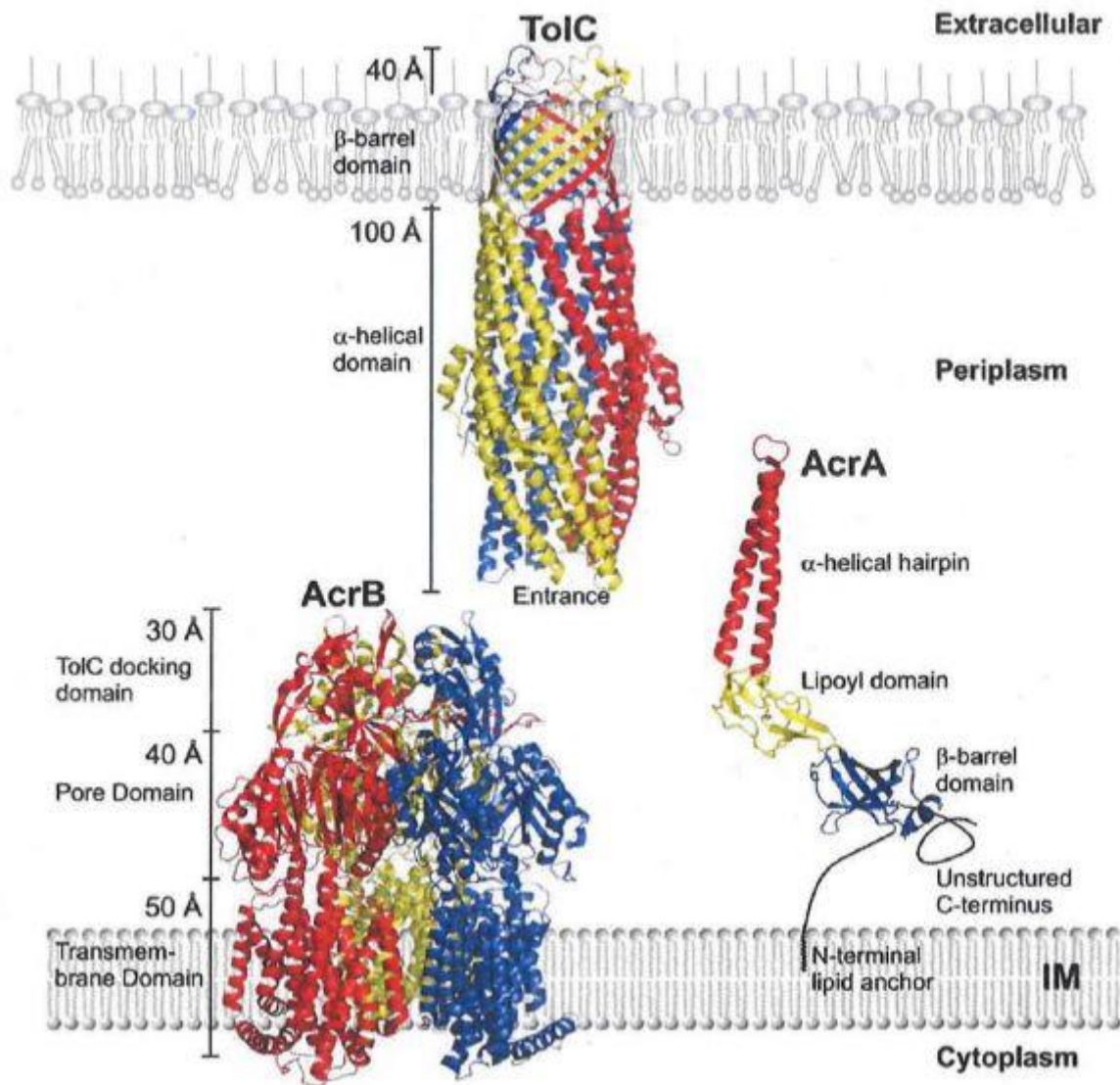


Fig 3. Structures of the proteins constituting the AcrAB-TolC efflux pump [44]

#### 1.1.3.2.2 The AcrB protein

AcrB is a member of the RND family which determines substrate specificity and energy transduction [45][49]. It forms a trimer where each AcrB monomer consists of 1049 amino acids and exhibits sequence homology and similar structural architecture between its N- and C-terminal half, indicating an early gene duplication event. AcrB consists of the following domains: transmembrane domain (50 Å long) and periplasmatic domain which comprises pore domain (50 Å long) and TolC docking domain (30 Å long) (Fig.3). The transmembrane domain is made up of twelve transmembrane  $\alpha$ -helices. The residues D407 and D408 from TM4 and K940 from TM10 are suggested to play an essential role in proton translocation. As far as periplasmic part of AcrB is concerned, the TolC docking domain exhibits a funnellike structure narrowing to a central pore located in the pore domain, the latter composed

of subdomains PN1, PN2, PC1 and PC2. The characteristic central pore is formed by three  $\alpha$ -helices, donated by the PN1 subdomains of each AcrB monomer. The pore has a small diameter and therefore does not allow drug passage in this conformation [50]. Residues located in the pore domain determine substrate specificity of the pump [51][52]. The PC1 and PC2 subdomains form a cleft at the periplasmic periphery of the pore domain which is suggested to accommodate AcrA [50]. The putative hydrophobic binding pocket in the binding (T) state conformation where doxorubicin and minocycline were demonstrated to bind is formed by phenylalanines 136, 178, 610, 615, 617 and 628 [53][54].

#### 1.1.3.2.3 The TolC protein

TolC is a homotrimer which consists of a 40 Å long  $\beta$ -barrel located in the outer membrane, a 100 Å long helical domain that spreads into the periplasm and a mixed  $\beta$  equatorial domain (Fig.3) [55]. The TolC channel has a volume of 43000 Å<sup>3</sup> and its accessible interior diameter amounts to 19.8 Å [56][57]. In a resting state, the periplasmic entrance of TolC is tightly sealed through hydrogen bonds and salt bridges formed between side chains of adjacent coiled-coil pairs in order to prevent the passage of even the smallest ions [55][56].

#### **1.1.3.3 Mechanism of action of the AcrAB-TolC efflux pump**

AcrB transports drugs by a three-step binding change mechanism. In the access state, the vestibule of the AcrB is open to the periplasm, but the binding site is still shrunken in size. In this state, potential substrates have access to the vestibule. In the binding state, the vestibule is kept open and the binding pocket is expanded to accommodate the substrate. Therefore, drugs enter into the vestibule from the surface of the cytoplasmic membrane, move through the uptake channel, and bind to the different locations in the aromatic pocket. At this stage, the exit from the binding site is blocked by the central helix inclined from the extrusion protomer. Then, in the extrusion state, the vestibule is closed, and the exit is opened because the central helix is inclined away. The bound drug is pushed out into the top funnel by shrinking of the binding pocket. These changes are expected to be coupled to proton translocation across the membrane [53].

#### **1.1.4 Strategies to circumvent efflux mechanism**

Research to restore efficacy of therapeutically inactive agents by circumventing efflux mechanism is underway. This purpose may be achieved in a number of ways. The main of them are:

- Modification of chemical design of previous antibiotics in order to reduce their affinity for binding sites and cavities located inside the pump transporter
- Increase of the influx of antibiotics using membrane permeabilizers that increase the intracellular concentration of drugs
- Down-regulation of the expression of efflux pump genes using antisense oligonucleotides or small interfering RNA
- Collapse of the energy required to support the drug transport using compounds such as carbonyl cyanide *m*-chlorophenylhydrazone (CCCP) or potassium cyanide. However, since these compounds are cytotoxic, they cannot be used in the clinic.
- Blockade of the pump using efflux pump inhibitors that enhance the action of antibiotics by preventing them from being expelled from the cell. The combination of a resistance inhibitor (other than efflux pump inhibitor) with an antibiotic has already proven its efficacy with the clavulanic acid (inhibitor of beta-lactamase) / amoxicillin association [58][59].

### 1.1.5 Efflux pumps inhibitors

Since the crystal structures of none of the efflux pumps found in *S. aureus* such as NorA or Qac have been solved yet, the research on efflux pumps inhibitors focused primarily on Gram-negative bacteria.

EPIs discovered so far belong to four groups:

#### 1.1.5.1 Peptidomimetics

The first EPI discovered in the group of peptidomimetics was Phe-Arg- $\beta$ -naphthylamide (PA $\beta$ N) (Fig. 4). PA $\beta$ N is an efflux pump inhibitor active against Gram-negative bacteria [60]. It was first described to act against RND efflux pumps of *Pseudomonas aeruginosa* [61]. PA $\beta$ N competes with antibiotics for binding sites in efflux pumps which increases intracellular concentration of antibiotics. It may bind to different sites in the binding pocket than some antibiotics (e.g. aminoglycosides,  $\beta$ -lactams) [62].

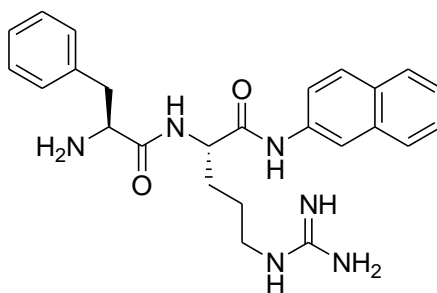


Fig. 4. Structure of PA $\beta$ N

A more stable and less toxic PA $\beta$ N derivative is MC-04,124 (Fig. 5) [63].

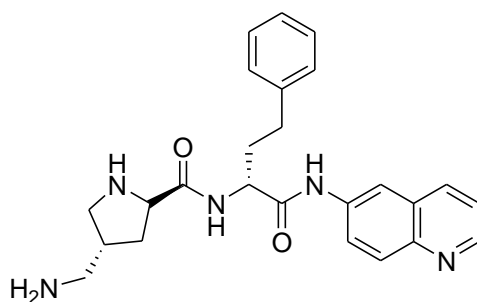
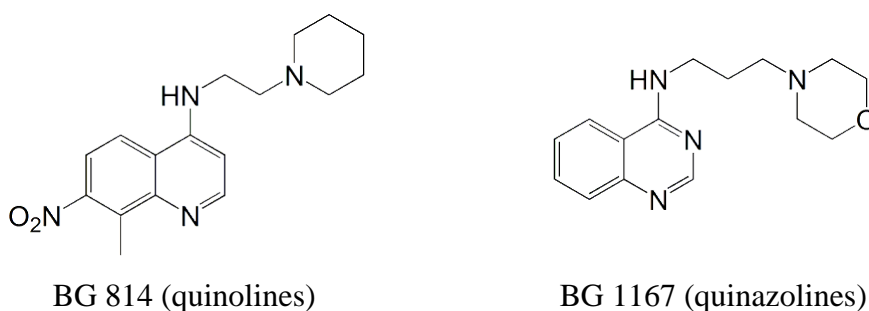


Fig. 5. Structure of MC-04,124

Approximately 10 years ago, Glaxo Smith Kline established cooperation with Mpx Pharmaceuticals to develop one of Mpx's PA $\beta$ N derivatives, but so far the compound has not entered clinical trials yet, and no information is available whether it has been discontinued or its development is still pursued [64].

#### 1.1.5.2 Quinolines and quinazolines

The structure of this group of inhibitors was designed based on similarity to quinolones which are the main substrate of efflux pumps. Thus, quinolines may act as competitive inhibitors. Several derivatives of quinoline were demonstrated to potentiate action of quinolones, phenicols and cyclines against *Enterobacter aerogenes* and *Klebsiella pneumoniae*. It is suggested that alkyl side chain bondage to the heterocyclic fragment of alkylaminoquinolines may play a fundamental role in EPI activity [65][66][67][68].



BG 814 (quinolines)

BG 1167 (quinazolines)

Fig. 6. Structure of representative quinolines and quinazolines

#### 1.1.5.3 Arylpiperidines and arylpiperazines

Among piperazine derivatives, NMP shows the best inhibitory properties (Fig. 7). It is an unsubstituted arylpiperazine active against *Enterobacteriaceae* and *Acinetobacter baumannii* which increases intracellular concentration of many antibiotics such as fluoroquinolones,

erythromycin, linezolid and chloramphenicol [69][70]. So far, the mechanism of NMP's activity has not been clarified yet. Furthermore, due to structural similarity to serotonin receptor agonists, this compound may turn out too toxic for clinical use [71].

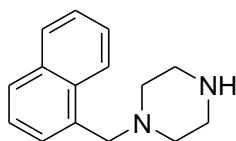
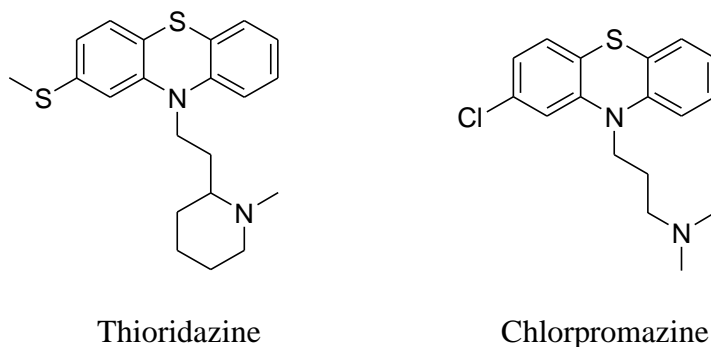


Fig. 7. Structure of NMP

#### 1.1.5.4 Phenothiazines

Phenothiazines are known to inhibit enzymes involved in generating cellular energy which is necessary for efflux [72]. Thioridazine (Fig. 8), a neuroleptic compound, some thioridazine derivatives and chlorpromazine (Fig. 8) were demonstrated to inhibit efflux pumps of *Mycobacterium tuberculosis* and thus showed a promising synergistic effect with anti-tuberculosis drugs such as isoniazid or rifampicin [73][74][75].



Thioridazine

Chlorpromazine

Fig.8. Structures of thioridazine and chlorpromazine

#### 1.1.6 Resistance of methicillin-resistant *S. aureus* to $\beta$ -lactam antibiotics

Methicillin-resistant *S. aureus* (MRSA) is a major nosocomial pathogen that is resistant not only to methicillin but also to other  $\beta$ -lactam antibiotics such as penicillin derivatives (e.g. oxacillin), cepheems such as cephalosporins and carbapenems. It is also often resistant to quinolones and aminoglycosides [76].

Staphylococci developed two mechanisms of resistance to  $\beta$ -lactam antibiotics. Firstly, they produce  $\beta$ -lactamases, enzymes that hydrolytically destroy  $\beta$ -lactams. Secondly, they are able to express a modified penicillin-binding protein (PBP) named PBP2a, which is not susceptible to inhibition by  $\beta$ -lactam antibiotics [77]. PBPs are membrane-bound enzymes

that participate in the biosynthesis of the bacterial cell wall: they catalyse the transpeptidation reaction that is necessary for cross-linkage of peptidoglycan chains [78]. Unmodified PBP is the target for  $\beta$ -lactam antibiotics: binding of a  $\beta$ -lactam antibiotic to the active centre of the PBP protein inactivates the enzyme and results in bacterial growth inhibition due to the inhibition of cell wall synthesis. In turn, the modified PBP protein (PBP2a) found in MRSA strains displays much lower affinity to  $\beta$ -lactam antibiotics thus rendering MRSA resistant to this group of antibiotics. Presence of the modified PBP2 protein in MRSA strains is caused by the acquisition of a mobile genetic element from an unknown bacterial source, SCCmec (Staphylococcal Cassette Chromosome). It contains the *mecA* gene that encodes the modified PBP protein (PBP2a). Upon the acquisition of SCCmec, MSSA (methicillin-sensitive *S. aureus*) changes to MRSA. Expression of the *mecA* gene is regulated by two proteins: methicillin resistance regulatory protein MecI (a repressor protein; marked in pink in Fig. 9) and methicillin resistance MecR1 protein (a signal transducer protein). When MecI binds to the promoter region of *mecA*, the transcription of *mecA* is repressed. The active site centre of MecR1 penicillin binding domain is the catalytic serine residue at the beginning of helix  $\alpha$ 3, Ser391. If MecR1 detects  $\beta$ -lactam antibiotics in the extracellular space via MecR1 penicillin binding domain (marked in green in Fig. 9), it becomes acylated at its active-site serine residue. Thus, when  $\beta$ -lactam antibiotics bind to MecR1, the polypeptide having protease activity (marked in yellow in Fig. 9) is released from MecR1 to degrade MecI, resulting in increased transcription of *mecA*. Consequently, a higher level of PBP2a is reached rendering MRSA resistant to  $\beta$ -lactams due to lower affinity of the PBP2a protein to this group of antibiotics [79].

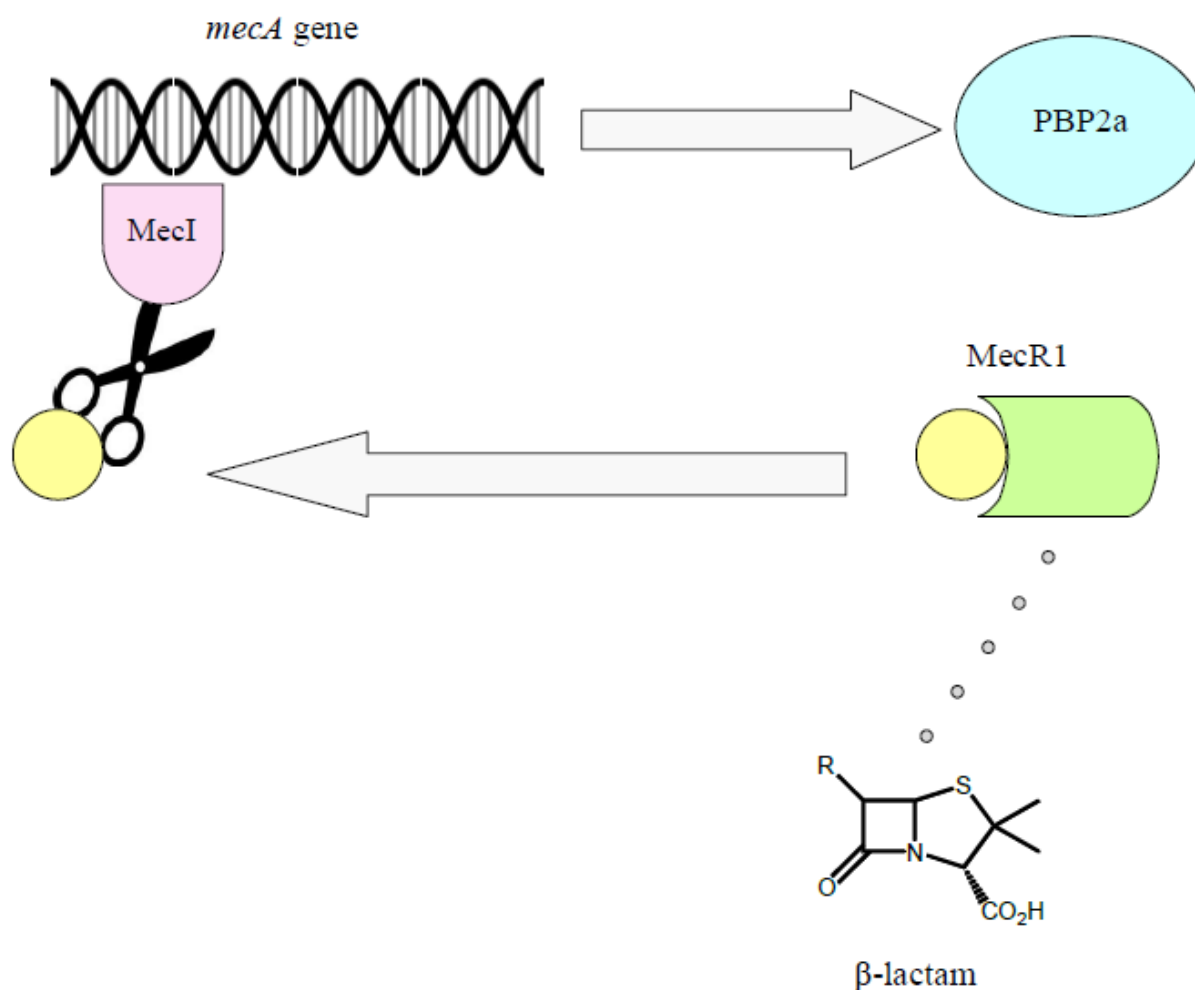


**Fig. 9.** Mechanism of PBP2a expression

*Staphylococcus aureus* has also a number of efflux pumps including those of the MF family (NorA, Mef, Tet; the efflux pump Qac is plasmid mediated) and the ABC family (Msr(A)) that are able to extrude antibiotics outside the cell, thus reducing the efficacy of the drugs [80].

Since MRSA is a worldwide problem in clinical medicine, there is a need for developing new therapeutic agents against this bacterium. One of the strategies is to search for adjuvants that enhance the action of antibiotics and may thus restore the efficacy of therapeutically inactive agents. The combination of a resistance inhibitor with an antibiotic has already proven its efficacy with the clavulanic acid (inhibitor of beta-lactamase) / amoxicillin association [59]. Lines of evidence indicated several chemical families [11-16] of inhibitors of the *S. aureus* efflux pumps, mainly the NorA efflux pump (Fig 1) [11].

## **1.2 CANCER DRUG RESISTANCE**

### **1.2.1 Mechanisms of cancer drug resistance**

Cancer cells develop resistance to anti-cancer drugs whereby several major mechanisms which often occur together, complicating attempts to combat them [81]. These mechanisms are:

#### ***1.2.1.1 Heterogeneity of tumor cells before treatment***

Cancers are populations of cells with a great degree of genetic and phenotypic heterogeneity. In a given type of tumor, various populations of cells with several clonogenic potentials exist. These populations consist of major and minor populations of tumor cells. During the treatment, the major populations are usually destroyed by cancer drugs and the minor resistant populations such as cancer stem cells (CSCs) survive and remain quiescent due to drug pressure. Stem cells are undifferentiated cells with renewing capacity for cell division that might be inactive for a long period. When activated under special conditions, they can differentiate and become a tissue or an organ with specialized functions. Thus, based on different conditions, such as the status of the immune system, age, and hormones, these minor populations may start to repopulate and establish another tumor, which is resistant to the first line treatment. A number of research has shown that treatment failure in several tumors has been attributed to the presence of CSCs [82].

#### ***1.2.1.2 Alteration of drug targets***

Drug targets may be altered due to changes in expression level of their genes or as a result of mutations. An example is post-treatment overexpression of the androgen receptor gene. It has been described in around 30% of recurrent prostate cancer patients that were treated by castration; however, untreated prostate cancer patients did not show amplification of the androgen receptor [82]. Point mutations are the most frequent mechanism of acquired resistance to tyrosine kinase inhibitors. The most common type of point mutations reduces the affinity of the target for the drug while the enzyme catalytic activity may not be affected. Another type of mutations are changes in the amino acids near the enzyme binding site which may reduce the accessibility of the target region for the inhibitor binding. There are also mutations which increase the affinity of the enzyme for ATP and thus decrease the effectiveness of type I inhibitors (ATP competitors) [82].

In addition to genetic alterations, other factors such as epigenetic factors may contribute to drug resistance. Epigenetic modifications, such as methylation of gene promoter or changes in

chromatin packaging that regulate the availability of DNA to special transcription factors, may change the expression of target genes. Modifications that induce drug resistance are associated with dysregulation of apoptotic factors and DNA repair enzymes as well as abnormal expression of drug efflux transporters [82]. An example is promoter CpG island hypermethylation which silences the gene for DNA/RNA helicase Schlafen-11 (SLFN11) enzyme that has been found to be associated with resistance to chemotherapeutic drugs such as platinum compounds [83].

If the target is part of a pathway activated by other molecules, then the cell may activate an alternative molecular mechanism [81]. An example comes from the work of Isoyama *et al.* who showed that acquired resistance to phosphatidylinositol 3-kinase (PI3K) inhibitors (such as ZSTK474) was due to the upregulation of insulin-like growth factor 1 receptor (IGF1R) pathway and that inhibition of this pathway with selective IGF1R inhibitors reversed the acquired resistance to PI3K inhibitors [84].

### **1.2.1.3 Drug activation or inactivation**

In order to exert their cytotoxic effects, many anti-cancer drugs must undergo metabolic activation. However, cancer cells may circumvent the effects of such treatments due to decreased drug activation. It is for example observed in the treatment of acute myelogenous leukemia with cytarabine (AraC), a nucleoside drug that is activated after multiple phosphorylation events that convert it to AraC-triphosphate. Down-regulation or mutation in this pathway can produce a decrease in the activation of AraC which can lead to AraC drug resistance [85].

Drug inactivation also plays a major role in the development of resistance. Major components of human detoxification system include cytochrome P450 (CYP) system, glutathione S-transferase (GST) superfamily, and uridine diphospho-glucuronosyltransferase (UGT) superfamily [85].

Cytochromes P450 (CYPs) are terminal enzymes in electron transfer chains which contain heme as a cofactor. They are located in the smooth endoplasmic reticulum of several tissues, primarily liver, but extrahepatic metabolism also occurs in the kidneys, skin, gastrointestinal tract, and lungs. The most common reaction catalyzed by cytochromes P450 is a monooxygenase reaction, e.g., insertion of one atom of oxygen into the aliphatic position of an organic substrate (RH) while the other oxygen atom is reduced to water. Many hydroxylation reactions also use CYP enzymes [86][87]. An example of an antineoplastic drug which has been shown to become inactivated via CYP450 is irinotecan, a topoisomerase

I inhibitor, used for treating colon cancer [84]. It is possible that mutations or alterations in CYP enzymes may change these proteins' metabolic capabilities, such as increasing the breakdown of drugs and their secretion by the kidneys [5]. In this case, the drug would not maintain proper levels in the patient [85].

Glutathione S-transferases (GSTs) are enzymes that catalyze the conjugation of the reduced form of glutathione (GSH) to xenobiotics thereby depriving them of their toxic properties. The mechanism of conjugation is based on the nucleophilic attack of the thiol group of glutathione on electrophilic carbon, sulfur, or nitrogen atoms of nonpolar xenobiotic substrates in order to make these compounds more water-soluble. The conjugates are then transported outside the cell and metabolized [88][89]. GSH conjugation to platinum drugs, such as oxaliplatin and cisplatin used in the treatment of various types of cancers, renders them substrates for ABC transporters. [84]. Elevated GST expression, and consequently enhanced detoxification of anticancer drugs, is found in many tumors [90][91][92][93]. Finally, binding of platinum drugs, particularly cisplatin, to metallothionein, a small cysteine-rich protein, is another means of drug inactivation [84].

Lastly, the UGT superfamily is a group of endoplasmic reticulum-bound enzymes that catalyze glucuronidation [87]. This process regulates the formation of inactive hydrophilic glucuronides with substrates such as steroids, bile acids, and xenobiotics including environmental carcinogens and cytotoxics. UGT family provides many tissues, such as the skin, breast, prostate gland, gut, and placenta, with a first line of metabolic defense from harmful substrates. Widespread down-regulation of *UGT1A1* transcription and microsomal activity occurs in certain cancerous states. The expression of *UGT1A1* is negatively regulated by DNA methylation at its promoter region [85][87].

#### **1.2.1.4 Reduced susceptibility to apoptosis**

Response of a cell to DNA damage is either to repair or to die. In such case, cell death is usually triggered through apoptosis which is defined as highly controlled programmed cell suicide led by biochemical events. Apoptosis is characterized by distinct morphological changes which include blebbing (protrusion of the plasma membrane of a cell), cell shrinkage, nuclear fragmentation, chromatin condensation, chromosomal DNA fragmentation, and global mRNA decay [94]. Resistance occurs due to the evasion of apoptotic pathways as a result of the acquisition of either inactivating mutations in genes coding for apoptotic proteins, such

as p53 or TNF, or activating mutations in genes coding for anti-apoptotic proteins, such as Bcl-2 or Mcl-1 or overexpression of these anti-apoptotic genes [84][82][95]. The gene coding for the p53 protein, *TP53*, is mutated in 50% of cancers [96]. Alternatively, inactivation of P53 regulators, such as caspase-9 and its cofactor Apaf-1, can also lead to drug resistance [85].

#### **1.2.1.5 DNA damage repair**

Defects in DNA repair pathways enable cancer cells to accumulate genomic alterations that contribute to their aggressive phenotype [97]. In response to chemotherapy drugs that either directly or indirectly damage DNA, DNA damage response (DDR) mechanisms can reverse the drug-induced damage. For example, resistance to platinum-based drugs often arises due to nucleotide excision repair and homologous recombination [85][95]. Cancer cells often have increased ability to repair DNA. O<sup>6</sup>-methylguanine DNA methyltransferase (MGMT) is a DNA repair protein. Many tumors have high MGMT levels, yielding them resistant to alkylating agents. Over-expression of *MGMT* has been shown to protect hematopoietic stem cells from alkylating agents. Studies also show that many glioma patients with epigenetically silenced *MGMT* genes have increased disease-free and overall survival rates [85].

Once a mutation is acquired cancers often become addicted to a different DNA repair pathway. A good example of this is BRCA1/2. As BRCA1/2 are key components of a DNA double strand repair pathway, cancers with mutations in these genes become dependent on another DNA repair component, PARP1, for replication fork progression. Thus, inhibition of PARP1 in these cancer cells should in theory result in their death [81]. However, despite the promising results these inhibitors showed, cancer cells once again were capable of evolving resistance to PARP inhibitors in preclinical and clinical settings [84].

#### **1.2.1.6 Steric hindrance**

Overexpression of other molecules that surround a target protein has been found to inhibit interaction of antineoplastic drugs with the target protein [98]. For instance, resistance of tumor HER2-overexpressing cells to a monoclonal antibody trastuzumab is related to high expression of MUC4, a membrane-associated glycoprotein, which binds to HER2 and thus inhibits binding of trastuzumab through steric hindrance [99].

#### **1.2.1.7 Extracellular vesicles**

Extracellular vesicles (EVs) (such as exosomes and microvesicles) are small particles (100-1000 nm) that are surrounded by phospholipid bilayer similar to the cell membrane. Their

primary function is intercellular transport. Extracellular vesicles transfer different molecules involved in resistance, such as microRNAs (miRNAs) and drug efflux pumps (P-gp, ABCG2, MRP1, ABCA3), to other cells by shedding from resistant cells and consequently induce drug resistance in non-resistant cells. They are also directly involved in the removal of cancer drugs, e.g. doxorubicin or several small molecule inhibitors, from treated cells. It is suggested that the hydrophobic characteristics of some drugs may enhance their interaction with lipid layer of vesicles [82].

#### **1.2.1.8 MicroRNAs (miRNAs)**

MicroRNAs are non-coding, single-stranded RNA molecules that consist of 19–22 nucleotides. These short RNAs behave as regulators of signaling pathways and are important key regulators in tumor progression. MiRNA deregulation in cancers has been found to be involved in deregulation of gene transcription, epigenetic modifications such as methylation of the CpG islands, induction of mutations, and alteration of DNA copy numbers. miR-7, miR-10, miR-15a, and miR-16 have been described to target MDR1, homeobox D10 (HOXD10), Bcl-2, and cyclin-D1 genes, respectively, and induce resistance to cisplatin, taxol, tamoxifen, and docetaxel in breast cancer. Microarray studies demonstrated that chronic exposure of A549 cell line with gefitinib increases the expression of 25 miRNAs and suppresses the expression of 18 others. This difference in the expression of miRNAs has been noted to be related to a 3-fold increase in IC<sub>50</sub> of gefitinib [82].

#### **1.2.1.9 Efflux pumps**

Several cell membrane transporter proteins have been linked to resistance to commonly used chemotherapeutics by promoting drug efflux [95]. Enhanced drug efflux is frequently caused by increased expression of ATP binding cassette (ABC) membrane transporters [84]. Out of 49 members of this protein family, 3 transporters are the best known: multi-drug resistance protein 1 (MDR1; also known as phenolic glycoprotein (P-glycoprotein) or ABCB1), multidrug resistance-associated protein 1 (MRP1) and breast cancer resistance protein (BCRP) [100].

ABC transporters are highly expressed in the epithelium of the liver and intestine, where they protect the body by pumping drugs and other harmful molecules into the bile duct and intestinal lumen [85].

Though some exceptions exist, ABC transporters are classified by the presence of two distinct domains—a highly conserved nucleotide binding domain and a more variable transmembrane domain (36) [85].

### **1.2.2 Expression of efflux pumps in tumors**

A study conducted in 2015 by Feldman *et al.* comprising over 50,000 patients diagnosed with different tumors revealed that the most frequently expressed in tumors efflux pump was MRP1 which was present in 81% of tumors. 66% of tumors were positive for BCRP and 23% for P-gp [101]. As shown in Fig. 10, gastrointestinal cancers exhibit the most abundant expression of all 3 efflux pumps. P-gp was the most widely expressed in gastrointestinal tumors, especially liver cancer where it was present in almost 75% of cases (Fig. 9). Patients were assessed by immunohistochemistry (IHC); IHC thresholds (positive =  $\geq 1+$  and  $\geq 10\%$ ) were used. [101].

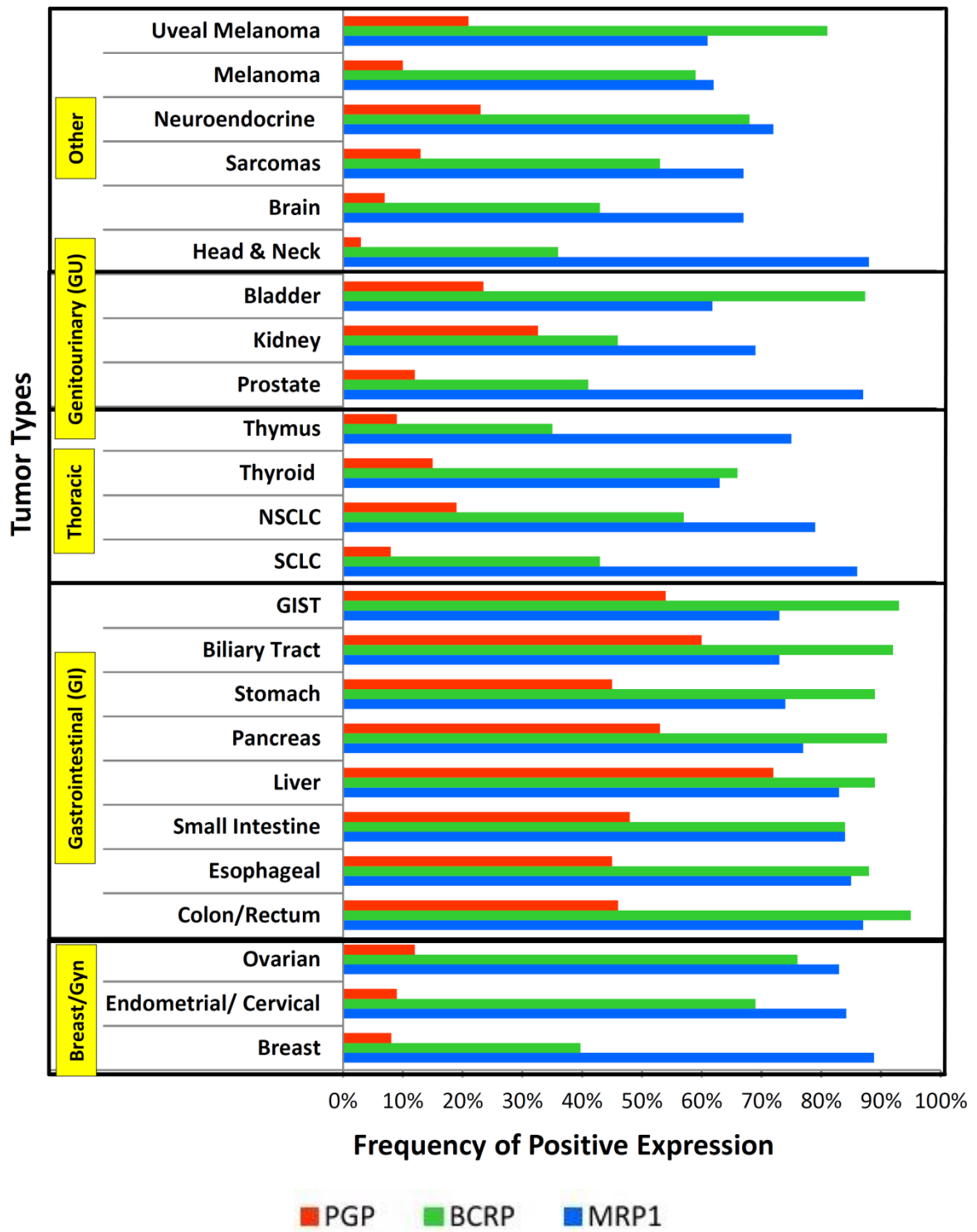


**Fig. 10.** Distribution of positive expression rates, according to tumor type [101]

The highest average combined expression of the 3 pumps was observed in liver cancers (81% of cases; Table 3) [101].

**Table 3.** Combined expression rates of P-gp, BCRP and MRP1, according to tumor type, and in order of decreasing frequency [101]

Tumor Type	Frequency
Liver	81%
Colon/Rectum	76%
Biliary Tract	75%
Pancreas	74%
GIST	73%
Esophageal	73%
Small Intestine	72%
Stomach	69%
Bladder	58%
Ovarian	57%
Neuroendocrine	54%
Uveal Melanoma	54%
Endometrial/Cervical	54%
NSCLC	52%
Kidney	49%
Thyroid	48%
Prostate	47%
SCLC	46%
Breast	46%
Sarcomas	44%
Melanoma	44%
Head & Neck	42%
Thymus	40%
Brain	39%

Abbreviations:

GIST stands for gastrointestinal stromal tumors

NSCLC stands for non-small-cell lung carcinoma

SCLC stands for small-cell lung carcinoma

### **1.2.3 P-glycoprotein**

P-glycoprotein was discovered in 1971 in a CHO cell line where it prevented the permeation of several unrelated drugs [102].

#### ***1.2.3.1 Expression of P-gp in healthy tissues***

P-gp is extensively distributed and expressed in the intestinal epithelium where it pumps xenobiotics (such as toxins or drugs) back into the intestinal lumen, in liver cells where it pumps them into bile ducts, in the cells of the proximal tubule of the kidney where it pumps them into urine-conducting ducts, and in the capillary endothelial cells composing the blood–brain barrier and blood-testis barrier, where it pumps them back into the capillaries [103].

#### ***1.2.3.2 Substrates of P-gp***

P-gp binds electrically neutral and positively charged hydrophobic drugs. It is extremely polyspecific, recognizing hundreds of structurally divergent compounds ranging in size from 100 daltons up to 4000 daltons [104]. P-gp transports various substrates across the cell membrane that occur naturally in the body as well as a number of drugs used in cancer chemotherapy, immunosuppression, hypertension, allergy, infection, and inflammation. Most P-gp substrates are hydrophobic and partition into the lipid bilayer [105]. Well-known P-gp substrates and compounds that induce P-gp expression are shown in Table 4 [106].

**Table 4.** Substrates and inducers of P-glycoprotein [106].

Substrates		Inducers
Aldosterone	Itraconazole	Amprenavir
Amprenavir	Ivermectin	Clotrimazole
Bilirubin	Loperamide	Dexamethasone
Cimetidine	Methylprednisolone	Indinavir
Colchicine	Morphine	Morphine
Cortisol	Nelfinavir	Nelfinavir
CPT-11	Paclitaxel	Phenothiazine
Cyclosporine	Quinidine	Retinoic acid
Dexamethasone	Ranitidine	Rifampin
Digoxin	Rhodamine	Ritonavir
Diltiazem	Saquinavir	Saquinavir
Domperidone	Sparfloxacin	St John's Wort
Doxorubicin	Terfenadine	( <i>Hypericum perforatum</i> )
Erythromycin	Tetracycline	
Estradiol-17B-D-glucuronide	Vecuronium	
Etoposide	Verapamil	
Fexofenadine	Vinblastine	
Indinavir		

### 1.2.3.3 Association between P-gp expression and cancer drug resistance

A growing body of evidence has suggested that the expression level of P-gp encoded by the *MDR1* gene is significantly associated with primary and acquired multi-drug resistance [107]. For example, measurements of the *MDR1* expression level in the National Cancer Institute (NCI) 60 cancer cell lines revealed dramatic inverse correlation between *MDR1* expression and paclitaxel sensitivity, indicating that the overexpression of *MDR1* contributes to the development of paclitaxel resistance in cancer [19][107].

A prognostic impact of P-gp is well documented in leukemia. It has been demonstrated that P-gp positivity in patients with acute myeloid leukemia is correlated with resistance to induction treatment [108] and poor treatment outcome [109][110], higher relapse rate [111][110][108] and shorter survival [112][110]. Shorter survival was also observed in case of P-gp positive patients with acute lymphoblastic leukemia [113][114]. Also in chronic myelogenous leukemia, patients in whom treatment has failed had significantly higher P-gp expression than responders [115].

Studies also show that P-gp positivity is associated with poor prognosis in breast cancer [116][117]. P-gp positive patients have been found to be at significantly greater risk for

disease recurrence [117]. Findings from a meta-analysis of 1232 treated and untreated patients with breast cancer showed that tumors with positive *MDR1* expression were 3 times more likely to fail to respond to chemotherapy than were tumors with negative *MDR1* expression [20][107]. P-gp can be used as a predictor for neoadjuvant therapy response in breast cancer that will also aid in avoiding the toxic side effects of neoadjuvant therapy in non-responders [118].

A correlation between P-gp expression and poor treatment outcome has also been observed in case of ovarian cancer [119][120] where it is suggested to be a useful predictive marker of chemotherapeutic response, gastric cancer [15][121], oral cavity cancer [122], nonsmall cell lung cancer [123], neuroblastoma [124], renal carcinoma, colon cancer and liver cancer [11][107]. In gallbladder carcinoma, patients with positive P-gp expression showed a significantly lower 2-year survival rate [125]. Also, the largest and most aggressive soft sarcomas exhibited the highest P-gp expression [34][107].

#### **1.2.3.4 Structure of P-gp**

The structure of the murine P-gp was solved by x-ray diffraction in 2009 (PDB code: 3G5U) [105]. It has 87% sequence identity to human P-gp which is composed of 1280 amino acids [105][126]. The structure of P-gp is presented in Figure 11. It is a 170 kDa transmembrane glycoprotein, which includes 10-15 kDa of N-terminal glycosylation. The N-terminal half of the molecule contains 6 transmembrane domains (TMDs), followed by a large cytoplasmic domain with an ATP-binding site (marked as nucleotide-binding domain (NBD)), and then a second section with 6 TMDs and an ATP-binding site that shows over 65% of amino acid similarity with the first half of the polypeptide [127]. These 2 halves are joined by a 60 amino acid linker region. This organization of the domains is characteristic of ATP binding cassette transporters [126][128]. The volume of the internal cavity within the lipid bilayer is substantial ( $\sim 6000 \text{ \AA}^3$ ) and can accommodate at least two compounds simultaneously. The major drug-binding site resides in the cell membrane in or near transmembrane helices TM6 and TM12 [105][126]. The drug-binding pocket is made up of mostly hydrophobic and aromatic residues. Although the upper half of the drug-binding pocket contains predominantly hydrophobic and aromatic residues, the lower half of the chamber has more polar and charged residues [105]. In addition to this, TM1, TM4, TM10, and TM11 also have drug-binding sites. Amino acids in TM1 are involved in the formation

of a binding pocket that plays a role in determining the suitable substrate size for P-gp, whereas Gly residues in TMs 2 and 3 are important in determining substrate specificity [126].

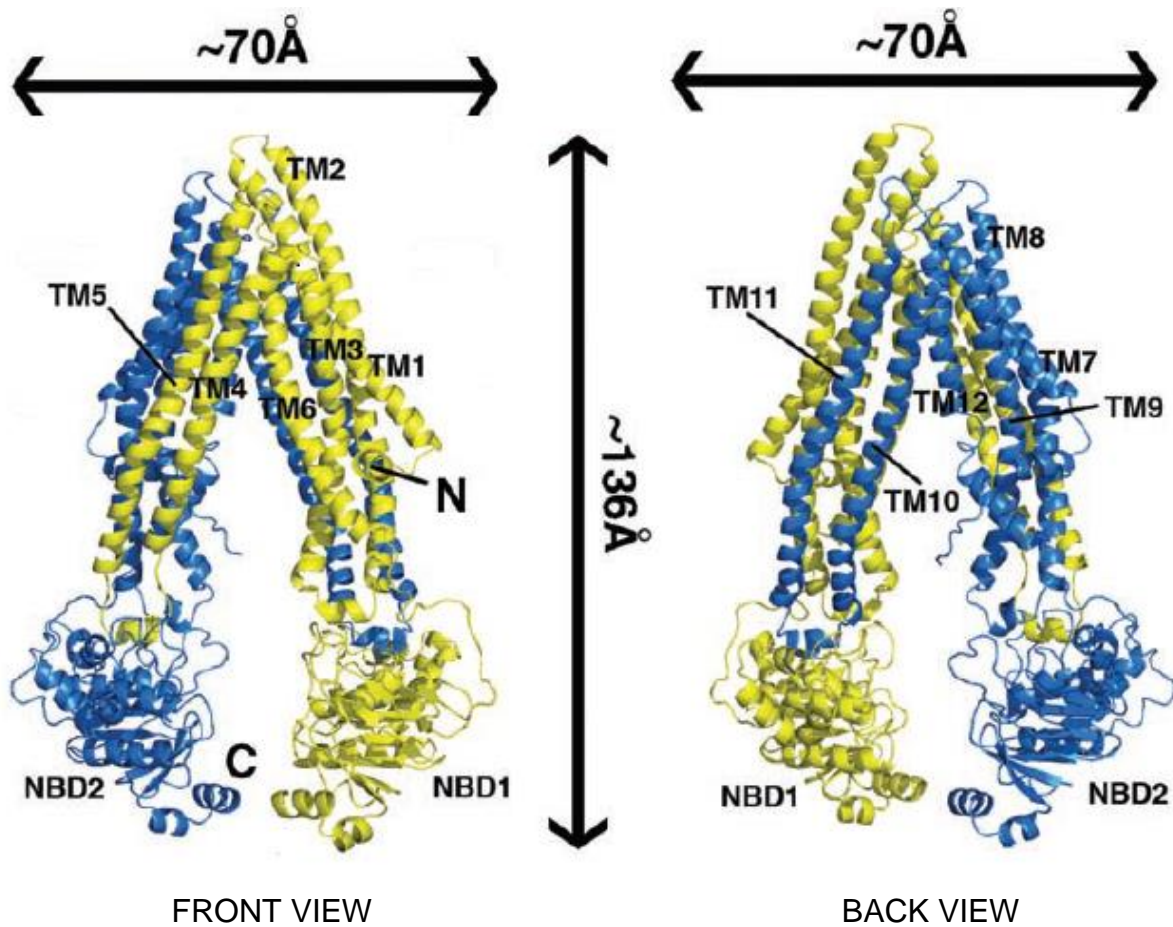


**Figure 11.** Structure of P-gp: front and back views [105].

#### 1.2.3.5 Mechanism of action of P-gp

Substrate (magenta, Fig. 12) enters the internal drug binding pocket through an open portal. The residues in the drug binding pocket (cyan spheres) interact with the substrate [105]. Binding of ATP (yellow) at the NBDs causes dimerization of NBDs and drives conformational changes in the TMDs that switch the transporter's overall conformation from inward-facing to outward-facing (inward/outward refer to the opening of the drug-binding pocket relative to the cell). This ATP-driven switch results in the transport of substrates out of the cell [129]. Exit of the substrate to the inner leaflet is sterically occluded, which provides unidirectional transport to the outside [105]. The hydrolysis of ATP and release of Pi/ADP are essential for resetting the transporter back to the inward-facing conformation [129].

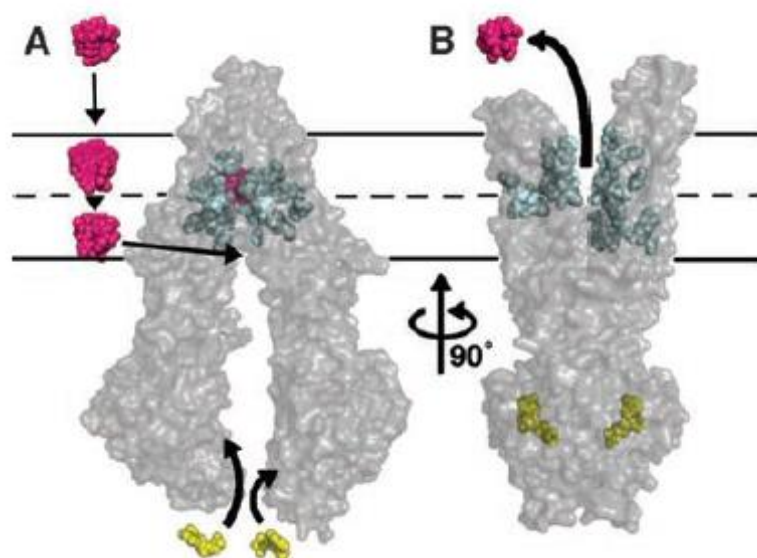


**Figure 12.** Model of substrate transport by P-gp [105].

Over the past 3 decades, P-gp inhibitors have been classified into 4 generations [107]:

### 1.2.4 P-gp inhibitors

Over the past 3 decades, P-gp inhibitors have been classified into 3 generations [107]:

#### *1.2.4.1 First-generation P-gp inhibitors*

First-generation P-gp inhibitors (Fig. 13) included calcium channel blockers such as verapamil, nifedipine and tetrandrine, an immunosuppressant cyclosporin A, an antimalarial drug quinine, and reserpine. Initially, verapamil, nifedipine, tetrandrine and reserpine were used to treat hypertension and cyclosporine A was administered in autoimmune diseases. Verapamil enabled to enhance intracellular accumulation of many anticancer drugs such as vincristine, vinblastine, doxorubicin and daunorubicin. Since first-generation compounds were drugs already in clinical use for other indications, the first consequence of their use as MDR modulators was intrinsic toxicity due to their pharmacological activity [130]. For example, serum concentration of verapamil required to reverse drug resistance results in severe cardiotoxicity and the effective dose of cyclosporin A is nephrotoxic and associated with nervous system disorders [107]. Therefore, these compounds were rejected in phase I clinical trials and their investigation was stopped [130].

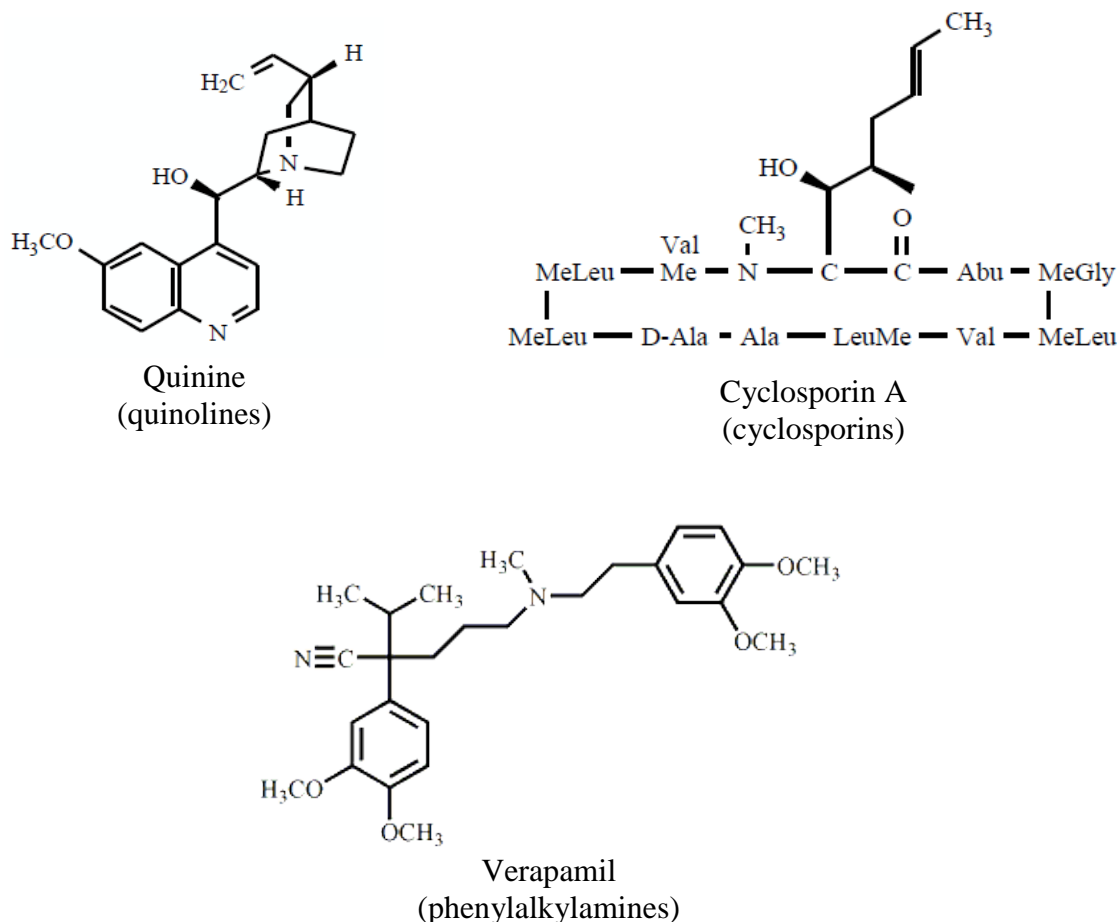


**Figure 13.** Structures of first-generation P-gp inhibitors

#### 1.2.4.2 Second-generation P-gp inhibitors

Following the failure of first-generation inhibitors, the second step was to identify their analogues that would be deprived of the pharmacological properties of the original molecule but able to potently and specifically inhibit P-gp [130].

This group of drugs (Fig. 14) included dexverapamil (one of the two enantiomers of racemic verapamil), valsopodar (PSC-833), dexnigulpidine and chinconine that are structural analogs of cyclosporin A, nifedipine and quinidine [130].

Compared with the first-generation agents, second-generation inhibitors exhibit higher selectivity and activity and lower toxicity, and they reverse drug resistance at lower concentrations. Dexverapamil was demonstrated to exert a 200-fold lower effect on calcium channels compared to verapamil, while the concentration of dexverapamil required to reverse drug resistance is 1/10 of the concentration of verapamil required to do the same *in vitro*. Valsopodar, the most studied second-generation compound, is a cyclosporine derivative which

inhibits P-gp with 10- to 20-fold greater activity than cyclosporine A and has much lower renal toxicity and no immunosuppressive activity [130][107]. It is believed to act as a non-competitive inhibitor that alters the conformation of P-gp and interferes with its ATPase activity [130].

Unfortunately these advantages did not translate into clinical success: clinical trials with dexverapamil were stopped due to elevated intrinsic toxicity and valsopodar did not improve treatment outcome in phase III clinical trials. Clinical trials with dexnigulpidine were stopped because of its poor efficacy, cinchonine development was discontinued in phase I clinical trials [131][130][132].

The drawback of second-generation inhibitors is suppression of hepatic and intestinal cytochrome P-450 (CYP) enzymes, which interferes with the clearance (e.g., *via* biliary elimination) and metabolism (e.g., *via* the CYP system) of substrate drugs and thereby results in unacceptable pharmacokinetic interactions and systemic toxicity. Furthermore, second-generation inhibitors often block other ABC transporters thus triggering side effects. In clinical trials, the most frequent unfavorable adverse events of second-generation P-gp inhibitors in combination with anticancer drugs were neutropenia, myelosuppression, agranulocytosis, thrombocytopenia and nonhematologic toxicity [107].

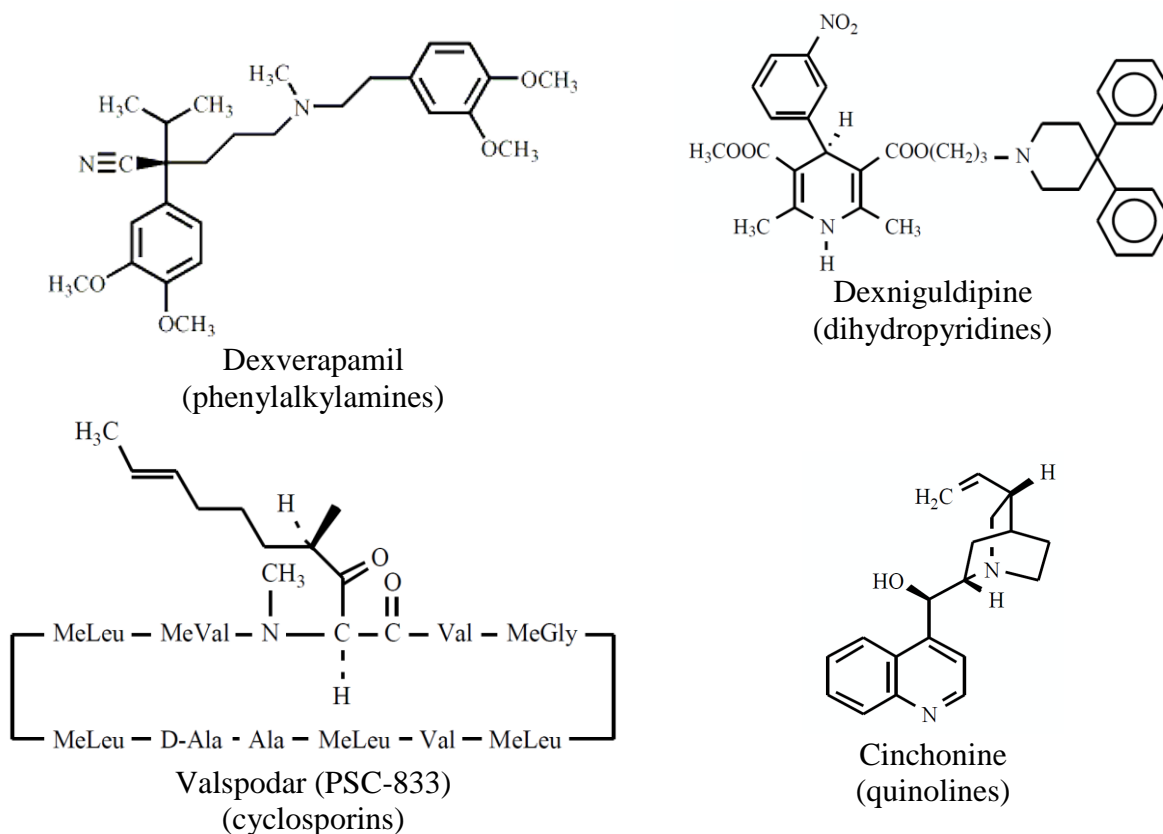


**Figure 14.** Structures of second-generation P-gp inhibitors

#### 1.2.4.3 Third-generation P-gp inhibitors

Third-generation P-gp inhibitors were developed using quantitative structure-activity relationships (QSARs) and combinatorial chemistry to circumvent the limitations of first- and second-generation inhibitors. These compounds have enhanced specificity, decreased toxicity and better affinity for P-gp, and they do not affect CYP enzymes at relevant concentrations. Therefore, they have limited pharmacokinetic interactions with chemotherapeutic agents [107]. Third-generation compounds that have been tested in clinical trials are the amido-keto-pipecolate derivative biricodar (VX-710), the acridocarboxamide derivative elacridar (GF-120918), the quinolyloxy-propanolamine derivative zosuquidar (LY-335979), the anthranilamide derivative tariquidar (XR-9576), and laniquidar (R-101933) which is structurally related to tricyclic antidepressants (Fig. 15) [130].

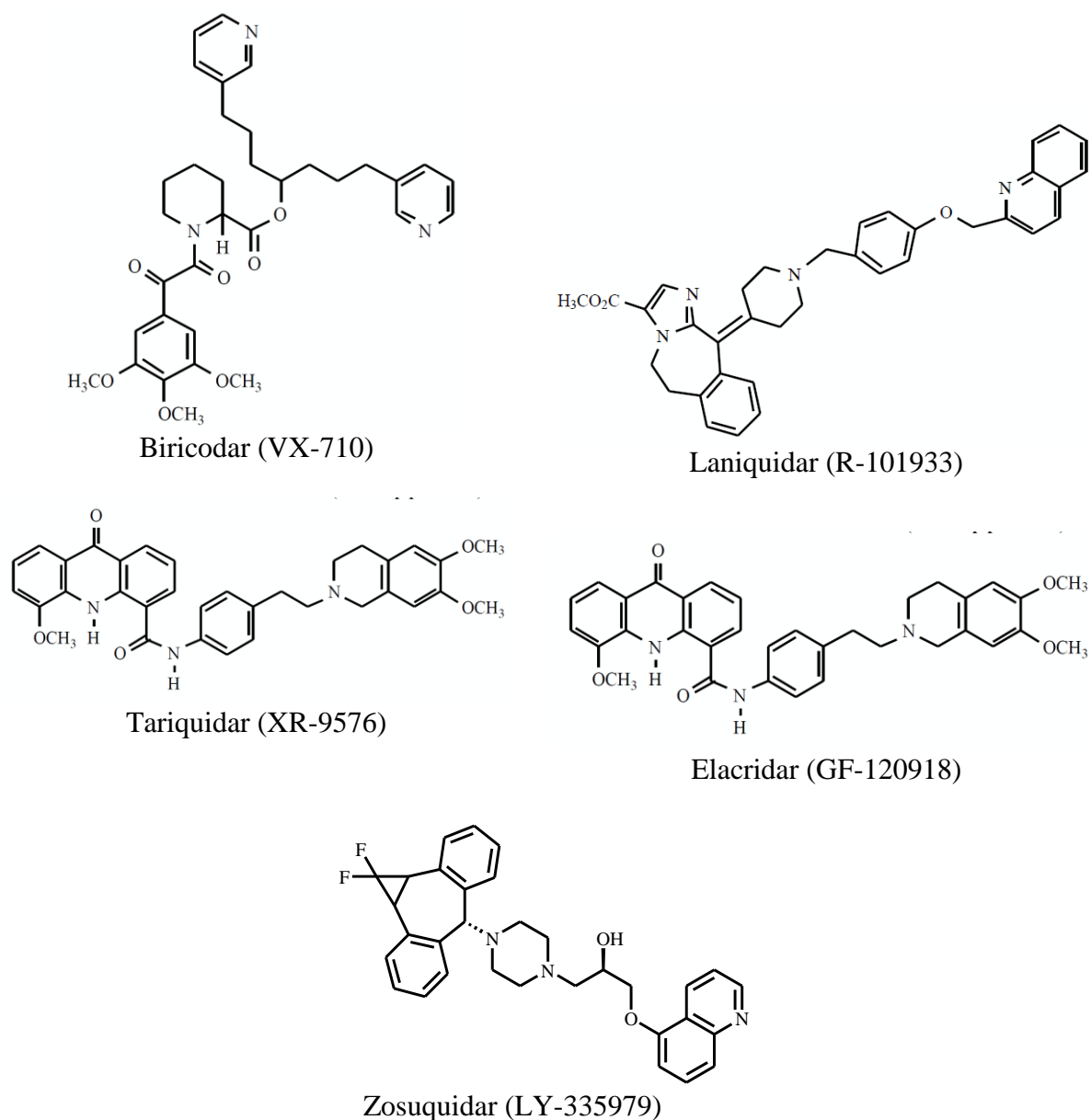


**Figure 15.** Structures of third-generation P-gp inhibitors

Biricodar (VX-710; developed by Vertex Pharmaceuticals) is a simplified analog of tacrolimus, that is the most widely studied immunosuppressive macrolactone. It is considered by some authors to be a second-generation compound probably because it is not a selective P-gp inhibitor as it acts both on P-gp and MRP1 [130]. Biricodar has not entered phase III clinical trials based on its limited efficacy in phase II clinical trials in patients with recurrent small cell lung cancer treated with doxorubicin and vincristine [133].

Elacridar (GF-120918; developed by GlaxoSmithKline) does not specifically inhibit P-gp; it has also been shown to act on BCRP but not on MRP1. No phase II clinical trials with this agent have been carried out after the encouraging results of phase I trials [130][134].

Zosuquidar (developed by Eli Lilly) is one of the most potent P-gp inhibitors described to date. It inhibits P-gp at nanomolar concentrations *in vitro* and *in vivo* and it has been proved that it is not an inhibitor of MRP or BCRP. The mechanism of action of zosuquidar is still unclear but a noncompetitive inhibition has been suggested since it is not a substrate of P-gp and it cannot be transported by this ABC transporter [130]. Zosuquidar development was discontinued after a phase III trial with cytarabine and daunorubicin for the treatment of acute myeloid leukemia (AML) and myelodysplastic syndrome because it did not meet its primary endpoint [135].

Tariquidar (XR-9576; developed by Xenova/QLT) both *in vitro* and *in vivo* reversed resistance to various anticancer drugs at nanomolar concentrations. Its mechanism of inhibitory action has not been completely clarified but a non-competitive mechanism has been suggested. However, phase III clinical trials with tariquidar in combination either with paclitaxel and carboplatin or with vinorelbine as first line therapy in non-small-cell lung cancer patients have been stopped due to increased toxicity [130].

Laniquidar (developed by NCI/EORTC Inc.) is a potent, orally active MDR inhibitor. Results of a phase II study in metastatic breast cancer patients of laniquidar in combination with taxanes are not available and it is unknown whether phase III is planned [130].

## 2. Purpose and scope of the research

---

The aim of this doctoral dissertation was to test selected hydantoin derivatives synthesized in the Department of Technology and Biotechnology of Drugs by various students under supervision of Professor Jadwiga Handzlik in terms of their activity against bacteria and cancer cells.

Hydantoins have pharmacological properties that are used to treat many human diseases. A well-known example of a drug featuring hydantoin is phenytoin (5,5-diphenylhydantoin), which has been used for decades to treat epilepsy [136][137]. A hydantoin derivative dantrolene is used as a muscle relaxant to treat muscle spasticity in conditions such as a spinal cord injury, stroke, cerebral palsy or multiple sclerosis. It is also used to prevent muscle stiffness and spasms caused by malignant hyperthermia (a rapid rise in body temperature and severe muscle contractions) that can occur during surgery with certain types of anesthesia [138]. Ropitoin is an example of antiarrhythmic hydantoin [139]. Nilutamide is a selective antagonist of the androgen receptor used in the treatment of metastatic prostate cancer [140].

The structures of imidazolidine-2,4-dione (hydantoin) and its sulphuric analog, 2-thiohydantoin, have been in the area of interest of the research group in the Department of Technology and Biotechnology of Drugs for more than twenty years. Many aromatic hydantoin derivatives obtained in the Department of Technology and Biotechnology of Drugs demonstrate various pharmacological properties such as antimicrobial [141][142][143][144], hypotensive, antiarrhythmic- or/and GPCR-agents [145][146][147][148][149][150][151].

### 2.1 Hydantoin derivatives against bacteria

Derivatives of hydantoin also seem to be an interesting target in pharmacological strategies for overcoming multidrug resistance. It has been observed that benzyhydantoins bind to the Mhp1 efflux pump of the bacteria *Microbacterium liquefaciens*, which suggests that such derivatives may inhibit efflux pumps [152]. A comparison of structural features of the 5-aromatic derivatives of hydantoin with potent efflux pump inhibitors belonging to the family of peptidomimetics (PAβN, MC-04,124) indicates some similarities which became a base to consider hydantoin-family as a good starting point for search for new modulators of bacterial multi-drug resistance (Fig. 16).

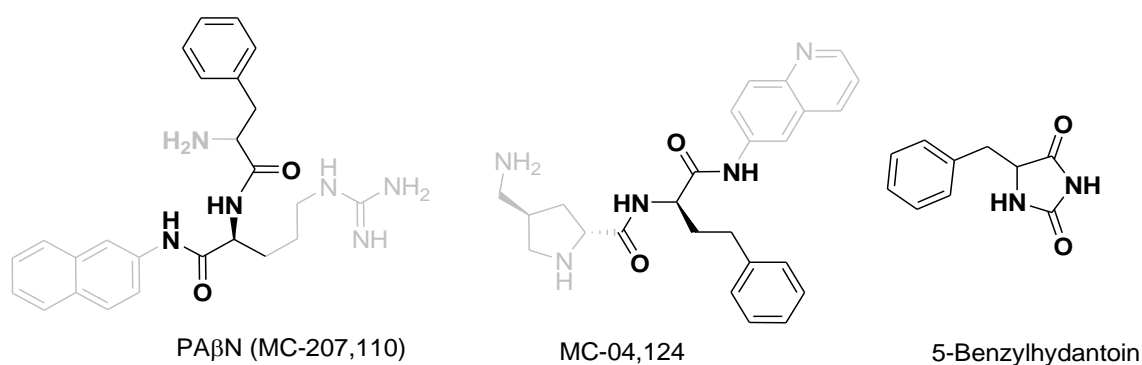


**Figure 16.** Structural similarities of aromatic hydantoin and peptidomimetics EPIs

Since arylpiperazines are known EPIs [153], this moiety was also used in compounds synthesized in our Department (group A of compounds: 2-piperazine derivatives of 5-arylideneimidazolone, group D of compounds: N-1 arylpiperazine derivatives of 5-phenylhydantoin (both groups described in detail in Tables 3.2.4A and 3.2.4D). NMP (structure presented on page 13) also contains a naphthalene ring and this moiety was used in EPIs from group C synthesized in our Department (amine derivatives of 5-naphthalen-5-methylhydantoin (described in detail in Table 3.2.4C)). This group of compounds contains also an amine fragment found in PAβN. Compounds with other amines have also been synthesized in our Department (group B of compounds: amine derivatives of 5-arylidenehydantoin (described in detail in Table 3.2.4B)). Results obtained for the first generation of phenylpiperazine derivatives of 5,5-diphenylhydantoin synthesized in our Department revealed two most promising chemosensitizers which contain methylcarboxylic acid N3-substituent (Fig. 17). This prompted further investigation of this group of compounds (group D of compounds: N-1 arylpiperazine derivatives of 5-phenylhydantoin (described in detail in Table 3.2.4D) [154].

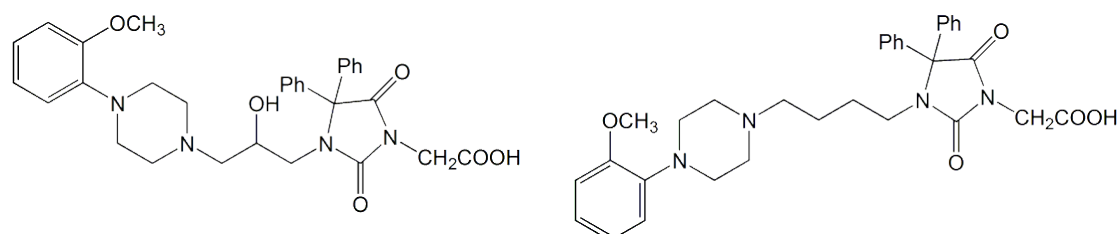


**Figure 17.** Two most promising chemosensitizers synthesized in our Department

The ability of aromatic hydantoin derivatives to inhibit multidrug resistance mechanisms in pathogenic bacteria, especially Gram-negative bacteria *Enterobacter aerogenes*, has been investigated in the Department of Technology and Biotechnology of Drugs since 2008. The studies have been conducted in collaboration with the research team of Prof. Jean-Marie Pagès: Dr Sandrine Alibert and Dr Jacqueline Chevalier (*UMR-MD-1, Transporteurs Membranaires, Chimiorésistance et Drug Design, Aix-Marseille Université/IRBA, Facultés de Médecine et de Pharmacie, Université de la Méditerranée*) under two research programs: ATENS COST action BM0701 and Polish-French collaboration program 757/N-POLONIUM/2010/0.

The promising preliminary results obtained for hydantoin derivatives against *Enterobacter aerogenes* prompted our research group to test hydantoin derivatives synthesized in our Department against other bacteria. Considering different structure and mechanism of action of efflux pumps found in Gram-positive and Gram-negative bacteria, representatives of both bacterial groups were selected: *Staphylococcus aureus* for Gram-positive bacteria and *Escherichia coli* for Gram-negative bacteria.

Thus, my research aimed to:

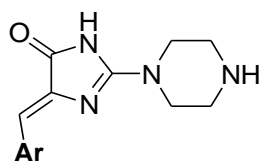
- determine direct antibacterial activity of the hydantoin derivatives presented in Tables 2.1-2.4 against *S. aureus* and *E. coli* strains
- determine ability of the compounds to increase/restore efficacy of selected antibiotics

For the active compounds, the research aimed to:

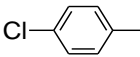
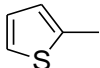
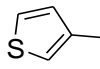
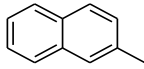
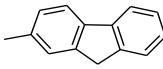
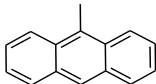
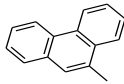
- determine their mechanism of action
- check their toxicity

Hydantoin derivatives selected for testing belonged to four groups. They were:

- **Group A: 2-piperazine derivatives of 5-arylideneimidazolone**

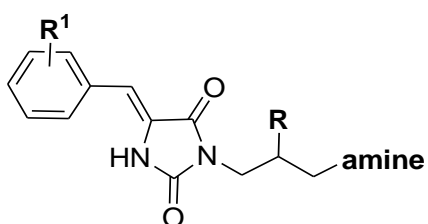


**Table 2.1.A.** 2-piperazine derivatives of 5-arylideneimidazolone selected for testing

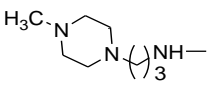
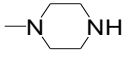
Compound	Substituents
	Ar
BM7b	
BM33	
BM34	
BM36	
BM38	
DS9	
DS11	

A list of chemical names of the compounds from this group is shown in Table 3.2.4A on page 55.

- Group B: amine derivatives of 5-arylidenehydantoin**

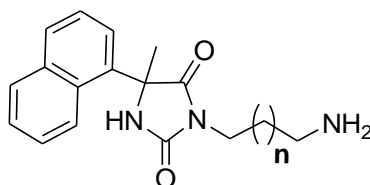


**Table 2.1.B.** Amine derivatives of 5-arylidenehydantoin selected for testing

Compound	Substituents		
	R	R <sup>1</sup>	amine
A2	H	4-OCH <sub>3</sub>	
A18	OH	2,4-diCl	

A list of chemical names of the compounds from this group is shown in Table 3.2.4B on page 56.

- **Group C: amine derivatives of 5-naphthalen-5-methylhydantoin**

**Table 2.1.C.** Amine derivatives of 5-naphthalen-5-methylhydantoin selected for testing

Compound	Substituents
	n
JM1	1
JM2	2
JM3	3

A list of chemical names of the compounds from this group is shown in Table 3.2.4C on page 56.

- **Group D: N-1 arylpiperazine derivatives of 5-phenylhydantoin**

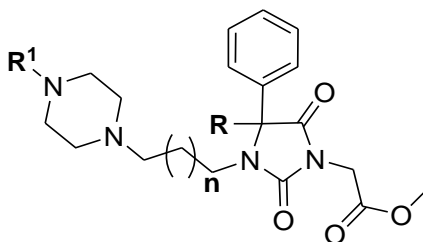


**Table 2.1.D.** N-1 arylpiperazine derivatives of 5-phenylhydantoin selected for testing

Compound	Substituents		
	R	R <sup>1</sup>	n
DK1	CH <sub>3</sub>		1
DK7	CH <sub>3</sub>		1
GG4			2
BG1			4
BG6			6

A list of chemical names of the compounds from this group is shown in Table 3.2.4D on page 57.

## 2.2 Hydantoin derivatives against cancer

The potential of hydantoin derivatives to inhibit efflux pumps found in cancer cells has not been extensively studied. Nevertheless, the existing studies are very promising: enzalutamide (structure presented in Fig. 18) was found to inhibit P-gp efflux activity by approximately 60%. This was enough to desensitize docetaxel-resistant prostate cancer DU145 cells to docetaxel treatment suggesting that combinatorial therapies with enzalutamide and docetaxel may be effective regimens to treat advanced prostate cancer [155].

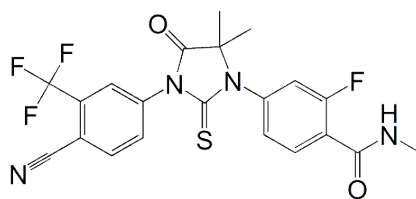
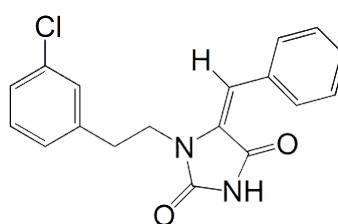
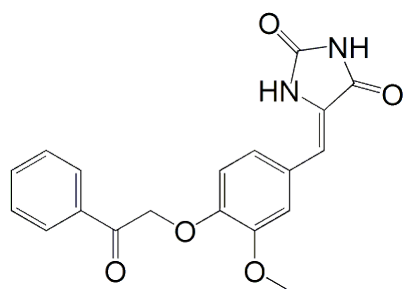


**Figure 18.** Structure of enzalutamide

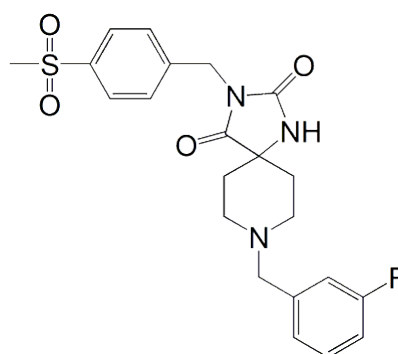
5-benzylidene hydantoins were reported as potent epidermal growth factor receptor (EGFR) inhibitors with antiproliferative activity on human lung cancer cell lines [156][157][158]. Marine-derived phenylmethylene hydantoin (PMH) derivatives were found to have antiproliferative and anti-metastatic activity against prostate cancer [159]. Azaspiro bicyclic hydantoin derivatives showed significant anti-proliferative activity against human ovarian cancer (SKOV-3 and OVSAHO cells). One derivative was also found to down regulate the secretion of VEGF in murine osteosarcoma cells (LM8 and LM8G7) which indicates its potential angioinhibitory effect [160].



5-benzylidene hydantoins



PMH derivative



Azaspiro bicyclic hydantoin derivative

**Figure 19.** Hydantoin derivatives active against cancer cells

As far as cancer cells are concerned, my research aimed to test the ability of the hydantoin derivatives synthesized in our Department to inhibit an efflux pump, P-glycoprotein, in mouse lymphoma cells.

Hydantoin derivatives selected for testing belonged to four groups. Group 1 and Group 2 of the compounds were selected based on the presence of a benzylidene moiety found in hydantoin derivatives active against cancer cells (Fig. 19). Group 3 of the compounds was selected based on a dimethyl moiety found in enzalutamide (Fig. 18).

The four groups of the compounds selected for testing were:

- **Group 1: Arylidene hydantoins (N-unsubstituted)**

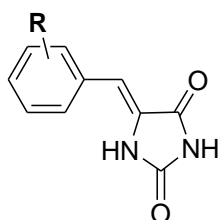


**Table 2.2.1** Arylidene hydantoins (N-unsubstituted) selected for testing

Compound	Substituents
	R
<b>HY83</b>	3-O-CH <sub>2</sub> -Ph-4-Cl
<b>HY84</b>	3-O-CH <sub>2</sub> -Ph
<b>HY110</b>	4-O-CH <sub>2</sub> -Ph-4-Cl
<b>HY111</b>	4-O-CH <sub>2</sub> -Ph-2,4-diCl
<b>HY112</b>	4-O-CH <sub>2</sub> -Ph
<b>HY115</b>	3,4-diO-CH <sub>2</sub> -Ph

A list of chemical names of the compounds from this group is shown in Table 3.1.3A on page 46.

- **Group 2: Arylidene hydantoins (N-3 phenylpiperazine derivatives)**

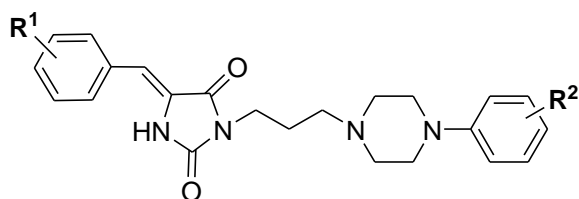


**Table 2.2.2** Arylidene hydantoins (N-3 phenylpiperazine derivatives) selected for testing

Compound	Substituents	
	R <sup>1</sup>	R <sup>2</sup>
R1	3-Cl	2-F
R2	3-Cl	2,3-diCl
R3	4-Cl	3,4-diCl
R4	4-Cl	2-F
R5	4-Cl	2,3-diCl
R6	4-Cl	3-Cl

A list of chemical names of the compounds from this group is shown in Table 3.1.3B on page 47.

- **Group 3: Dimethylhydantoins (N-1 phenylpiperazine derivatives)**

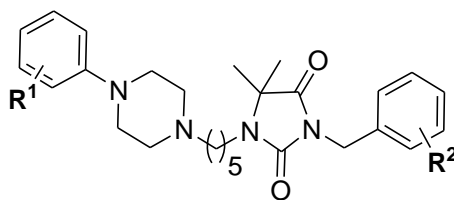


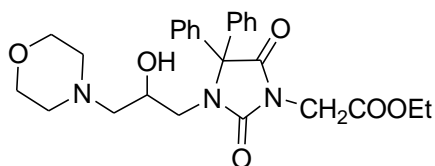
**Table 2.2.3** Dimethylhydantoin (N-1 phenylpiperazine derivatives) selected for testing

Compound	Substituents	
	R <sup>1</sup>	R <sup>2</sup>
PI1A	H	H
PI2A	2-OCH <sub>3</sub>	H
PI3A	3-OCH <sub>3</sub>	H
PI4A	2-F	H
PI5A	4-F	H
PI6A	2,4-diF	H
PI7A	2,4-diF	4-F
PI8A	4-F	4-F
PI9A	2,3-diCl	2,4-diCl
PI10A	3,4-diCl	2,4-diCl
PI11A	4-Cl	2,4-diCl

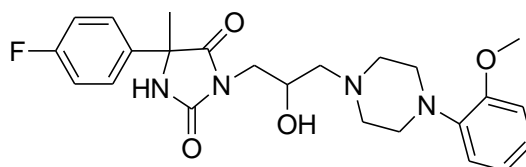
A list of chemical names of the compounds from this group is shown in Table 3.1.3C on page 48.

- **Group 4: Other hydantoin derivatives**

**KF4**



**MF8**



A list of chemical names of the compounds from this group is shown in Table 3.1.3D on page 49.

# Experimental part

## 3. Materials and Methods

---

### 3.1. Cancer assays: assessment of the inhibition of P-glycoprotein

The list of equipment and all reagents used in the assessment of the inhibition of P-glycoprotein is shown in Annex 1, section 6.1.

#### 3.1.1. Cell line

L5178 mouse T-cell lymphoma cells transfected with pHa ABCB1/A retrovirus (ECACC cat. no. 87111908 obtained from FDA, Silver Spring, MD, USA) was used in the study. The cell line was constructed by the group of Professor Joseph Molnar in the Institute of Medical Microbiology and Immunology at the University of Szeged in Hungary.

The *ABCB1*-expressing cell line (MDR) was selected by culturing the infected cells with 60 ng/ml of colchicine to maintain the MDR phenotype. The L5178Y human *ABCB1*-transfected subline was cultured in McCoy's 5A medium supplemented with 10% heat-inactivated horse serum, 200 mM L-glutamine and a penicillin-streptomycin mixture in concentrations of 100 IU/ml and 100 µg/ml, respectively. The cell lines were incubated at 37°C, in a 5% CO<sub>2</sub>, 95% air atmosphere.

#### 3.1.2. Method of assessment of the inhibition of P-glycoprotein

Inhibition of P-glycoprotein was evaluated using ethidium bromide accumulation assay. The quaternarium ammonium compound ethidium bromide (EB), structurally related to the antibiotic group of quinolones, has been a popular fluorescence probe of real-time monitoring of resistance mechanisms in bulk cells and is a common substrate of efflux pumps in bacteria [161][162][163][164]. Because EB is also recognized and extruded by ATP-binding cassette (ABC) transporters and these have similarity to P-gp, the method has been extended for the evaluation of agents that can inhibit the extrusion of EB on a real-time basis by mouse

lymphoma cells containing the human ABCB1 (mdr1) gene [165]. EB emits weaker fluorescence in an aqueous environment and becomes strongly fluorescent in a non-polar or hydrophobic environment. Thus, the semi-automated EB method enables real-time detection of EB accumulation inside cells and can be used to evaluate compounds for their ability to inhibit efflux [161].

Prior to the experiment, maximum concentration of EB which can be extruded by the cells was determined. This was done by adding different concentrations of EB to the cell suspension and analysing accumulation curves. The maximum concentration of EB that the cells are able to extrude corresponds to the first curve below the first curve for which accumulation can be observed. On the graph showing the relationship between relative fluorescence index (RFI; y axis) and time (x axis), accumulation is seen as a clearly upward curve, as opposed to relatively stable curves that represent efflux (Fig. 4.1.1; page 61).

The cells were adjusted to a density of  $2 \times 10^6$  cells/ml, centrifuged at  $2000 \times g$  for 2 minutes and re-suspended in phosphate-buffered saline (PBS) containing 0.6% glucose (a source of metabolic energy) at pH 7.4. The cell suspension was distributed in 90  $\mu$ l aliquots into 0.2 ml tubes. 2  $\mu$ l of the stock solutions of the tested compounds (final concentration of the tested compounds: 20  $\mu$ g/ml) and 3  $\mu$ l of water (to make up the final volume 100  $\mu$ l) were added into each tube. The samples were incubated for 10 minutes at room temperature (approx. 25°C). After incubation, 5  $\mu$ l (1 mg/l final concentration) of EB (20 mg/l stock solution) were added to the samples, the tubes were placed into a Rotor-Gene™ 3000 thermocycler (Corbett Research, Sydney, Australia) and the fluorescence was monitored on a real-time basis. All experiments were conducted in four repetitions. Prior to the assay, the instrument was programmed for temperature (37°C), the appropriate excitation and emission wavelengths of EB (530 nm bandpass and 585 nm highpass, respectively), and the assay time (60 minutes). The results were evaluated by Rotor-Gene Analysis Software 6.1 (Build 93) provided by Corbett Research. A progressive increase of fluorescence of EB induced by the compound under study provides an estimate of the inhibition of EB efflux promoted by that agent. From the real-time data, the activity of the compound, i.e. the relative final fluorescence index (RFI) of the last time point (minute 60) of the EB accumulation assay, was calculated according to the formula:

$$RFI = \frac{RF_{treated} - RF_{untreated}}{RF_{untreated}}$$

where  $RF_{treated}$  is the relative fluorescence (RF) at the last time point of EB retention curve in the presence of a potential inhibitor and  $RF_{untreated}$  is the relative fluorescence at the last time point of the EB retention curve of the control, i.e. sample without any tested compound. The greater the difference between the  $RF_{treated}$  and  $RF_{untreated}$  control, the greater the degree of EB accumulated and, therefore, the greater the degree of inhibition of the efflux pump system of the cells by the compound. Dividing the RFI by the number of micromoles of the hydantoin compound used in the assay provides the specific activity of inhibition of the efflux pump of MDR mouse lymphoma cells transfected with the human *ABCB1* gene (Tables 4.1A (page 63) – 4.1D (page 65); Fig. 4.1.2 (page 62)).

### 3.1.3. Tested compounds

The purity of all the tested compounds was >95%, estimated by the use of the LC-MS analytical method. The tested compounds belonged to four groups. They were:

- Arylidene hydantoins (N-unsubstitued)

**Table 3.1.3A.** Arylidene hydantoins (N-unsubstitued) selected for testing

Compound	Chemical name
HY83	(Z)-5-(3-(4-chlorobenzyloxy)benzylidene)imidazolidine-2,4-dione
HY84	(Z)-5-(3-(benzyloxy)benzylidene)imidazolidine-2,4-dione
HY110	(Z)-5-(4-(4-chlorobenzyloxy)benzylidene)imidazolidine-2,4-dione
HY111	(Z)-5-(4-(2,4-dichlorobenzyloxy)benzylidene)imidazolidine-2,4-dione
HY112	(Z)-5-(4-(benzyloxy)benzylidene)imidazolidine-2,4-dione
HY115	(Z)-5-(3,4-dibenzyloxybenzylidene)imidazolidine-2,4-dione

The structures of the compounds are presented in Table 2.2.1 on page 41.

The compounds were synthesized by Maria Kaleta, a technician working in the Department of Technology and Biotechnology of Drugs, under supervision of Professor Katarzyna Kieć-Kononowicz.

- **Arylidene hydantoins (N-3 phenylpiperazine derivatives)**

**Table 3.1.3B.** Arylidene hydantoins (N-3 phenylpiperazine derivatives) selected for testing

Compound	Chemical name
R1	(Z)-5-(3-chlorobenzylidene)-3-(3-(4-(2-fluorophenyl)piperazin-1-yl)propyl)imidazolidine-2,4-dione
R2	(Z)-5-(3-chlorobenzylidene)-3-(3-(4-(2,3-dichlorophenyl)piperazin-1-yl)propyl)imidazolidine-2,4-dione
R3	(Z)-5-(4-chlorobenzylidene)-3-(3-(4-(3,4-dichlorophenyl)piperazin-1-yl)propyl)imidazolidine-2,4-dione
R4	(Z)-5-(4-chlorobenzylidene)-3-(3-(4-(2-fluorophenyl)piperazin-1-yl)propyl)imidazolidine-2,4-dione
R5	(Z)-5-(4-chlorobenzylidene)-3-(3-(4-(2,3-dichlorophenyl)piperazin-1-yl)propyl)imidazolidine-2,4-dione
R6	(Z)-5-(4-chlorobenzylidene)-3-(3-(4-(3-chlorophenyl)piperazin-1-yl)propyl)imidazolidine-2,4-dione

The structures of the compounds are presented in Table 2.2.2 on page 42.

The compounds were synthesized by a master student Renata Wójcik and Maria Kaleta, a technician working in the Department of Technology and Biotechnology of Drugs, under supervision of Professor Katarzyna Kieć-Kononowicz.

- **Dimethylhydantoins (N-1 phenylpiperazine derivatives)**

**Table 3.1.3C.** Dimethylhydantoins (N-1 phenylpiperazine derivatives) selected for testing

Compound	Chemical name
PI1A	3-benzyl-5,5-dimethyl-1-(5-(4-phenylpiperazin-1-yl)pentyl)imidazolidine-2,4-dione hydrochloride
PI2A	3-benzyl-1-(5-(4-(2-methoxyphenyl)piperazin-1-yl)pentyl)-5,5-dimethylimidazolidine-2,4-dione hydrochloride
PI3A	3-benzyl-1-(5-(4-(3-methoxyphenyl)piperazin-1-yl)pentyl)-5,5-dimethylimidazolidine-2,4-dione hydrochloride
PI4A	3-benzyl-1-(5-(4-(2-fluorophenyl)piperazin-1-yl)pentyl)-5,5-dimethylimidazolidine-2,4-dione hydrochloride
PI5A	3-benzyl-1-(5-(4-(4-fluorophenyl)piperazin-1-yl)pentyl)-5,5-dimethylimidazolidine-2,4-dione hydrochloride
PI6A	3-benzyl-1-(5-(4-(2,4-difluorophenyl)piperazin-1-yl)pentyl)-5,5-dimethylimidazolidine-2,4-dione hydrochloride
PI7A	3-(4-fluorobenzyl)-1-(5-(4-(2,4-difluorophenyl)piperazin-1-yl)pentyl)-5,5-dimethylimidazolidine-2,4-dione hydrochloride
PI8A	3-(4-fluorobenzyl)-1-(5-(4-(4-fluorophenyl)piperazin-1-yl)pentyl)-5,5-dimethylimidazolidine-2,4-dione hydrochloride
PI9A	3-(2,4-dichlorobenzyl)-1-(5-(4-(2,3-dichlorophenyl)piperazin-1-yl)pentyl)-5,5-dimethylimidazolidine-2,4-dione hydrochloride
PI10A	3-(2,4-dichlorobenzyl)-1-(5-(4-(3,4-dichlorophenyl)piperazin-1-yl)pentyl)-5,5-dimethylimidazolidine-2,4-dione hydrochloride
PI11A	3-(2,4-dichlorobenzyl)-1-(5-(4-(4-chlorophenyl)piperazin-1-yl)pentyl)-5,5-dimethylimidazolidine-2,4-dione hydrochloride

The structures of the compounds are presented in Table 2.2.3 on page 43.

The compounds were tested as hydrochlorides.

The compounds were synthesized by a master student Paula Idzik under supervision of Professor Jadwiga Handzlik.

- **Other hydantoin derivatives**

**Table 3.1.3D.** Other hydantoin derivatives selected for testing

Compound	Chemical name
KF4	ethyl 2-(3-(2-hydroxy-3-(4-(2-hydroxyethyl)piperazin-1-yl)propyl)-2,5-dioxo-4,4-diphenylimidazolidin-1-yl)acetate
MF8	5-(4-fluorophenyl)-3-(2-hydroxy-3-(4-(2-methoxyphenyl)piperazin-1-yl)propyl)-5-methylimidazolidine-2,4-dione hydrochloride

The structures of the compounds are presented on page 43.

The compound KF4 was synthesized by Maria Kaleta, a technician working in the Department of Technology and Biotechnology of Drugs, under supervision of Professor Katarzyna Kieć-Kononowicz [147].

The compound MF8 was synthesized by a master student Małgorzata Frączek under supervision of Professor Jadwiga Handzlik.

Stock solutions of the compounds (10 mg/ml, 1 mg/ml) were prepared in sterile DMSO suitable for cell culture (Sigma-Aldrich). The final concentration of DMSO in the assay did not exceed 2% and had no effect on the viability of cells. The compounds were tested at the concentration 20 µg/ml.

Prior to the assay, this concentration of all the compounds was tested by the trypan blue method to confirm that it did not affect viability of the cells. The trypan blue exclusion assay is based on the principle that viable cells have intact cell membranes that exclude certain dyes, such as trypan blue, eosin or propidium, whereas dead cells are permeable for these dyes. The cell suspension was mixed with the trypan blue solution (Sigma-Aldrich) in 1:1 proportion and the compounds and then visually examined under a microscope to determine whether the cells took up or excluded the dye: the cytoplasm of viable cells is clear whereas the cytoplasm of nonviable cells is blue [166]. Since over 95% of the cells were uncoloured, it proved that this concentration of the compounds did not harm the cells.

The P-gp modulator verapamil was used at a concentration of 20 µg/ml as the positive control. The results were read after 1-hour incubation.

## 3. 2. Bacterial assays: assessment of restoration of antibiotic efficacy

The list of equipment and all reagents used in the assessment of restoration of antibiotic efficacy is shown in Annex 1, section 6.3.

### 3.2.1. Bacterial strains

The following bacterial *Staphylococcus aureus* strains were used in the study:

- multi-drug resistant clinical strain *S. aureus* HEMSA 5 (resistant to oxacillin)
- a reference strain *S. aureus* ATCC 25923 (susceptible to oxacillin)

The strains were donated by Professor Leonard Amaral (Group of Mycobacteriology, Unit of Medical Microbiology, Institute of Hygiene and Tropical Medicine, Universidade Nova de Lisboa, Lisbon, Portugal)

#### Characterization of *S. aureus* HEMSA 5

The strain is an MRSA strain that contains  $\beta$ -lactamases, *mecA* cassette, and efflux pumps.

The presence of the penicillin binding protein 2a (PBP2a) protein that makes *S. aureus* methicillin resistant was confirmed using a slide latex agglutination assay SLIDEX MRSA Detection (bioMérieux). The assay is based on the principle that latex particles sensitized with a monoclonal antibody directed against PBP2a will specifically react with MRSA to cause agglutination visible to the naked eye. Methicillin-susceptible *S. aureus* (MSSA) do not agglutinate the latex particles. The reference strain *S. aureus* ATCC 25923 was used as a negative control. The test was performed according to the manufacturer's instructions [167]. The procedure consists of two steps: PBP2a extraction and latex agglutination. In PBP2a extraction procedure, for each of the tested strains, three 1  $\mu$ l loops were filled with isolated colonies of either *S. aureus* HEMSA 5 or *S. aureus* ATCC 25923 and placed in microcentrifuge tubes containing 4 drops of Extraction reagent 1. The tubes were vortexed and placed on a heating block at 95-100°C for 3 minutes. When the tubes cooled down to room temperature, 1 drop

of Extraction reagent 2 was added, vortexed and centrifuged at 1500 g for 5 minutes. In latex agglutination procedure, the supernatants were used as specimens. For each of the tested strains, one drop of sensitized latex was added onto one circle of the test card. Similarly, 1 drop of negative control latex was added onto another circle of the test card. 50  $\mu$ l of specimens were added into each of the circles. The samples were mixed well and spread over the total surface of the circle. The test cards were rotated by hand for 3 minutes and the agglutination was observed [167].

The presence of  $\beta$ -lactamases was confirmed by comparing minimum inhibitory concentration of a  $\beta$ -lactamase sensitive antibiotic (ampicillin) in presence and absence of a  $\beta$ -lactamase inhibitor (sulbactam). The assay was conducted by means of a serial dilution broth microplate method according to the requirements presented in [168]. The ratio of sulbactam to ampicillin used in the assay was 1 gram : 2 grams, and it was consistent with the ratio used in commercial formulations [169]. Serial two-fold dilutions of ampicillin (starting with 2400  $\mu$ g/ml; Sigma-Aldrich) were prepared in 75  $\mu$ l of the Mueller-Hinton broth (Merck). In the other row of the microplate plate (Nunc), serial two-fold dilutions of ampicillin (starting with 2400  $\mu$ g/ml) and sulbactam (starting with 1200  $\mu$ g/ml; Sigma-Aldrich) were prepared in 75  $\mu$ l of the Mueller-Hinton broth (Merck). Bacterial suspensions were diluted to OD = 0.5. The resulting suspensions were then diluted 1:100 and added in the volume of 75  $\mu$ l into the serial dilutions of ampicillin. The results were read after 20-hour incubation at 37°C. In case of *S. aureus* HEMSA 5, the minimum inhibitory concentration of ampicillin was over 600  $\mu$ g/ml, whereas the MIC of ampicillin in the presence of sulbactam was reduced to 75  $\mu$ g/ml. This shows that the strain contains  $\beta$ -lactamases. In case of *S. aureus* ATCC 25923, no decrease in the MIC of ampicillin was observed after the addition of sulbactam what indicates that the strain is devoid of  $\beta$ -lactamases.

The presence of efflux pumps was confirmed by an Ethidium Bromide-agar Cartwheel method by the group of Professor Leonard Amaral (Group of Mycobacteriology, Unit of Medical Microbiology, Institute of Hygiene and Tropical Medicine, Universidade Nova de Lisboa, Lisbon, Portugal) [170]. The principle of the method relies on the ability of the bacteria to expel a fluorescent molecule that is a substrate for most efflux pumps, ethidium bromide (EB). The concentration of EB that is required to produce

fluorescence in bacterial strains overexpressing efflux systems is considerably higher than that which produces fluorescence of the reference strain. Bacterial strains were grown in 5 ml of tryptic soy broth (TSB; Merck) until they reached an optical density (OD) 0.6 at 600 nm. The OD of the cultures was adjusted with PBS to 0.5 of a McFarland standard. Agar plates containing EB concentrations ranging from 0 to 2.5 mg/l were prepared on the same day of the experiment and protected from light. OD adjusted cultures were swabbed on EB-agar plates starting from the centre of the plate and spreading towards the edges. The wild-type strain *S. aureus* ATCC 25923 served as a comparative control. The swabbed EB-agar plates were then incubated at 37°C for 16 h and examined under a UV transilluminator. The minimum concentration of EB (MC<sub>EB</sub>) that produced fluorescence of the bacterial mass was recorded. The capacity to efflux EB of the bacterial strain was ranked relative to the reference strain according to the following formula [170]:

$$Index = \frac{MC_{EB}(MDR) - MC_{EB}(REF)}{MC_{EB}(REF)}$$

The MC<sub>EB</sub> (mg/l) and index values for both *S. aureus* strains are shown in the Table 3.2.1A.

**Table 3.2.1A** MC<sub>EB</sub> (mg/l) and index values for the *S. aureus* strains

	MC <sub>EB</sub> (mg/l)	Index
<i>S. aureus</i> HEMSA 5	1.5	2
<i>S. aureus</i> ATCC 25923	0.5	0

[170]

The following bacterial *Escherichia coli* strains were used in the study:

- *E. coli* HEMEC 10 (resistant to ciprofloxacin)
- a reference strain *E. coli* ATCC 25922 (susceptible to ciprofloxacin)

HEMEC10 was donated by Professor Isabel Couto and Professor Leonard Amaral (Group of Mycobacteriology, Unit of Medical Microbiology, Institute of Hygiene and Tropical Medicine, Universidade Nova de Lisboa, Lisbon, Portugal)

*E. coli* ATCC 25922 was donated by Professor Alicja Budak (Jagiellonian University Medical College, Faculty of Pharmacy).

The  $MC_{EB}$  (mg/l) and index values for both *E.coli* strains are shown in the Table 3.2.1B.

**Table 3.2.1B**  $MC_{EB}$  (mg/l) and index values for the *E.coli* strains

	$MC_{EB}$ (mg/l)	Index
<i>E. coli</i> HEMEC10	2.5	5
<i>E. coli</i> ATCC 25922	0.5	0

[170]

The breakpoints for antibiotic susceptibility / resistance given in chapter 4.2 were cited according to the European Committee on Antimicrobial Susceptibility Testing (EUCAST) of the European Society of Clinical Microbiology and Infectious Diseases.

### **3.2.2. Method of assessment of direct antibacterial activity of the compounds**

The list of equipment and all reagents used in the assessment of direct antibacterial activity of the compounds is shown in Annex 1, section 6.3.

Direct antibacterial activity of the compounds was tested by determining their minimum inhibitory concentrations. Minimum inhibitory concentrations (MICs) are defined as the lowest concentration of an antimicrobial that will inhibit the visible growth of a microorganism after overnight incubation and are considered the ‘gold standard’ for determining the susceptibility of organisms to antimicrobials [168]. The assay was conducted by means of a serial dilution broth microplate method according to the requirements presented in [168]. Prior to the experiment, *E. coli* strains were grown in Lysogeny broth (LB) and *S. aureus* strains were grown in tryptone soya broth (TSB). Serial two-fold dilutions of the tested compounds (section 3.2.4) were prepared in 75  $\mu$ l of the Mueller-Hinton broth.

Bacterial suspensions were diluted to OD = 0.5. The resulting suspensions were then diluted 1:100 and added in the volume of 75 µl into the serial dilutions of the compounds. The results were read after 20-hour incubation at 37°C. The experiments were conducted in three repetitions.

### **3.2.3. Method of assessment of the compounds' ability to restore antibiotic efficacy**

The list of equipment and all reagents used in the assessment of the compounds' ability to restore antibiotic efficacy is shown in Annex 1, section 6.3.

The ability of the four groups of the compounds to increase/restore antibiotic efficacy was tested by investigating if / to what extent they reduce the minimum inhibitory concentrations of selected antibiotics. The compounds were tested in combination with oxacillin (*S. aureus*) and ciprofloxacin (*E. coli*). Selected compounds (representatives of each chemical group) were also tested with other β-lactam antibiotics: cloxacillin (resistant to β-lactamases), ampicillin (susceptible to β-lactamases) in combination with sulbactam (a β-lactamase inhibitor), fluoroquinolones (ciprofloxacin) and aminoglycosides (neomycin) using the same *S. aureus* strains.

The assay was conducted by means of a serial dilution broth microplate method according to the requirements presented in [168]. Prior to the experiment, *E. coli* strains were grown in Lysogeny broth (LB) and *S. aureus* strains were grown in tryptone soya broth (TSB). Total volume in a single well of the 96-well plate was 150 µl. Serial two-fold dilutions of the antibiotics (oxacillin, ciprofloxacin, cloxacillin, ampicillin/sulbactam, neomycin) were prepared in 65 µl of the Mueller-Hinton broth at the microplate. Suitable concentrations of the compounds (not exceeding ¼ of their MICs; total volume 10 µl) were then added into the microplate. Bacterial suspensions were diluted to OD = 0.5. The resulting suspensions were then diluted 1:100 and added in the volume of 75 µl into the serial dilutions of the antibiotics with the compounds. The results were read after 20-hour incubation at 37°C. Activity gains (AG) were calculated according to the following equation:

$$AG = \frac{MIC \text{ of antibiotic in absence of compound}}{MIC \text{ of antibiotic in presence of compound}}$$

Reduction of resistance was considered as significant if the MIC in the presence of a compound was reduced at least 4-fold. The experiments were conducted in three repetitions.

### 3.2.4. Tested compounds

The tested compounds belonged to several groups:

- **2-piperazine derivatives of 5-arylideneimidazolone**

**Table 3.2.4A** 2-piperazine derivatives of 5-arylideneimidazolone selected for testing

Compound	Chemical name
<b>BM7b</b>	(Z)-5-(4-chlorobenzylidene)-2-(piperazin-1-yl)-3H-imidazol-4(5H)-one hydrochloride
<b>BM33</b>	(Z)-2-(piperazin-1-yl)-5-(thiophen-2-ylmethylene)-3H-imidazol-4(5H)-one hydrochloride
<b>BM34</b>	(Z)-2-(piperazin-1-yl)-5-(thiophen-3-ylmethylene)-3H-imidazol-4(5H)-one hydrochloride
<b>BM36</b>	(Z)-5-(naphthalen-2-ylmethylene)-2-(piperazin-1-yl)-3H-imidazol-4(5H)-one hydrochloride
<b>BM38</b>	(Z)-5-(fluorene-2-ylmethylene)-2-(piperazin-1-yl)-3H-imidazol-4(5H)-one hydrochloride
<b>DS9</b>	(Z)-5-(anthracene-9-ylmethylene)-2-(piperazin-1-yl)-3H-imidazol-4(5H)-one hydrochloride
<b>DS11</b>	(Z)-5-(phenanthren-9-ylmethylene)-2-(piperazin-1-yl)-3H-imidazol-4(5H)-one hydrochloride

The structures of the compounds are presented in Table 2.1.A on page 36 and 37.

The compounds were tested as hydrochlorides.

The compounds BM7b, BM33, BM34, BM36, BM38 were synthesized by a master student Beata Studnicka under supervision of Professor Jadwiga Handzlik. The compounds DS-9 and

DS-11 were synthesized by a master student Daria Studnicka under supervision of Professor Jadwiga Handzlik.

- **Amine derivatives of 5-arylidenehydantoin**

**Table 3.2.4B** Amine derivatives of 5-arylidenehydantoin selected for testing

Compound	Chemical name
<b>A2</b>	(Z)-5-(4-methoxybenzylidene)-3-(3-(3-(4-methylpiperazin-1-yl)propylamino)propyl)imidazolidine-2,4-dione hydrochloride
<b>A18</b>	(Z)-5-(2,4-dichlorobenzylidene)-3-(2-hydroxy-3-(piperazin-1-yl)propyl)imidazolidine-2,4-dione hydrochloride

The structures of the compounds are presented in Table 2.1.B on page 38.

The compounds were tested as hydrochlorides.

The compounds A2 and A18 were synthesized by a PhD student Ewa Otrębska under supervision of Professor Jadwiga Handzlik.

- **Amine derivatives of 5-naphthalen-5-methylhydantoin**

**Table 3.2.4C** Amine derivatives of 5-naphthalen-5-methylhydantoin selected for testing

Compound	Chemical name
<b>JM1</b>	3-(3-aminopropyl)-5-methyl-5-(naphthalen-1-yl)imidazolidine-2,4-dione hydrochloride
<b>JM2</b>	3-(4-aminobutyl)-5-methyl-5-(naphthalen-1-yl)imidazolidine-2,4-dione hydrochloride
<b>JM3</b>	3-(5-aminopentyl)-5-methyl-5-(naphthalen-1-yl)imidazolidine-2,4-dione hydrochloride

The structures of the compounds are presented in Table 2.1.C on page 37 and 38.

The compounds were tested as hydrochlorides.

The compounds JM-1, JM-2 and JM-3 were synthesized by a master student Jakub Schabikowski (Mazurkiewicz) under supervision of Professor Jadwiga Handzlik.

- **N-1 arylpiperazine derivatives of 5-phenylhydantoin**

**Table 3.2.4D** N-1 arylpiperazine derivatives of 5-phenylhydantoin selected for testing

Compound	Chemical name
<b>DK1</b>	methyl 2-(5-methyl-2,4-dioxo-5-phenyl-1-(3-(4-phenylpiperazin-1-yl)propyl)imidazolidin-3-yl)acetate hydrochloride
<b>DK7</b>	methyl 2-(5-methyl-2,4-dioxo-5-phenyl-1-(3-(4-(4-fluorophenyl)piperazin-1-yl)propyl)imidazolidin-3-yl)acetate hydrochloride
<b>GG4a</b>	methyl 2-(3-(3-(4-(4-fluorophenyl)piperazin-1-yl)propyl)-2,5-dioxo-4,4-diphenylimidazolidin-1-yl)acetate hydrochloride
<b>BG1</b>	methyl 2-(2,4-dioxo-5,5-diphenyl-1-(4-(4-phenylpiperazin-1-yl)butyl)imidazolidin-3-yl)acetate hydrochloride
<b>BG6</b>	methyl 2-(2,4-dioxo-5,5-diphenyl-1-(8-(4-(2-methoxyphenyl)piperazin-1-yl)hexyl)imidazolidin-3-yl)acetate hydrochloride

The structures of the compounds are presented in Table 2.1.D on page 39.

The compounds were tested as hydrochlorides.

The compounds DK-1 and DK-7 were synthesized by a master student Karolina Dębska under supervision of Professor Jadwiga Handzlik. The compound GG4a was synthesized by an Erasmus student Giovanni Di Gregorio under supervision of Professor Jadwiga Handzlik. The compounds BG-1 and BG-7 were synthesized by Professor Jadwiga Handzlik.

### **3.3. Determination of the mechanism of action of the most active compounds against bacteria by molecular modeling**

Crystal structures of PBP2a (PDB ID: 1VQQ) and binding domain of MecR1 (PDB ID: 2IWB) were fetched from the PDB database [171]. Three-dimensional conformations of all newly synthesized compounds and oxacillin were generated using LigPrep (version 2.5) from Schrödinger Suite 2013 (Schrödinger, LLC, New York, NY). All molecules tested against bacteria were generated in protonation states at pH 7+/-2 using OPLS\_2005 force field [172].

The compounds were docked into the binding sites of MecR1 and PBP2a using Schrödinger Glide in extra precision mode (maximum 5 poses for each instance from Ligprep were enabled).

For the most active compounds **BM36**, **DS9** as well as structurally-related **DS11** (group 2-piperazine derivatives of 5-arylideneimidazolone), oxacillin and cloxacillin (for comparison) molecular dynamic simulation studies were performed. The simulations were carried out using Schrödinger Desmond (Desmond Molecular Dynamics System, version 3.6, D.E. Shaw Research, New York, NY, 2013). Protein structure was preprocessed and optimized in Schrödinger Protein Preparation Wizard (Schrödinger Suite 2013: Epik version 2.6, Impact version 6.1, Prime version 3.3). The system was composed of protein, chemical compound and solvent (TIP3P model of water). The input poses for molecular dynamics (MD) were obtained from docking and complexes with the best docking scores were selected; as conformations of **DS9** and **DS11** for the ligand-protein complexes were slightly different, **DS11** underwent additional simulation with the analogous starting conformation as **DS9**. The aim of this procedure was to check whether the obtained ligand-protein complexes are stable. Each simulation lasted for 20 ns, and was performed using OPLS\_2005 force field.

## 3.4. Toxicity assays

### 3.4.1. *In-silico* toxicity prediction

Toxicity was predicted *in-silico* using a free online tool Molecular Property Explorer for all compounds tested against bacteria.

Three parameters were calculated: mutagenicity, tumorigenicity and teratogenicity.

Mutagenicity is the ability of an agent to cause mutations: permanent alterations of the nucleotide sequence in the genome. Mutations may be either point mutations (changes to one base in the DNA code such as substitution of a base, insertion of a base, deletion of a base and inversion of bases) or may involve larger parts of the gene or the genome i.e. more bases (deletions, translocations or inversions).

Tumorigenicity is defined as the ability of cultured cells to give rise to either benign or malignant progressively growing tumours showing viable and mitotically active cells in immunologically nonresponsive animals over a limited observation period.

Teratogenicity is the ability of an agent to produce congenital malformations.

The prediction process relies on a precomputed set of structural fragments that give rise to toxicity alerts if they are encountered in the structure currently drawn. These fragment lists

were created by rigorously shredding all compounds of the Registry of Toxic Effects of Chemical Substances database (RTECS database) known to be active in a certain toxicity class (e.g. mutagenicity) [173]. The RTECS database contains critical toxicity data on more than 174,000 chemical substances) [174]. During the shredding any molecule was first cut at every rotatable bonds leading to a set of core fragments. These in turn were used to reconstruct all possible bigger fragments being a substructure of the original molecule. Afterwards, a substructure search process determined the occurrence frequency of any fragment (core and constructed fragments) within all compounds of that toxicity class. It also determined these fragments' frequencies within the structures of more than 3000 traded drugs. Based on the assumption that traded drugs are largely free of toxic effects, any fragment was considered a risk factor if it occurred often as substructure of harmful compounds but never or rarely in traded drugs [173].

The drug score (0-1 range) combines druglikeness, cLogP, logS, molecular weight and toxicity risks in one handy value than may be used to judge the compound's overall potential to qualify for a drug [173].

### **3.4.2. Proliferation assay**

The list of equipment and all reagents used in the proliferation assay is shown in Annex 1, section 6.2.

Compounds with the highest activity against resistant bacterial strains were tested for their anti-proliferative properties. *In vitro* proliferation assay was conducted using HEK-293 cell line and a commercial kit EZ4U (cat. no.: BI-5000, Biomedica) according to the manufacturer's instructions [175]. The kit contains uncoloured tetrazolium salt that is reduced by living cells into intensely coloured formazan derivative. This conversion is presumably accomplished by NADPH or NADH produced by dehydrogenase enzymes in metabolically active cells [176]. The reduction process requires functional mitochondria, which are inactivated within a few minutes after cell death. Thus, the method enables to distinguish living cells from the dead ones [175,177].

Three stock solutions of the compounds (0.25 mM, 10  $\mu$ M, 0.1 $\mu$ M) were prepared from the 25 mM master stock solutions of the compounds (prepared in DMSO) using DMEM medium.

HEK-293 cell line was cultured in Dulbecco's Modified Eagle's complete growth Medium (DMEM) containing 10% fetal bovine serum (FBS), 100 µg/ml streptomycin and 100 IU/ml penicillin. The cells were cultured at 37°C in an atmosphere containing 5% CO<sub>2</sub>. The cells were seeded in 96-well plates at a concentration of  $1.5 \times 10^4$  cells/well in 200 µl culture medium and incubated for 24 h at 37°C and 5% CO<sub>2</sub> to reach 60% confluence. After the incubation, the medium was discarded from the microplate and replaced with the fresh one and appropriate volumes of the stock solutions of the tested compounds (final concentrations 0.01–250 µM in 200 µl volume). . The cells were incubated with the compounds for 48 h at 37°C and 5% CO<sub>2</sub>. Then, 20 µl of EZ4U labeling mixture was added and the cells were incubated for 5 h under the same conditions. The absorbance of the samples was measured using a microplate reader (PerkinElmer) at 492 nm. The activity of the standard drug doxorubicin (DX) was estimated in the same way at the concentrations 0.005–100 µM by using EZ4U. All experiments were conducted in four repetitions. GraphPad Prism 5.01 software was used to calculate the experimental IC<sub>50</sub> values.

## 4. Results

### 4.1. Cancer assays: assessment of the inhibition of P-glycoprotein

The maximum concentration of EB that the mouse lymphoma cells are able to extrude (1  $\mu\text{g/ml}$ ) was selected based on previous studies [165] using the graph presented in Fig. 4.1.1. Accumulation is seen as clearly upward curves, as opposed to relatively stable curves that represent efflux.

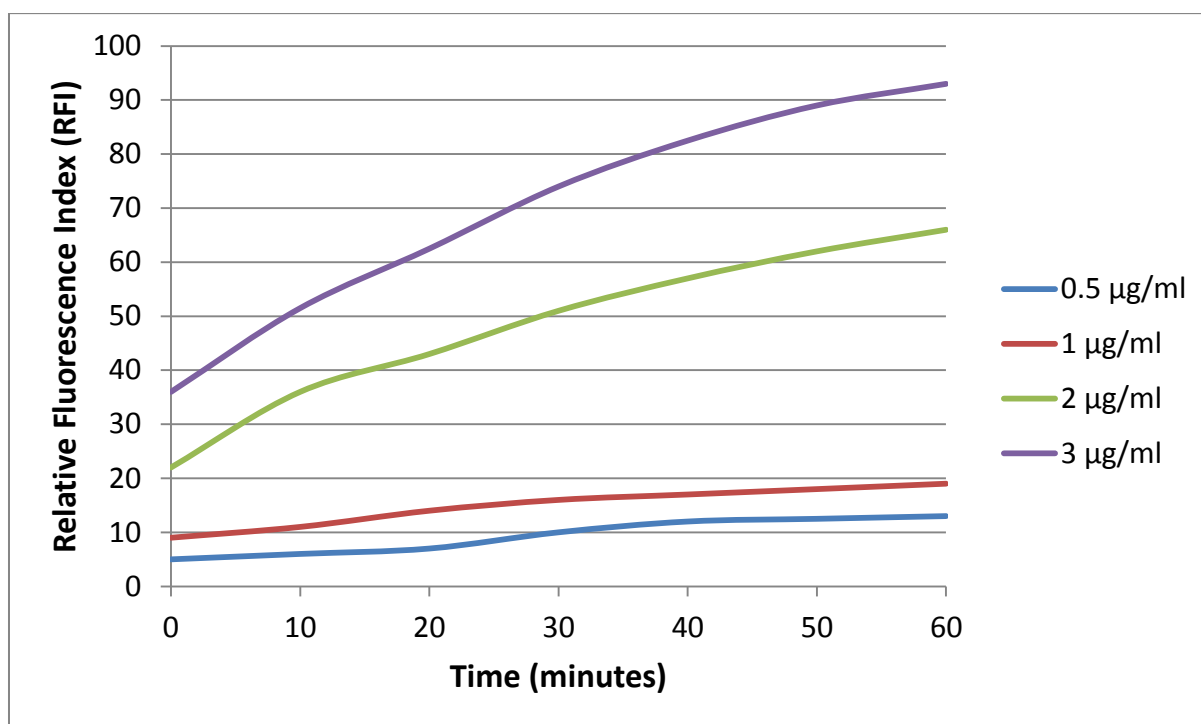
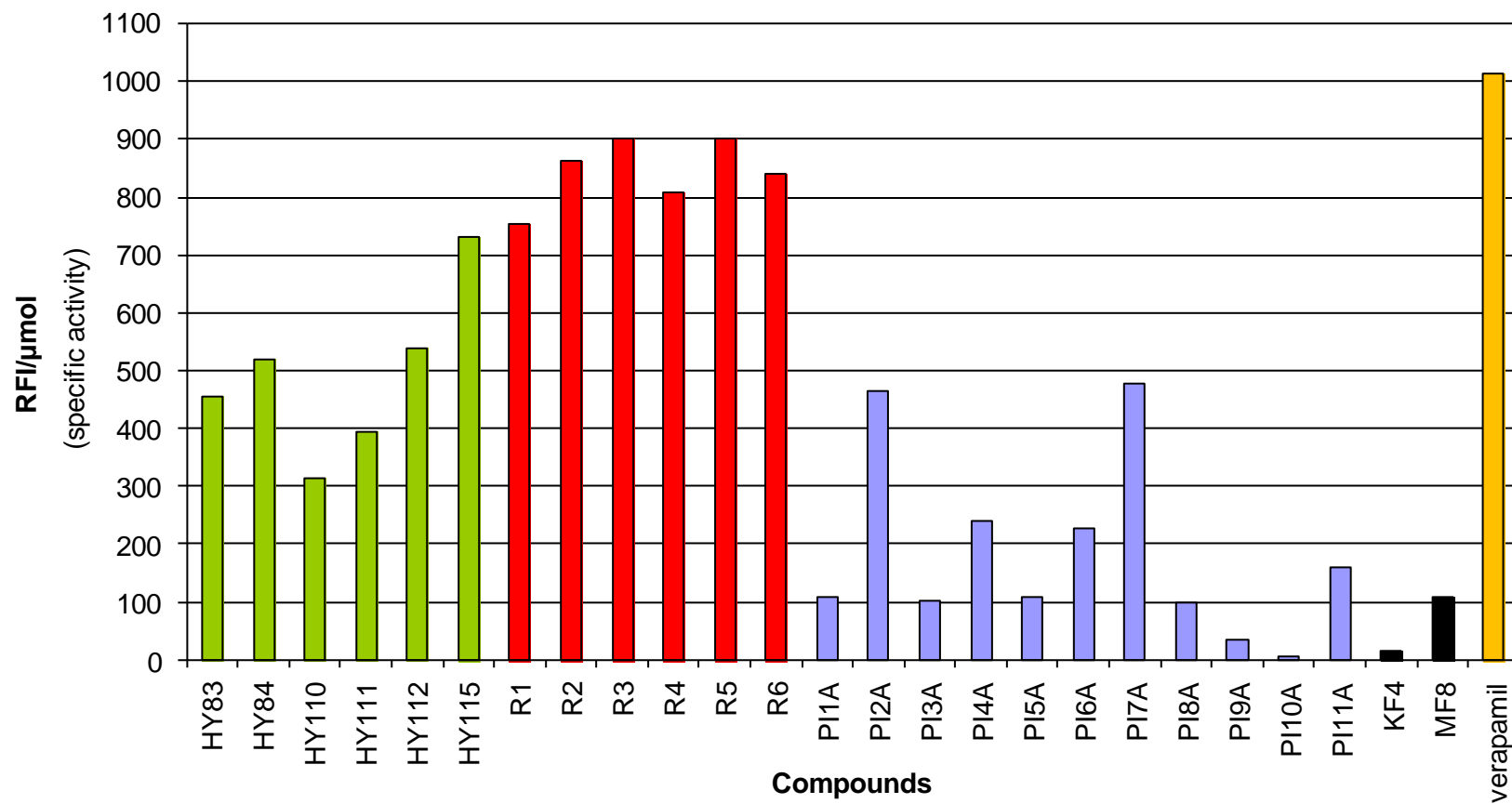


**Figure 4.1.1.** Accumulation/efflux of different concentrations of EB by L5178 mouse lymphoma cells transfected with human *ABCB1* gene

The effect of the tested compounds on the inhibition of P-gp in L5178 mouse lymphoma cells transfected with human *ABCB1* gene is shown in Fig. 4.1.2.

Values represent the mean of  $n=4$  experiments.

**Figure 4.1.2.** Assessment of the inhibition of P-gp: EB accumulation assay



Arylidene hydantoin (N-unsubstituted)

Arylidene hydantoin (N-3 phenylpiperazine derivatives)

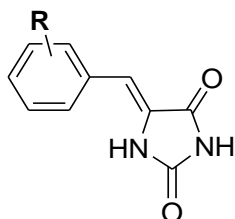
Dimethylhydantoin (N-1 phenylpiperazine derivatives)

Other hydantoin derivatives

Detailed numerical results of RFI/ $\mu\text{mol}$  obtained in the EB accumulation assay for arylidene hydantoins (N-unsubstituted), arylidene hydantoins (N-3 phenylpiperazine derivatives), dimethylhydantoins (N-1 phenylpiperazine derivatives) and other hydantoin derivatives are shown in the tables 4.1A – 4.1D. Values represent the mean of n= 4 experiments.

**Table 4.1A**

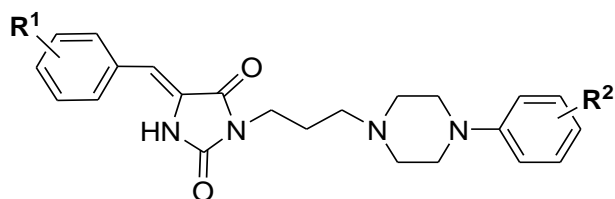
EB accumulation assay: arylidene hydantoins (N-unsubstituted)



Substituents	Compound	RFI/ $\mu\text{mol}$
R		
3-O-CH <sub>2</sub> -Ph-4-Cl	<b>HY83</b>	456
3-O-CH <sub>2</sub> -Ph	<b>HY84</b>	520
4-O-CH <sub>2</sub> -Ph-4-Cl	<b>HY110</b>	314.4
4-O-CH <sub>2</sub> -Ph-2,4-diCl	<b>HY111</b>	394.6
4-O-CH <sub>2</sub> -Ph	<b>HY112</b>	538
3,4-diO-CH <sub>2</sub> -Ph	<b>HY115</b>	731.9
	<b>Verapamil</b>	1012.6

**Table 4.1B**

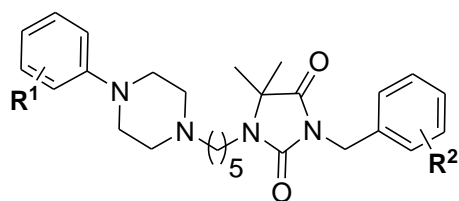
EB accumulation assay: arylidene hydantoin (N-3 phenylpiperazine derivatives)



Substituents		Compound	RFI/ $\mu\text{mol}$
R <sup>1</sup>	R <sup>2</sup>		
3-Cl	2-F	R1	754.6
3-Cl	2,3-diCl	R2	863.5
4-Cl	3,4-diCl	R3	902.6
4-Cl	2-F	R4	809.6
4-Cl	2,3-diCl	R5	902.6
4-Cl	3-Cl	R6	839.7
		Verapamil	1012.6

**Table 4.1C**

EB accumulation assay: dimethylhydantoin (N-1 phenylpiperazine derivatives)



Substituents		Compound	RFI/ $\mu\text{mol}$
R <sup>1</sup>	R <sup>2</sup>		
H	H	PI1A	107.2
2-OCH <sub>3</sub>	H	PI2A	465.7
3-OCH <sub>3</sub>	H	PI3A	103.2
2-F	H	PI4A	241.5
4-F	H	PI5A	108
2,4-diF	H	PI6A	227.3
2,4-diF	4-F	PI7A	477.6
4-F	4-F	PI8A	99.8
2,3-diCl	2,4-diCl	PI9A	34.1
3,4-diCl	2,4-diCl	PI10A	7.1
4-Cl	2,4-diCl	PI11A	159
		Verapamil	1012.6

**Table 4.1D**

EB accumulation assay: other hydantoin derivatives

Compound	RFI/ $\mu\text{mol}$
KF4	13.9
MF8	109.5
Verapamil	1012.6

Summary of the results of P-gp inhibition assay (EB accumulation assay) in L5178 mouse lymphoma cells transfected with human *ABCB1* gene:

- The most active compounds were arylidene hydantoin, especially phenylpiperazine derivatives (R3=R5, R2, R6, R4, R1).
- Among dimethylhydantoin (N-1 phenylpiperazine derivatives), the most active were derivatives containing methoxy group in the ortho position of the benzene ring (PI2A) and 3 fluorine atoms in the benzene ring and benzyl substituent (PI7A).
- Other hydantoin derivatives were not very active.

## **4. 2. Bacterial assays: assessment of restoration of antibiotic efficacy**

The ability of the four groups of the compounds to increase/restore antibiotic efficacy was tested by investigating if / to what extent they reduce the minimum inhibitory concentrations of selected antibiotics. The assay was conducted by means of a serial dilution broth microplate method. First, MICs of the antibiotics against the strains used were determined in the laboratory. They were then compared with the breakpoints for antibiotic susceptibility / resistance of the European Committee on Antimicrobial Susceptibility Testing (EUCAST) of the European Society of Clinical Microbiology and Infectious Diseases in order to find out how resistant the strains are.

The MICs the antibiotics, the MIC of each compound as well as the MIC of the antibiotic in presence of the compound were determined based on three repetitions.

### **4.2.1. Restoration of ciprofloxacin efficacy**

EUCAST classification of *E. coli* strains for determining resistance / susceptibility:

Resistant: MIC of ciprofloxacin > 1 µg/ml (>3.02 µM) [178]

Susceptible: MIC of ciprofloxacin ≤ 0.5 µg/ml (≤ 1.51 µM) [178]

Values determined in the laboratory as part of my research:

MIC of ciprofloxacin of *E. coli* HEMEC 10: 20 µg/ml (60.35 µM) (resistant)

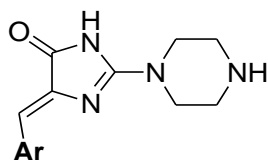
MIC of ciprofloxacin of *E. coli* ATCC 25922: 15 ng/ml (45 nM) (susceptible)

The effect of the tested compounds on the restoration of ciprofloxacin efficacy is shown in the tables 4.2.1.1A – 4.2.1.1D (*E.coli* HEMEC 10) and 4.2.1.2A – 4.2.1.2D (*E.coli* ATCC 25922).

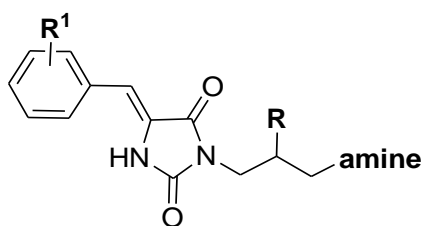
#### 4.2.1.1. *E. coli* HEMEC 10

**Table 4.2.1.1A.**

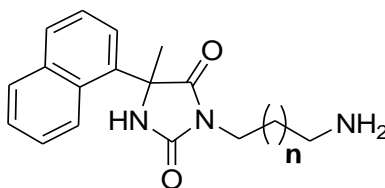
*E. coli* HEMEC 10 + ciprofloxacin: 2-piperazine derivatives of 5-arylideneimidazolone



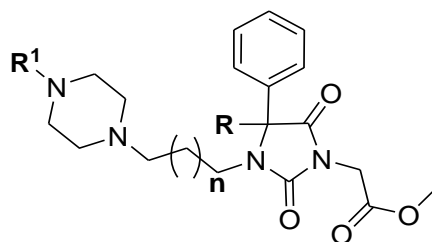
Substituents	Compound	MIC of compound [mM]	Tested concentration of compound [mM]	Activity gain	Numerical value of MIC reduction
Ar					
	<b>BM7b</b>	>1	0.5	2-fold	from 60 $\mu$ M to 30 $\mu$ M (from 20 $\mu$ g/ml to 10 $\mu$ g/ml)
	<b>BM33</b>	>1	0.5	no effect	—
	<b>BM34</b>	>1	0.5	no effect	—
	<b>BM36</b>	0.5	0.125	2-fold	from 60 $\mu$ M to 30 $\mu$ M (from 20 $\mu$ g/ml to 10 $\mu$ g/ml)
	<b>BM38</b>	0.125	0.0312	2-fold	from 60 $\mu$ M to 30 $\mu$ M (from 20 $\mu$ g/ml to 10 $\mu$ g/ml)
	<b>DS9</b>	1	0.25	2-fold	from 60 $\mu$ M to 30 $\mu$ M (from 20 $\mu$ g/ml to 10 $\mu$ g/ml)
	<b>DS11</b>	0.0625	0.0156	2-fold	from 60 $\mu$ M to 30 $\mu$ M (from 20 $\mu$ g/ml to 10 $\mu$ g/ml)

**Table 4.2.1.1B.***E. coli* HEMEC 10 + ciprofloxacin: amine derivatives of 5-arylidenehydantoin

Substituents			Compound	MIC of compound [mM]	Tested concentration of compound [mM]	Activity gain	Numerical value of MIC reduction
R	R <sup>1</sup>	amine					
H	2-OCH <sub>3</sub>		<b>A2</b>	>1	0.5	2-fold	from 60 μM to 30 μM (from 20 μg/ml to 10 μg/ml)
OH	2,4-diCl		<b>A18</b>	>1	0.5	2-fold	from 60 μM to 30 μM (from 20 μg/ml to 10 μg/ml)

**Table 4.2.1.1C.***E. coli* HEMEC 10 + ciprofloxacin: amine derivatives of 5-naphthalen-5-methylhydantoin

Substituents		Compound	MIC of compound [mM]	Tested concentration of compound [mM]	Activity gain	Numerical value of MIC reduction
n						
1		<b>JM1</b>	>2	0.5	no effect	—
2		<b>JM2</b>	>2	0.5	no effect	—
3		<b>JM3</b>	>1	0.5	2-fold	from 60 μM to 30 μM (from 20 μg/ml to 10 μg/ml)

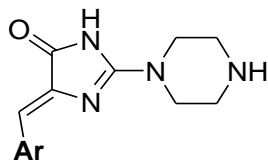
**Table 4.2.1.1D.***E. coli* HEMEC 10 + ciprofloxacin: N-1 arylpiperazine derivatives of 5-phenylhydantoin

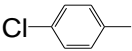
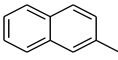
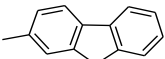
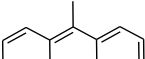
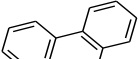
Substituents			Compound	MIC of compound [mM]	Tested concentration of compound [mM]	Activity gain	Numerical value of MIC reduction
R	R <sup>1</sup>	n					
CH <sub>3</sub>		1	<b>DK1</b>	>2	0.5	no effect	—
CH <sub>3</sub>		1	<b>DK7</b>	>2	0.5	no effect	—
		2	<b>GG4</b>	>2	0.5	no effect	—
		4	<b>BG1</b>	1	0.25	no effect	—
		6	<b>BG6</b>	0.25	0.0625	no effect	—

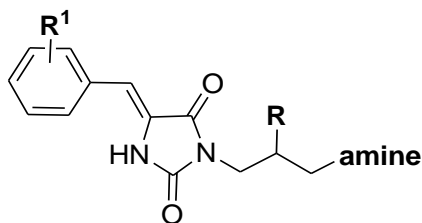
#### 4.2.1.2. *E. coli* ATCC 25923

**Table 4.2.1.2A.**

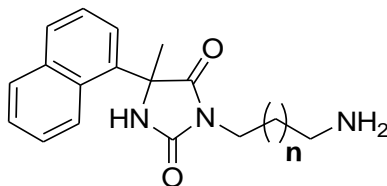
*E. coli* ATCC 25922 + ciprofloxacin: 2-piperazine derivatives of 5-arylideneimidazolone



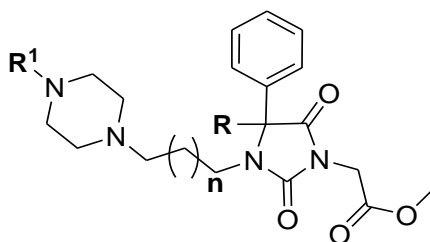
Substituents	Compound	MIC of compound [mM]	Tested concentration of compound [mM]	Activity gain	Numerical value of MIC reduction
Ar					
	<b>BM7b</b>	>1	0.5	2-fold	from 45 nM to 22.5 nM (from 15 ng/ml to 7.5 ng/ml)
	<b>BM33</b>	>1	0.5	4-fold	from 45 nM to 11.25 nM (from 15 ng/ml to 3.75 ng/ml)
	<b>BM34</b>	>1	0.5	4-fold	from 45 nM to 11.25 nM (from 15 ng/ml to 3.75 ng/ml)
	<b>BM36</b>	0.5	0.125	2-fold	from 45 nM to 22.5 nM (from 15 ng/ml to 7.5 ng/ml)
	<b>BM38</b>	0.0625	0.0156	no effect	—
	<b>DS9</b>	1	0.25	2-fold	from 45 nM to 22.5 nM (from 15 ng/ml to 7.5 ng/ml)
	<b>DS11</b>	0.0625	0.0156	2-fold	from 45 nM to 22.5 nM (from 15 ng/ml to 7.5 ng/ml)

**Table 4.2.1.2B.***E. coli* ATCC 25922 + ciprofloxacin: amine derivatives of 5-arylidenehydantoin

Substituents			Compound	MIC of compound [mM]	Tested concentration of compound [mM]	Activity gain	Numerical value of MIC reduction
R	R <sup>1</sup>	amine					
H	2-OCH <sub>3</sub>		<b>A2</b>	>1	0.5	2-fold	from 45 nM to 22.5 nM (from 15 ng/ml to 7.5 ng/ml)
OH	2,4-diCl		<b>A18</b>	>1	0.5	2-fold	from 45 nM to 22.5 nM (from 15 ng/ml to 7.5 ng/ml)

**Table 4.2.1.2C.***E. coli* ATCC 25922 + ciprofloxacin: amine derivatives of 5-naphthalen-5-methylhydantoin

Substituents		Compound	MIC of compound [mM]	Tested concentration of compound [mM]	Activity gain	Numerical value of MIC reduction
n						
1		<b>JM1</b>	>2	0.5	4-fold	from 45 nM to 11.25 nM (from 15 ng/ml to 3.75 ng/ml)
2		<b>JM2</b>	0.5	0.125	2-fold	from 45 nM to 22.5 nM (from 15 ng/ml to 7.5 ng/ml)
3		<b>JM3</b>	>1	0.5	2-fold	from 45 nM to 22.5 nM (from 15 ng/ml to 7.5 ng/ml)

**Table 4.2.1.2D.***E. coli* ATCC 25922 + ciprofloxacin: N-1 arylpiperazine derivatives of 5-phenylhydantoin

Substituents			Compound	MIC of compound [mM]	Tested concentration of compound [mM]	Activity gain	Numerical value of MIC reduction
R	R <sup>1</sup>	n					
CH <sub>3</sub>		1	<b>DK1</b>	>2	0.5	no effect	—
CH <sub>3</sub>		1	<b>DK7</b>	>2	0.5	no effect	—
		2	<b>GG4</b>	2	0.5	no effect	—
		4	<b>BG1</b>	1	0.25	no effect	—
		6	<b>BG6</b>	0.25	0.0625	no effect	—

Summary of the results *E. coli* + ciprofloxacin:

No compounds were active against the resistant *E. coli* HEMEC10 strain. As far as *E. coli* ATCC 25923 is concerned, there were 3 compounds which increased the activity of ciprofloxacin 4-fold (BM33, BM34 and JM1).

**4.2.2. Restoration of oxacillin efficacy**

EUCAST classification of *S. aureus* strains for determining resistance / susceptibility:

Resistant: methicillin resistant staphylococci are resistant to oxacillin (isolates with oxacillin MIC values > 2 µg/ml (> 4.72 µM) are mostly methicillin resistant (MRSA) due to the presence of the *mecA* gene (PBP2a protein)) [178]

Susceptible: no clear breakpoint given, but it may be assumed that isolates with oxacillin MIC values ≤ 2 µg/ml (< 4.72 µM) are susceptible, if no PBP2a protein is present [178]

Values determined in the laboratory as part of my research:

MIC of oxacillin of *S. aureus* HEMSA 5: 300 µg/ml (710 µM) (resistant, positive for PBP2a protein)

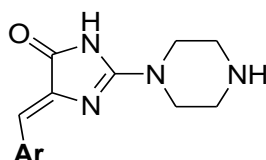
MIC of oxacillin of *S. aureus* ATCC 25923: 0.2 µg/ml (0.47 µM) (susceptible, negative for PBP2a protein)

The effect of the tested compounds on the restoration of oxacillin efficacy is shown in the tables 4.2.2.1A – 4.2.2.1D (*S. aureus* MRSA HEMSA 5) and 4.2.2.2A – 4.2.2.2D (*S. aureus* ATCC 25923).

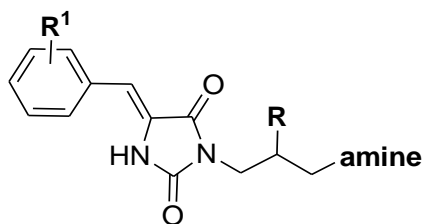
#### 4.2.2.1. *S. aureus* MRSA HEMSA 5

**Table 4.2.2.1A.**

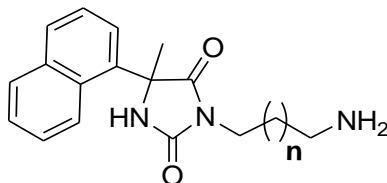
*S. aureus* MRSA HEMSA 5 + oxacillin: 2-piperazine derivatives of 5-arylideneimidazolone



Substituents	Compound	MIC of compound [mM]	Tested concentration of compound [mM]	Activity gain	Numerical value of MIC reduction
Ar					
	<b>BM7b</b>	0.5	0.125	no effect	—
	<b>BM33</b>	>1	0.5	no effect	—
	<b>BM34</b>	1	0.25	no effect	—
	<b>BM36</b>	0.5	0.125	128-fold	from 710 µM to 5.55 µM (from 300 µg/ml to 2.34 µg/ml)
	<b>BM38</b>	0.0313	0.0078	no effect	—
	<b>DS9</b>	0.5	0.125	64-fold	from 710 µM to 11.09 µM (from 300 µg/ml to 4.69 µg/ml)
	<b>DS11</b>	0.0156	0.0039	no effect	—

**Table 4.2.2.1B.***S. aureus* MRSA HEMSA 5 + oxacillin: amine derivatives of 5-arylidenehydantoin

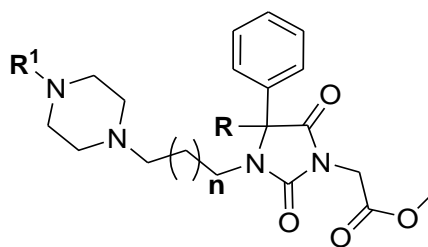
Substituents			Compound	MIC of compound [mM]	Tested concentration of compound [mM]	Activity gain	Numerical value of MIC reduction
R	R <sup>1</sup>	amine					
H	2-OCH <sub>3</sub>		<b>A2</b>	>1	0.5	2-fold	from 710 μM to 355 μM (from 300 μg/ml to 150 μg/ml)
OH	2,4-diCl		<b>A18</b>	>1	0.5	no effect	—

**Table 4.2.2.1C.***S. aureus* MRSA HEMSA 5 + oxacillin: amine derivatives of 5-naphthalen-5-methylhydantoin

Substituents		Compound	MIC of compound [mM]	Tested concentration of compound [mM]	Activity gain	Numerical value of MIC reduction
n						
1		<b>JM1</b>	>1	0.5	no effect	—
2		<b>JM2</b>	>1	0.5	no effect	—
3		<b>JM3</b>	1	0.25	no effect	—

**Table 4.2.2.1D.**

*S. aureus* MRSA HEMSA 5 + oxacillin: N-1 arylpiperazine derivatives of 5-phenylhydantoin

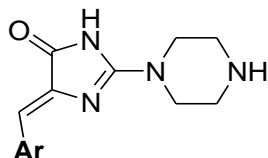


Substituents			Compound	MIC of compound [mM]	Tested concentration of compound [mM]	Activity gain	Numerical value of MIC reduction
R	R <sup>1</sup>	n					
CH <sub>3</sub>		1	<b>DK1</b>	>2	0.5	no effect	—
CH <sub>3</sub>		1	<b>DK7</b>	>2	0.5	no effect	—
		2	<b>GG4</b>	0.5	0.125	2-fold	from 710 μM to 355 μM (from 300 μg/ml to 150 μg/ml)
		4	<b>BG1</b>	0.5	0.125	8-fold	from 710 μM to 88.75 μM (from 300 μg/ml to 37.5 μg/ml)
		6	<b>BG6</b>	0.25	0.0625	no effect	—

#### 4.2.2.2. *S. aureus* ATCC 25923

**Table 4.2.2.2A.**

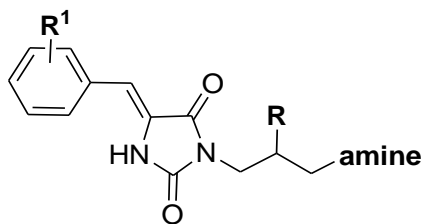
*S. aureus* ATCC 25923 + oxacillin: 2-piperazine derivatives of 5-arylideneimidazolone



Substituents	Compound	MIC of compound [mM]	Tested concentration of compound [mM]	Activity gain	Numerical value of MIC reduction
Ar					
	<b>BM7b</b>	>1	0.5	no effect	—
	<b>BM33</b>	>1	0.5	no effect	—
	<b>BM34</b>	>1	0.5	no effect	—
	<b>BM36</b>	0.25	0.0625	2-fold	from 0.47 $\mu$ M to 0.23 $\mu$ M (from 0.2 $\mu$ g/ml to 0.1 $\mu$ g/ml)
	<b>BM38</b>	0.0156	0.0039	2-fold	from 0.47 $\mu$ M to 0.23 $\mu$ M (from 0.2 $\mu$ g/ml to 0.1 $\mu$ g/ml)
	<b>DS9</b>	0.5	0.125	2-fold	from 0.47 $\mu$ M to 0.23 $\mu$ M (from 0.2 $\mu$ g/ml to 0.1 $\mu$ g/ml)
	<b>DS11</b>	0.0019	0.0005	no effect	—

**Table 4.2.2.2B.**

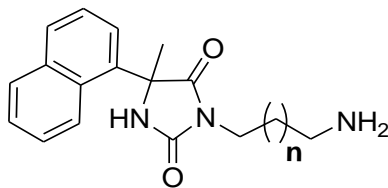
*S. aureus* ATCC 25923 + oxacillin: amine derivatives of 5-arylidenehydantoin



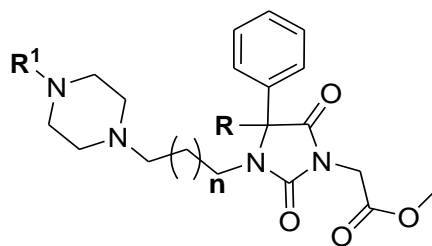
Substituents			Compound	MIC of compound [mM]	Tested concentration of compound [mM]	Activity gain	Numerical value of MIC reduction
R	R <sup>1</sup>	amine					
H	2-OCH <sub>3</sub>		<b>A2</b>	>1	0.5	no effect	—
OH	2,4-diCl		<b>A18</b>	>1	0.5	no effect	—

**Table 4.2.2.2C.**

*S. aureus* ATCC 25923 + oxacillin: amine derivatives of 5-naphthalen-5-methylhydantoin



Substituents		Compound	MIC of compound [mM]	Tested concentration of compound [mM]	Activity gain	Numerical value of MIC reduction
n						
1		<b>JM1</b>	>1	0.5	no effect	—
2		<b>JM2</b>	>1	0.5	no effect	—
3		<b>JM3</b>	>1	0.5	no effect	—

**Table 4.2.2.D.***S. aureus* ATCC 25923 + oxacillin: N-1 arylpiperazine derivatives of 5-phenylhydantoin

Substituents			Compound	MIC of compound [mM]	Tested concentration of compound [mM]	Activity gain	Numerical value of MIC reduction
R	R <sup>1</sup>	n					
CH <sub>3</sub>		1	<b>DK1</b>	>2	0.5	no effect	—
CH <sub>3</sub>		1	<b>DK7</b>	>2	0.5	no effect	—
		2	<b>GG4</b>	0.5	0.125	8-fold	from 0.47 μM to 0.059 μM (from 0.2 μg/ml to 0.025 μg/ml)
		4	<b>BG1</b>	0.5	0.125	no effect	—
		6	<b>BG6</b>	0.125	0.0312	no effect	—

Summary of the results *S. aureus* + oxacillin:

Most of the compounds had no impact on oxacillin activity. The most active compound was BM36, which decreased the MIC of oxacillin against MRSA HEMSA 5 128-fold. Another active compound (DS9) was able to reduce the MIC of oxacillin against the same strain 64-fold.

Since these two compounds proved to be very active, they, and some other selected compounds, were also tested with other β-lactam antibiotics: cloxacillin (resistant to β-lactamases) and ampicillin (susceptible to β-lactamases) in combination with sulbactam (a β-lactamase inhibitor) in order to check whether the activity involves other β-lactam antibiotics too. The results of these assays are presented in the tables 4.2.3 – 4.2.4.

### 4.2.3. Restoration of cloxacillin efficacy

EUCAST classification of *S. aureus* strains for determining resistance / susceptibility:

Resistant: methicillin resistant staphylococci are resistant to cloxacillin [178]

Susceptible: methicillin susceptible staphylococci negative for penicillinase (  $\beta$ -lactamase) are susceptible to cloxacillin [178]

*S. aureus* MRSA HEMSA 5: resistant to cloxacillin (methicillin resistant)

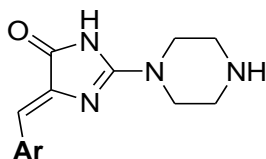
*S. aureus* ATCC 25923: susceptible to cloxacillin (methicillin susceptible, negative for penicillinase)

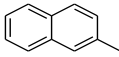
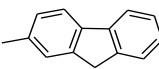
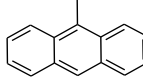
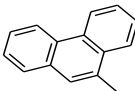
The effect of the tested compounds on the restoration of cloxacillin efficacy is shown in the tables 4.2.3.1A – 4.2.3.1C (*S.aureus* MRSA HEMSA 5) and section 4.2.3.2 (*S. aureus* ATCC 25923).

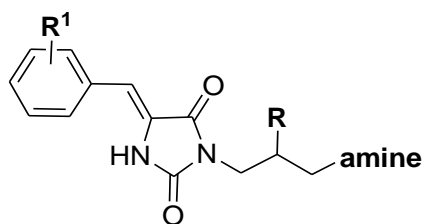
#### 4.2.3.1. *S. aureus* MRSA HEMSA 5

**Table 4.2.3.1A.**

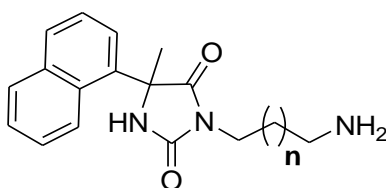
*S. aureus* MRSA HEMSA 5 + cloxacillin: 2-piperazine derivatives of 5-arylideneimidazolone



Substituents	Compound	MIC of compound [mM]	Tested concentration of compound [mM]	Activity gain	Numerical value of MIC reduction
Ar					
	<b>BM33</b>	>1	0.5	no effect	—
	<b>BM34</b>	1	0.25	no effect	—
	<b>BM36</b>	0.5	0.125	256-fold	from 315 $\mu$ M to 1.23 $\mu$ M (from 145 $\mu$ g/ml to 0.57 $\mu$ g/ml)
	<b>BM38</b>	0.0313	0.0078	8-fold	from 315 $\mu$ M to 39.37 $\mu$ M (from 145 $\mu$ g/ml to 18.12 $\mu$ g/ml)
	<b>DS9</b>	0.5	0.125	8-fold	from 315 $\mu$ M to 39.37 $\mu$ M (from 145 $\mu$ g/ml to 18.12 $\mu$ g/ml)
	<b>DS11</b>	0.0156	0.0039	2-fold	from 315 $\mu$ M to 157.5 $\mu$ M (from 145 $\mu$ g/ml to 72.5 $\mu$ g/ml)

**Table 4.2.3.1B.***S. aureus* MRSA HEMSA 5 + cloxacillin: amine derivatives of 5-arylidenehydantoin

Substituents			Compound	MIC of compound [mM]	Tested concentration of compound [mM]	Activity gain	Numerical value of MIC reduction
R	R <sup>1</sup>	amine					
H	2-OCH <sub>3</sub>		A2	>1	0.5	8-fold	from 315 μM to 39.37 μM (from 145 μg/ml to 18.12 μg/ml)

**Table 4.2.3.1C.***S. aureus* MRSA HEMSA 5 + cloxacillin: amine derivatives of 5-naphthalen-5-methylhydantoin

Substituents		Compound	MIC of compound [mM]	Tested concentration of compound [mM]	Activity gain	Numerical value of MIC reduction
n						
1		JM1	>1	0.5	no effect	—

#### 4.2.3.2. *S. aureus* ATCC 25923

None of the tested compounds (BM33, BM34, BM36, BM38, DS9, DS11, A2, JM1) had any impact on minimal inhibitory concentration (MIC) of cloxacillin against *S. aureus* ATCC 25923.

#### Summary of the results *S. aureus* + cloxacillin:

Out of the 8 tested compounds, 3 compounds (BM38, DS9 and A2) reduced the MIC of cloxacillin against *E. coli* HEMEC10 8-fold. Another compound (BM36), proved to be

exceptionally active as it increased cloxacillin activity as much as 256-fold against the same strain.

#### **4.2.4. Restoration of ampicillin + sulbactam efficacy**

EUCAST classification of *S. aureus* strains for determining resistance / susceptibility:

Resistant: methicillin resistant staphylococci are resistant to ampicillin +  $\beta$ -lactamase inhibitor [178]

Susceptible: methicillin susceptible staphylococci negative for penicillinase (  $\beta$ -lactamase) are susceptible to ampicillin; methicillin susceptible staphylococci positive for penicillinase (  $\beta$ -lactamase) are susceptible to ampicillin +  $\beta$ -lactamase inhibitor [178].

Values determined in the laboratory as part of my research:

MIC of ampicillin of *S. aureus* HEMSA 5: > 600  $\mu$ g/ml (>1.62 mM)

MIC of ampicillin + sulbactam of *S. aureus* HEMSA 5: 75  $\mu$ g/ml (202  $\mu$ M)

MIC of ampicillin of *S. aureus* ATCC 25923: 0.2  $\mu$ g/ml (0.54  $\mu$ M)

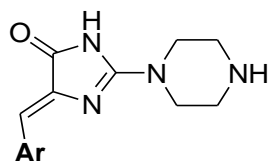
MIC of ampicillin + sulbactam of *S. aureus* ATCC 25923: 0.2  $\mu$ g/ml (0.54  $\mu$ M)

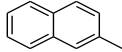
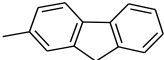
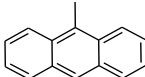
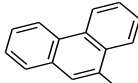
The effect of the tested compounds on the restoration of ampicillin + sulbactam efficacy is shown in the tables 4.2.4.1A – 4.2.4.1C (*S. aureus* MRSA HEMSA 5) and section 4.2.4.2. (*S. aureus* ATCC 25923).

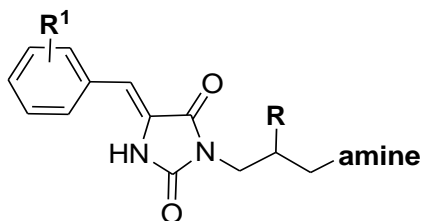
#### 4.2.4.1. *S. aureus* MRSA HEMSA 5

**Table 4.2.4.1A.**

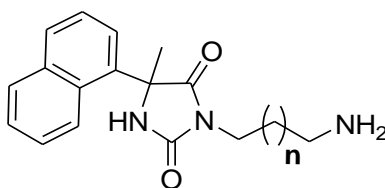
*S. aureus* MRSA HEMSA 5 + ampicillin + sulbactam: 2-piperazine derivatives of 5-arylideneimidazolone



Substituents	Compound	MIC of compound [mM]	Tested concentration of compound [mM]	Activity gain	Numerical value of MIC reduction
Ar					
	<b>BM33</b>	>1	0.5	no effect	—
	<b>BM34</b>	1	0.25	no effect	—
	<b>BM36</b>	0.5	0.125	4-fold	from 202 $\mu$ M to 50.5 $\mu$ M (from 75 $\mu$ g/ml to 18.75 $\mu$ g/ml)
	<b>BM38</b>	0.0313	0.0078	no effect	—
	<b>DS9</b>	0.5	0.125	no effect	—
	<b>DS11</b>	0.0156	0.0039	no effect	—

**Table 4.2.4.1B.***S. aureus* MRSA HEMSA 5 + ampicillin + sulbactam: amine derivatives of 5-arylidenehydantoin

Substituents			Compound	MIC of compound [mM]	Tested concentration of compound [mM]	Activity gain	Numerical value of MIC reduction
R	R <sup>1</sup>	amine					
H	2-OCH <sub>3</sub>		A2	>1	0.5	2-fold	from 202 μM to 101 μM (from 75 μg/ml to 37.5 μg/ml)

**Table 4.2.4.1C.***S. aureus* MRSA HEMSA 5 + ampicillin + sulbactam: amine derivatives of 5-naphthalen-5-methylhydantoin

Substituents		Compound	MIC of compound [mM]	Tested concentration of compound [mM]	Activity gain	Numerical value of MIC reduction
n						
1		JM1	>1	0.5	no effect	—

#### 4.2.4.2. *S. aureus* ATCC 25923

None of the tested compounds (BM33, BM34, BM36, BM38, DS9, DS11, A2, JM1) had any impact on minimal inhibitory concentration (MIC) of ampicillin + sulbactam against *S. aureus* ATCC 25923.

#### Summary of the results *S. aureus* + ampicillin + sulbactam:

The compounds were practically inactive against the *S. aureus* strains. Only one compound (BM36) reduced the MIC of ampicillin + sulbactam against *S. aureus* HEMSA 5 4-fold.

The two the most active compounds (BM36 and DS9) and some other selected compounds were also tested with antibiotics that act through a different mechanism of action than  $\beta$ -lactam antibiotics: ciprofloxacin (fluoroquinolones) and neomycin (aminoglycosides). The results of these assays are presented in sections 4.2.5 and 4.2.6.

#### **4.2.5. Restoration of ciprofloxacin efficacy**

EUCAST classification of *S. aureus* strains for determining resistance / susceptibility:

Resistant: MIC of ciprofloxacin  $> 1 \mu\text{g/ml}$  ( $> 3.02 \mu\text{M}$ ): [178]

Susceptible: MIC of ciprofloxacin  $\leq 1 \mu\text{g/ml}$  ( $\leq 3.02 \mu\text{M}$ ): [178]

Values determined in the laboratory as part of my research:

MIC of ciprofloxacin of *S. aureus* HEMSA 5:  $5 \mu\text{g/ml}$  ( $15.09 \mu\text{M}$ ) (resistant)

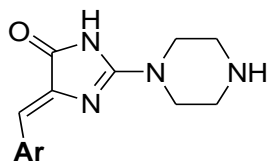
MIC of ciprofloxacin of *S. aureus* ATCC 25923:  $0.12 \mu\text{g/ml}$  ( $0.38 \mu\text{M}$ ) (susceptible)

The effect of the tested compounds on the restoration of ciprofloxacin efficacy is shown in the tables 4.2.5.1A – 4.2.5.1C (*S. aureus* MRSA HEMSA 5) and section 4.2.5.2 (*S. aureus* ATCC 25923).

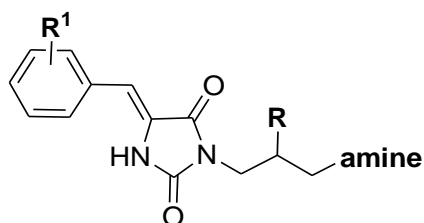
#### 4.2.5.1. *S. aureus* MRSA HEMSA 5

**Table 4.2.5.1A.**

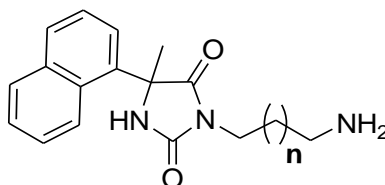
*S. aureus* MRSA HEMSA 5 + ciprofloxacin: 2-piperazine derivatives of 5-arylideneimidazolone



Substituents	Compound	MIC of compound [mM]	Tested concentration of compound [mM]	Activity gain	Numerical value of MIC reduction
Ar					
	<b>BM33</b>	1	0.25	no effect	—
	<b>BM34</b>	0.5	0.125	no effect	from 15.1 $\mu$ M to 3.77 $\mu$ M (from 5 $\mu$ g/ml to 1.25 $\mu$ g/ml)
	<b>BM36</b>	0.0313	0.0078	4-fold	—
	<b>BM38</b>	0.5	0.125	no effect	—
	<b>DS9</b>	0.5	0.125	no effect	—
	<b>DS11</b>	0.0156	0.0039	no effect	—

**Table 4.2.5.1B.***S. aureus* MRSA HEMSA 5 + ciprofloxacin: amine derivatives of 5-arylidenehydantoin

Substituents			Compound	MIC of compound [mM]	Tested concentration of compound [mM]	Activity gain	Numerical value of MIC reduction
R	R <sup>1</sup>	amine					
H	2-OCH <sub>3</sub>		A2	>1	0.5	2-fold	from 15.1 μM to 7.55 μM (from 5 μg/ml to 2.5 μg/ml)

**Table 4.2.5.1C.***S. aureus* MRSA HEMSA 5 + ciprofloxacin: amine derivatives of 5-naphthalen-5-methylhydantoin

Substituents		Compound	MIC of compound [mM]	Tested concentration of compound [mM]	Activity gain	Numerical value of MIC reduction
n						
1		JM1	>1	0.5	no effect	—

#### 4.2.5.2. *S. aureus* ATCC 25923

None of the tested compounds (BM33, BM34, BM36, BM38, DS9, DS11, A2, JM1) had any impact on minimal inhibitory concentration (MIC) of ciprofloxacin against *S. aureus* ATCC 25923.

#### Summary of the results *S. aureus* + ciprofloxacin:

The only compound that showed any activity was BM36 (4-fold activity gain).

## 4.2.6. Restoration of neomycin efficacy

No established breakpoints available for neomycin [178].

Values determined in the laboratory as part of my research:

MIC of neomycin of *S. aureus* HEMSA 5: 175 µg/ml (245 µM)

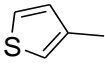
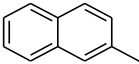
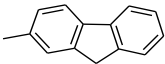
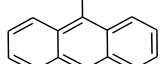
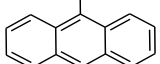
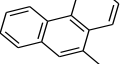
MIC of neomycin of *S. aureus* ATCC 25923: 0.75 µg/ml (1.05 µM)

The effect of the tested compounds on the restoration of neomycin efficacy is shown in the tables 4.2.6.1A – 4.2.6.1C (*S. aureus* MRSA HEMSA 5) and section 4.2.6.2. (*S. aureus* ATCC 25923).

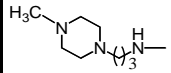
### 4.2.6.1. *S. aureus* MRSA HEMSA 5

**Table 4.2.6.1A.**

*S. aureus* MRSA HEMSA 5 + neomycin: 2-piperazine derivatives of 5-arylideneimidazolone

Substituents	Compound	MIC of compound [mM]	Tested concentration of compound [mM]	Activity gain	Numerical value of MIC reduction
Ar					
	<b>BM33</b>	1	0.25	no effect	—
	<b>BM34</b>	0.5	0.125	no effect	—
	<b>BM36</b>	0.0313	0.0078	no effect	—
	<b>BM38</b>	0.5	0.125	no effect	—
	<b>DS9</b>	0.5	0.125	no effect	—
	<b>DS11</b>	0.0156	0.0039	no effect	—

**Table 4.2.6.1B.***S. aureus* MRSA HEMSA 5 + neomycin: amine derivatives of 5-arylidenehydantoin

Substituents			Compound	MIC of compound [mM]	Tested concentration of compound [mM]	Activity gain	Numerical value of MIC reduction
R	R <sup>1</sup>	amine					
H	2-OCH <sub>3</sub>		A2	>1	0.5	no effect	—

**Table 4.2.6.1C.***S. aureus* MRSA HEMSA 5 + neomycin: amine derivatives of 5-naphthalen-5-methylhydantoin

Substituents		Compound	MIC of compound [mM]	Tested concentration of compound [mM]	Activity gain	Numerical value of MIC reduction
n						
1		JM1	>1	0.5	no effect	—

#### 4.2.6.2. *S. aureus* ATCC 25923

None of the tested compounds (BM33, BM34, BM36, BM38, DS9, DS11, A2, JM1) had any impact on minimal inhibitory concentration (MIC) of neomycin against *S. aureus* ATCC 25923.

#### Summary of the results *S. aureus* + neomycin:

No compounds were active.

Since the two the most active compounds (BM36 and DS9) were active virtually only with  $\beta$ -lactam antibiotics against the MRSA HEMSA 5 strain, and the corresponding reduction in the reference strain in all of these cases was negligent, this suggests that the modulation of bacterial resistance in the MRSA HEMSA 5 strain by the compounds BM36 and DS9 may involve proteins responsible for  $\beta$ -lactam resistance in MRSA strains: PBP2a and MecR1. This hypothesis was verified by molecular modeling.

**Table 4.2.7.** Summary of the results of microbiological assays, where: **A:** 2-piperazine derivatives of 5-arylidenimidazolone, **B:** amine derivatives of 5-arylidenhydantoin, **C:** amine derivatives of 5-naphthalen-5-methylhydantoin, **D:** N-1 arylpiperazine derivatives of 5-phenylhydantoin

Chemical group	Compound	resistant strains						reference strains					
		E. coli HEMEC 10 + ciprofloxacin	S. aureus MRSA HEMSA 5					E. coli ATCC 25922 + ciprofloxacin	S. aureus ATCC 25923				
			β-lactam antibiotics			other antibiotics			β-lactam antibiotics			other antibiotics	
			oxacillin	cloxacillin	ampicillin + sulbactam	ciprofloxacin	neomycin		oxacillin	cloxacillin	ampicillin + sulbactam	ciprofloxacin	neomycin
A	<b>BM7b</b>	2-fold	no effect					2-fold	no effect				
	<b>BM33</b>	no effect	no effect	no effect	no effect	no effect	no effect	4-fold	no effect	no effect	no effect	no effect	no effect
	<b>BM34</b>	no effect	no effect	no effect	no effect	no effect	no effect	4-fold	no effect	no effect	no effect	no effect	no effect
	<b>BM36</b>	2-fold	128-fold	256-fold	4-fold	4-fold	no effect	2-fold	2-fold	no effect	no effect	no effect	no effect
	<b>BM38</b>	2-fold	no effect	8-fold	no effect	no effect	no effect	no effect	2-fold	no effect	no effect	no effect	no effect
	<b>DS9</b>	2-fold	64-fold	8-fold	no effect	no effect	no effect	2-fold	2-fold	no effect	no effect	no effect	no effect
	<b>DS11</b>	2-fold	no effect	2-fold	no effect	no effect	no effect	2-fold	no effect	no effect	no effect	no effect	no effect
B	<b>A2</b>	2-fold	2-fold	8-fold	2-fold	2-fold	no effect	2-fold	no effect	no effect	no effect	no effect	no effect
	<b>A18</b>	2-fold	no effect					2-fold	no effect				
C	<b>JM1</b>	no effect	no effect	no effect	no effect	no effect	no effect	4-fold	no effect	no effect	no effect	no effect	no effect
	<b>JM2</b>	no effect	no effect					2-fold	no effect				
	<b>JM3</b>	2-fold	no effect					2-fold	no effect				
D	<b>DK1</b>	no effect	no effect					no effect	no effect				
	<b>DK7</b>	no effect	no effect					no effect	no effect				
	<b>GG4a</b>	no effect	2-fold					no effect	8-fold				
	<b>BG1</b>	no effect	8-fold					no effect	no effect				
	<b>BG6</b>	no effect	no effect					no effect	no effect				

## **4.3. Determination of the mechanism of action of the most active compounds by molecular modeling**

### **4.3.1. Docking results**

First, molecular docking experiments were performed to find out with which protein (MecR1 or PBP2a) the tested compounds potentially interact – all the tested compounds were docked into the crystal structures of MecrR1 and PBP2a. The results are presented in the Table 4.3.1.1.

**Table 4.3.1.1.** Number of poses obtained for each compound in the procedure of docking into the crystal structures of PBP2a and MecR1 binding domain.

Compound	Number of 3D conformations	Number of poses obtained by docking	
		MecR1	PBP2a
BM7b	3	2	0
BM33	8	9	5
BM34	4	4	2
BM36	3	1	0
BM38	3	0	0
DS9	6	10	3
DS11	6	7	3
A2	6	6	6
A18	2	3	0
JM1	1	1	1
JM2	1	1	2
JM3	1	2	1
DK1	2	0	2
DK7	2	0	2
GG4a	1	0	1
BG1	1	0	1
BG6	2	0	2
oxacillin	1	1	2

Docking results revealed that all of the tested compounds were much more successful in interacting with MecR1 than PBP2a as the number of the obtained ligand-protein complexes was much higher in case of MecR1 in comparison to the modified PBP (Table 4.3.1.1). The only compound for which the same number of ligand-protein complexes was obtained in case of MecR1 and PBP2a was A2. Compound A2 was also the one which caused 2-fold increase in oxacillin activity. This increase is only minor and fits in the method's inaccuracy range.

As one of the active compounds (DS9; an anthracene derivative) exhibits a very high structural similarity to compound DS11 (a phenathrene derivative) (inactive in *in vitro* tests),

a careful analysis of the binding of BM36 (a naphthalene derivative), DS9 (an anthracene derivative) and DS11 (a phenanthrene derivative) to MecR1 was performed. The docking studies revealed that these compounds bind in slightly different orientation modes and interact with different amino acids of MecR1. For each molecule, amino acids that interacted exclusively with one of these three compounds were identified (Figure 4.3.1.1).

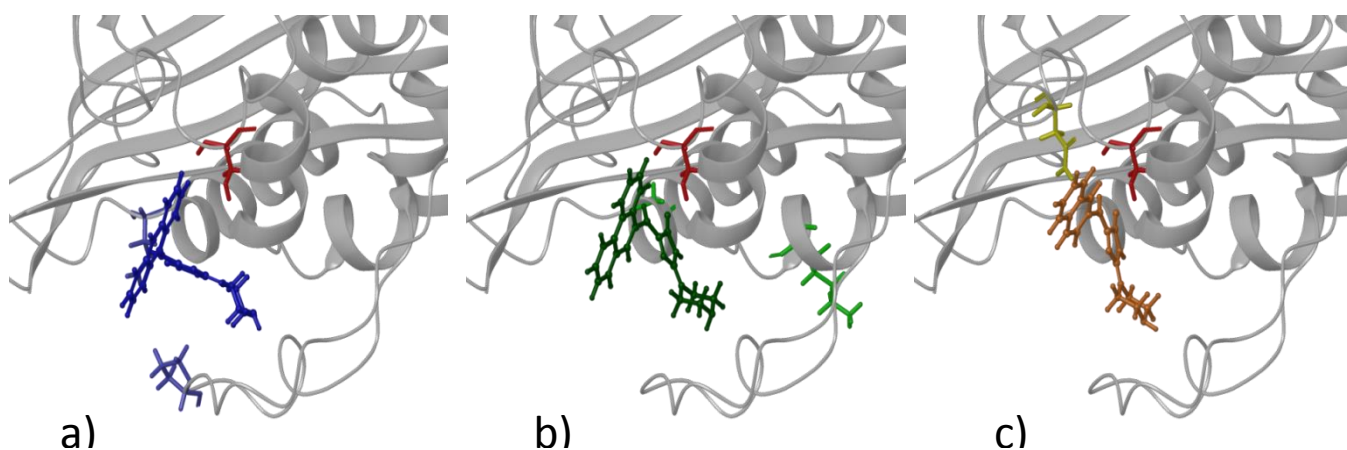


**Figure 4.3.1.1.** Interaction mode of **DS9** (a), **DS11** (b) and **BM36** (c) with MecR1 binding domain (complexes with the lowest docking score were selected). a) Amino acids that interact only with **DS9** (an anthracene derivative) are marked in blue; b) amino acids that interact only with **DS11** (a phenanthrene derivative) are marked in green; c) amino acids that interact only with **BM36** (a naphthalene derivative) are marked in yellow; Ser391 is marked in red.

As far as the antibiotics are concerned, docking studies were performed only for oxacillin and cloxacillin for two reasons. First of all, oxacillin and cloxacillin were the only antibiotics whose efficacy was substantially increased by the addition of some of the tested compounds (BM36, BM38, DS9, A2). Secondly, similar mechanism of action of both oxacillin and cloxacillin is closely connected with the PBP protein and differs from the mechanism of action of other antibiotics used in the *in vitro* studies. Docking results show that both oxacillin and cloxacillin fit into the binding site of MecR1 close to Ser391 (Fig. 4.3.1.2).

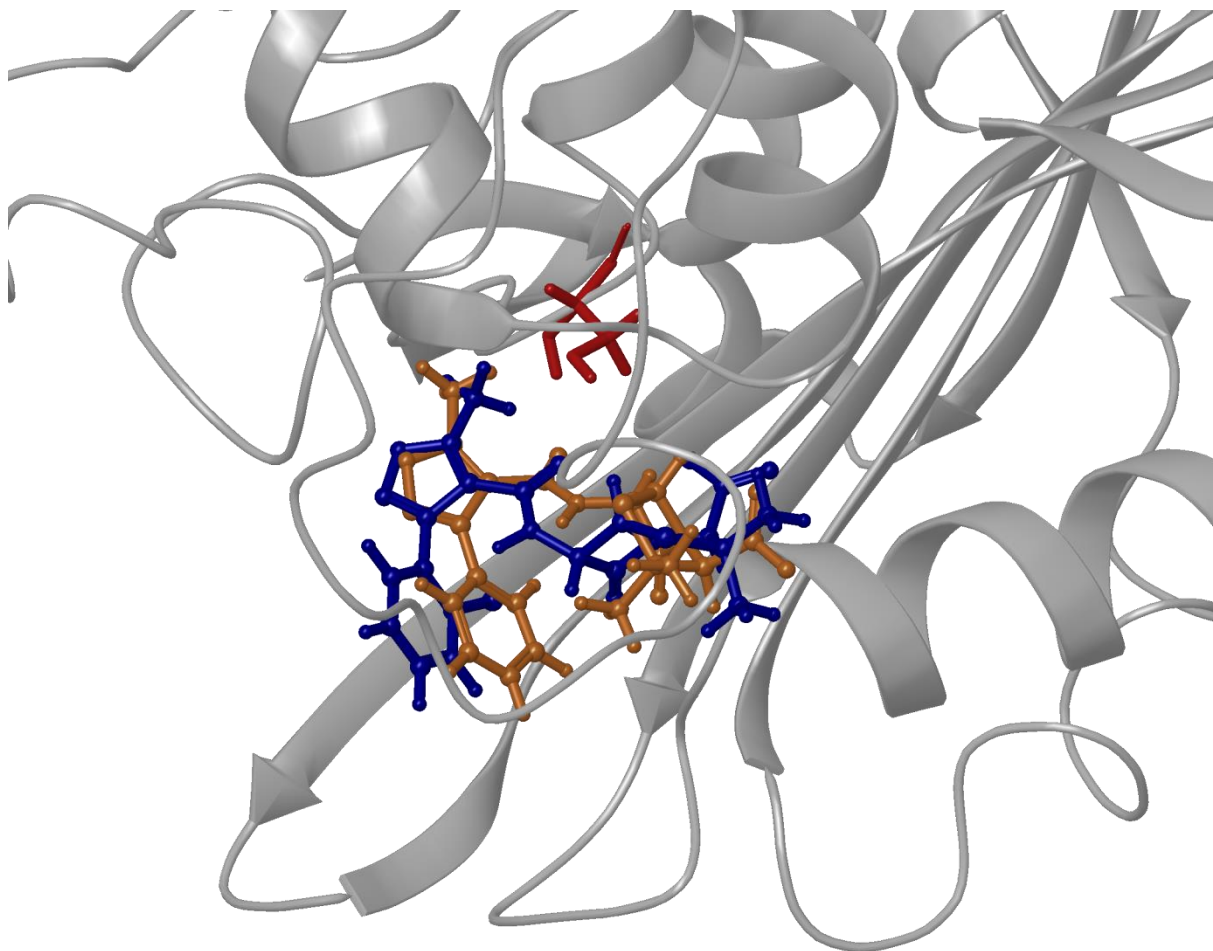


**Figure 4.3.1.2.** Visualisation of oxacillin (orange) and cloxacillin (blue) docking to MecR1 binding site.

The comparison of oxacillin binding mode to the binding mode of DS9 (an anthracene derivative) (Fig. 4.3.1.3A) and the binding mode of cloxacillin to the binding mode of BM36 (a naphthalene derivative) (Fig. 4.3.1.3B) revealed that in case of both pair compounds, the parts of the latter molecules that come into close proximity of Ser391 are parts of aromatic rings in contrast to free methyl groups and oxygen atoms from the ketone approaching Ser391 in the case of the antibiotic molecules.

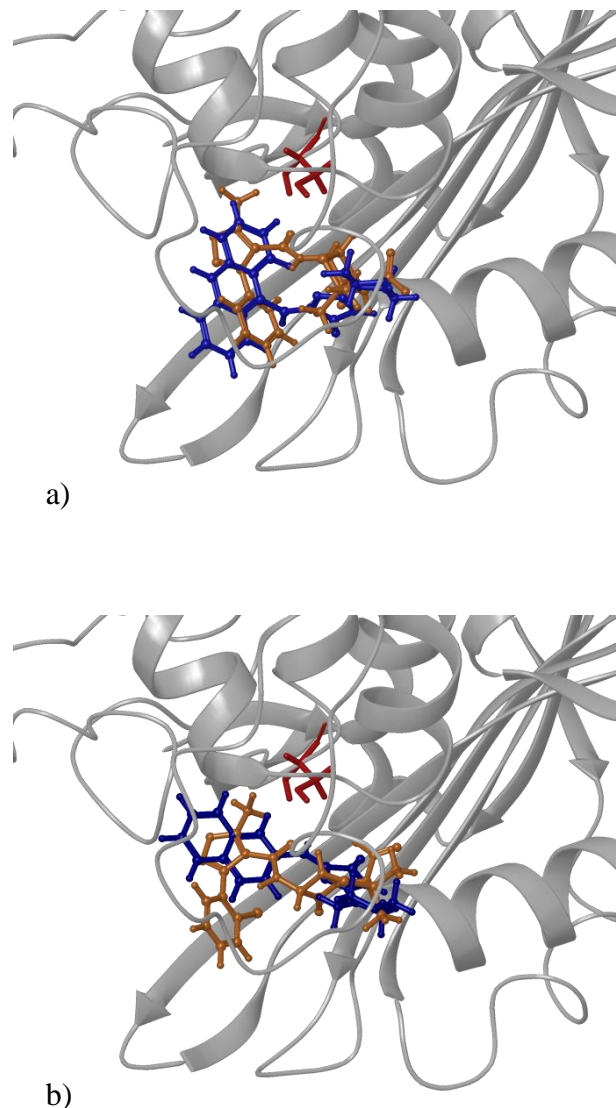


**Figure 4.3.1.3.** Comparison of docking results of oxacillin (orange) and **DS9** (an anthracene derivative) (blue) (a) and cloxacillin (orange) and **BM36** (a naphthalene derivative) (blue) (b) to MecR1. Ser391 is highlighted in red.

#### 4.3.2 Molecular Dynamics simulation

Next, with the use of molecular dynamic simulations, differences in ability to restore the antibiotic efficacy against the resistant *S. aureus* strain of the selected compounds were analyzed.

*In vitro* experiments showed that the compounds which managed to overcome antibiotic resistance to the greatest extent were BM36 (a naphthalene derivative) and DS9 (an anthracene derivative). They are structurally different from all compounds but one: DS11 (a

phenanthrene derivative). Therefore, these three compounds were selected for further evaluation in molecular dynamics studies. Due to extremely high similarity of the compounds DS9 (an anthracene derivative) and DS11 (a phenanthrene derivative), they were analyzed in detail.

The compounds DS9 (an anthracene derivative) and DS11 (a phenanthrene derivative) are similar in topology. Nevertheless, only DS9 enhances oxacillin antibacterial activity *in vitro*. Molecular dynamics simulation was performed for MecR1-DS9, MecR1-DS11 and MecR1-oxacillin (for comparison) complexes in order to reveal differences in interaction scheme of the compounds. All simulations were conducted under the same conditions, with the starting conformations of the compounds from their complexes with MecR1 of the lowest values of docking score. As conformations with the lowest values of docking score were slightly different for DS9 (an anthracene derivative) and DS11 (a phenanthrene derivative), additional simulation for compound DS11 was run with the starting conformation analogous to the one of the compound DS9.

During the entire simulations (20 ns), both compounds DS9 (an anthracene derivative) (Fig. 4.3.2.1) and BM36 (a naphthalene derivative) (Fig. 4.3.2.2) tend to stay in the entrance to the binding cavity of the MecR1 sensor domain, similar to oxacillin and cloxacillin which remain close to Ser391 (Figs. 4.3.2.1A and 4.3.2.2A). In contrast, compound DS11 (a phenanthrene derivative) leaves its initial position and locates nearby the cavity in experiments with the starting pose with the lowest value of docking score (Fig. 4.3.2.1B) or flips in a way that the moiety of condensed aromatic rings does not block the entrance to the binding cavity in experiments with the starting pose of DS11 (a phenanthrene derivative) being analogous to DS9 (an anthracene derivative) (Fig. 4.3.2.1C). Both oxacillin and cloxacillin stay in the proximity of the active site during the whole simulation (Figs. 4.3.2.1D and 4.3.2.2B).

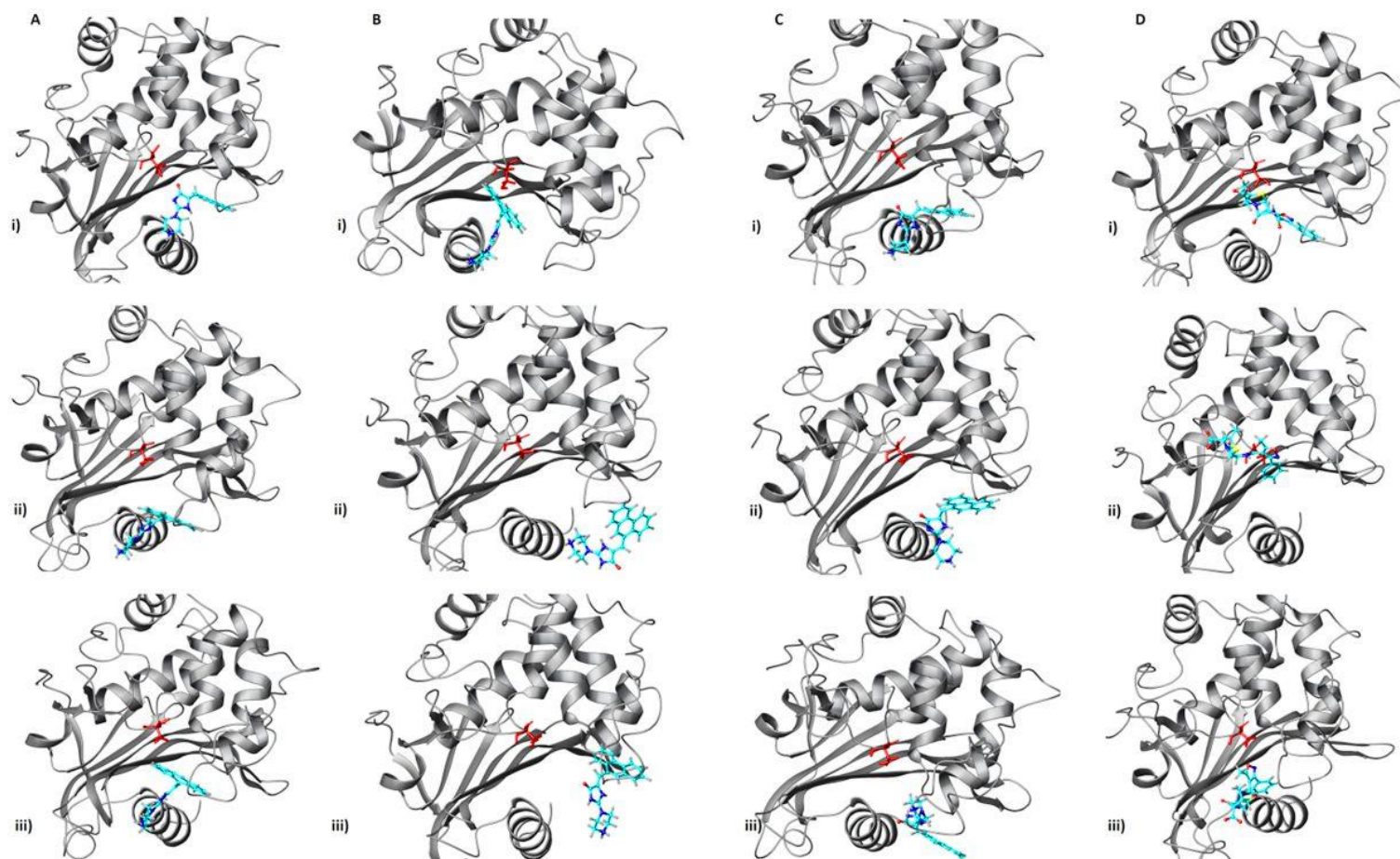


**Figure 4.3.2.1.** Snapshots of simulations of MecR1 and **DS9** (A), **DS11** (B, C) and oxacillin (D) from the first (i), central (ii) and last (iii) frames of MD simulations. B refers to studies with starting pose of **DS11** with the lowest docking score, C – to starting pose of **DS11** analogous to **DS9**. **DS9** (an anthracene derivative), **DS11** (a phenanthrene derivative) and oxacillin are marked in blue, Ser391 is marked in red.

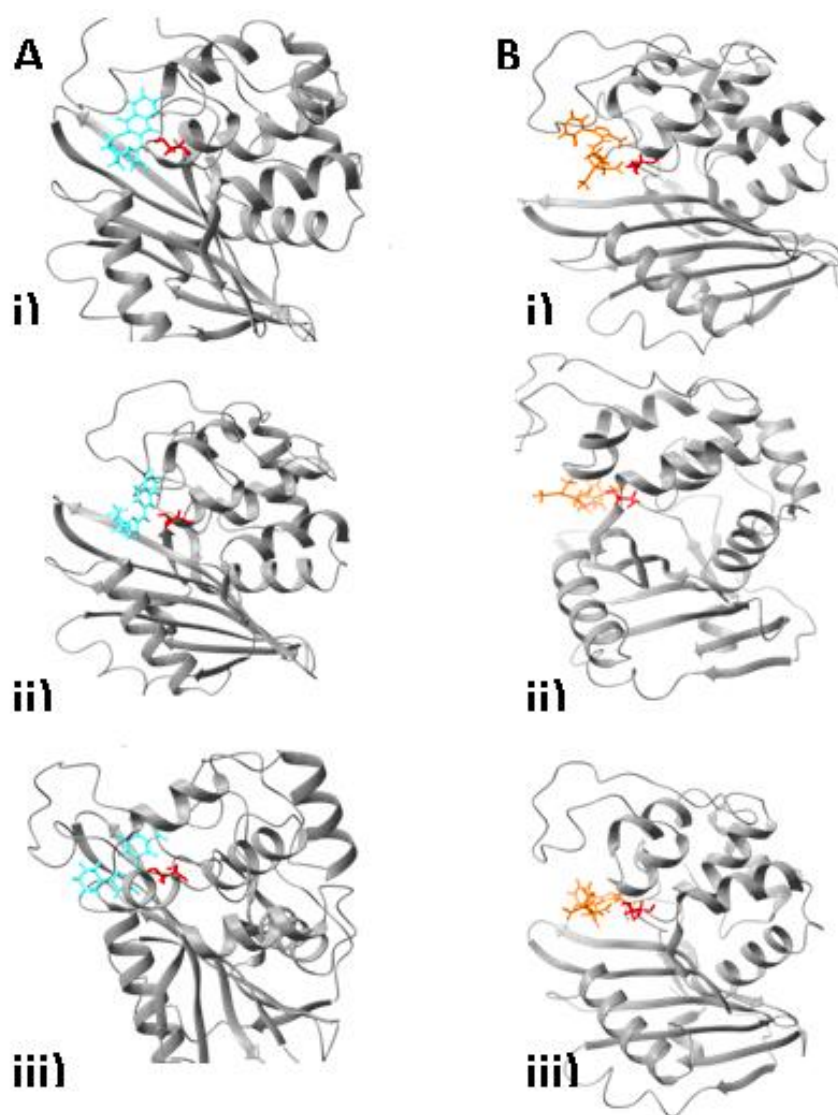


**Figure 4.3.2.2.** Snapshots of simulations of MecR1 and **BM36** (A) and cloxacillin (B) from the first (i), central (ii) and last (iii) frames of MD simulations. **BM36** (a naphthalene derivative) is marked in blue, cloxacillin is marked in yellow, Ser391 is marked in red.

On the basis of the molecular modeling studies, it may be postulated that the mechanism of action of BM36 (a naphthalene derivative) and DS9 (an anthracene derivative) is connected with the MecR1 protein. Docking results show that BM36 and DS9 are likely to bind in the region of entrance to the MecR1 active site. Thus, it can be suggested that they prevent antibiotics from binding to the active site of MecR1.

## 4.4. Toxicity assays

### 4.4.1. *In-silico* toxicity prediction

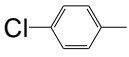
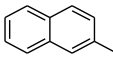
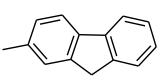
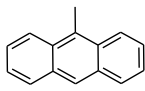
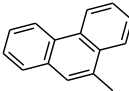
The results of toxicity predicted *in-silico* using a free online tool Molecular Property Explorer for all compounds tested against bacteria are presented in the tables 4.4.1.1 – 4.4.1.6.

Green colour denotes low risk of a given type of toxicity.

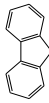
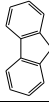
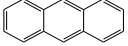
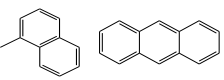
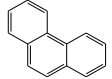
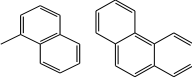
Yellow colour denotes medium risk of a given type of toxicity.

Red colour denotes high risk of a given type of toxicity.

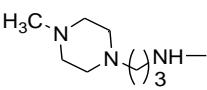
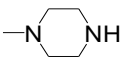
**Table 4.4.1.1.** *In silico* toxicity prediction: 2-piperazine derivatives of 5-arylidenimidazolone

Substituents	Name	mutagenicity	tumorigenicity	teratogenicity	drug score
Ar					
	BM7b	Green	Green	Green	0.89
	BM33	Green	Green	Green	0.93
	BM34	Green	Green	Green	0.94
	BM36	Green	Green	Green	0.79
	BM38	Red	Red	Green	0.24
	DS9	Red	Red	Green	0.12
	DS11	Yellow	Red	Green	0.28

**Table 4.4.1.2.** Substructures responsible for toxicity

Compound	Toxicity	Substructure
BM38	mutagenicity	
	tumorigenicity	
DS9	mutagenicity	
	tumorigenicity	
DS11	mutagenicity	
	tumorigenicity	

**Table 4.4.1.3.** *In silico* toxicity prediction: amine derivatives of 5-arylidenehydantoin

Substituents			Name	mutagenicity	tumorigenicity	teratogenicity	drug score
R	R <sup>1</sup>	amine					
H	2-OCH <sub>3</sub>		<b>A2</b>				0.84
OH	2,4-diCl		<b>A18</b>				0.88

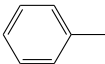
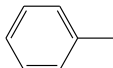
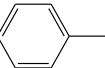
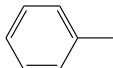
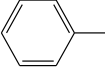
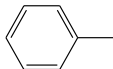
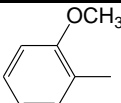
**Table 4.4.1.4.** *In silico* toxicity prediction: amine derivatives of 5-naphthalen-5-methylhydantoin

Substituents			Name	mutagenicity	tumorigenicity	teratogenicity	drug score
n							
1			JM1				0.5
2			JM2				0.48
3			JM3				0.44

**Table 4.4.1.5.** Substructures responsible for toxicity

Compound	Toxicity	Substructure
JM1, JM2, JM3	tumorigenicity	

**Table 4.4.1.6.** *In silico* toxicity prediction: N-1 arylpiperazine derivatives of 5-phenylhydantoin

Substituents			Name	mutagenicity	tumorigenicity	teratogenicity	drug score
R	R <sup>1</sup>	n					
CH <sub>3</sub>		1	DK1				0.74
CH <sub>3</sub>		1	DK7				0.7
		2	GG4				0.54
		4	BG1				0.39
		6	BG6				0.27

#### 4.4.2. Proliferation assay

The most promising compounds active against resistant bacterial strains were tested for their anti-proliferative properties against mammalian HEK293 cells in order to check how cytotoxic the compounds are. The compounds belonged to two groups: 2-piperazine derivatives of 5-arylideneimidazolone and N-1 arylpiperazine derivatives of 5-phenylhydantoin.

In the graphs and tables below (Figures 4.4.2.1A – 4.4.2.1C, 4.4.2.2A, Tables 4.4.2, 4.4.2.1A–4.4.2.1C, 4.4.2.2A), values represent the mean of n= 4 experiments. [M] (x axis) stands for molar concentration. Viability (y axis) denotes cell viability (% of control i.e. untreated cells). Doxorubicin is a positive control.

The anti-proliferative effect of doxorubicin is shown in each graph for comparison and in the Table 4.4.2.

**Table 4.4.2.** Anti-proliferative effect of doxorubicin

doxorubicin concentration [μM]	doxorubicin concentration [M]	log [M]	% viability	
			mean	SD
0.005	0.000000005	-8.3	96.02	9.04
0.01	0.00000001	-8	96.66	4.45
0.1	0.0000001	-7	98.78	1.04
0.5	0.0000005	-6.3	63.44	3.07
1	0.000001	-6	38.63	3.33
10	0.00001	-5	30.50	2.32
50	0.00005	-4.3	27.22	3.11
100	0.0001	-4	25.10	0.77

##### 4.4.2.1 Anti-proliferative properties of 2-piperazine derivatives of 5-arylideneimidazolone

The anti-proliferative effect of **BM36** (the most active compound: 128-fold oxacillin activity gain against *S. aureus* HEMSA 5 and 256-fold cloxacillin activity gain against *S. aureus* HEMSA 5) is presented in Fig. 4.4.2.1A and in the Table 4.4.2.1A. The compound was tested in the following micromolar concentrations: 0.1, 1, 10, 50 and 100 μM.

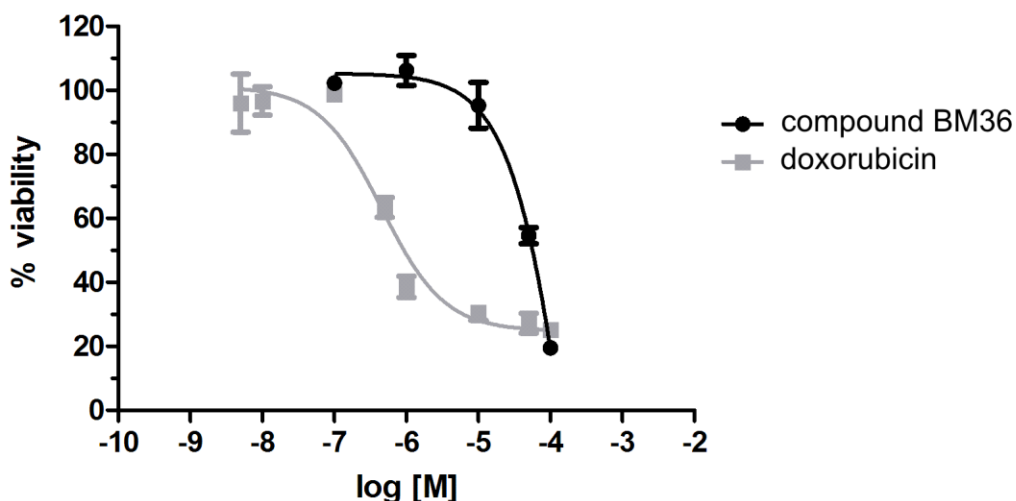


**Figure 4.4.2.1A.** Anti-proliferative effect of compound BM36

**Table 4.4.2.1A** Anti-proliferative effect of compound BM36

BM36 concentration [μM]	BM36 concentration [M]	log [M]	% viability	
			mean	SD
0.1	0.0000001	-7	102.23	1.78
1	0.000001	-6	106.20	4.67
10	0.00001	-5	95.27	7.16
50	0.00005	-4.3	54.63	2.55
100	0.0001	-4	19.51	0.34

At lower concentrations, **BM36** was less toxic than doxorubicin, but unfortunately at 100 μM (concentration active in microbiological tests: 125 μM) the viability of the cells was lower than in case of doxorubicin.

The anti-proliferative effect of **DS9** (64-fold oxacillin activity gain against *S. aureus* HEMSA 5) is presented in Fig. 4.4.2.1B and Table 4.4.2.1B. The compound was tested in the following micromolar concentrations: 0.01, 0.1, 0.5, 1, 5, 10, 50, 100, 125 and 250 μM.

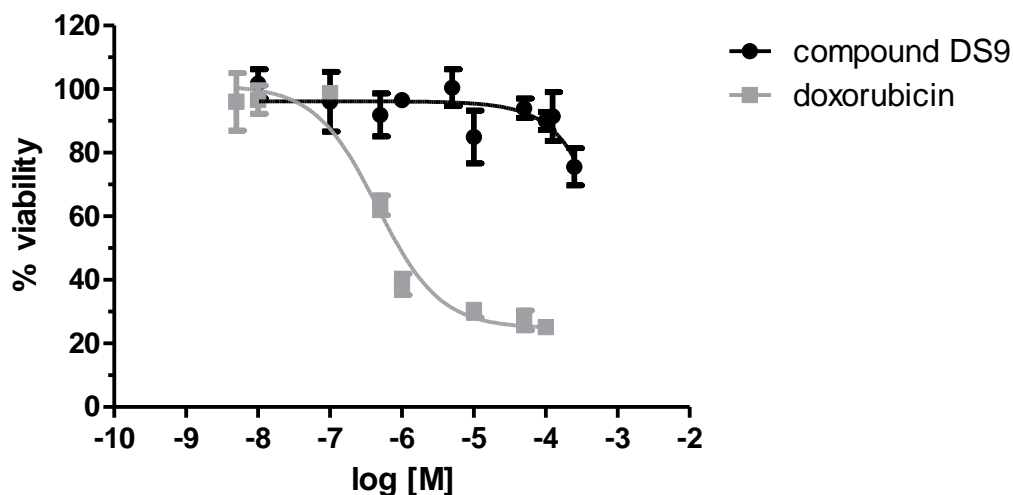


**Figure 4.4.2.1B.** Anti-proliferative effect of compound DS9

**Table 4.4.2.1B** Anti-proliferative effect of compound DS9

DS9 concentration [μM]	DS9 concentration [M]	log [M]	% viability	
			mean	SD
0.01	0.00000001	-8	101.70	4.51
0.1	0.0000001	-7	96.04	9.42
0.5	0.0000005	-6.3	91.88	6.75
1	0.000001	-6	96.56	0.49
5	0.000005	-5.3	100.45	5.84
10	0.00001	-5	84.97	8.31
50	0.00005	-4.3	94.00	3.07
100	0.0001	-4	90.02	2.88
125	0.000125	-3.9	91.40	7.67
250	0.00025	-3.6	75.60	5.86

Compound DS9 did not exert any significant anti-proliferative effect against HEK-293 cell line: the viability of the cells exposed to its 125 μM concentration (active against MRSA) was 91% ± 7.67% (versus 25.5% for doxorubicin; IC50 of doxorubicin: 0.458 μM). This makes compound DS9 a drug-like one and a good candidate for further pre-clinical tests.

The anti-proliferative effect of **BM38** (8-fold cloxacillin activity gain against *S. aureus* HEMSA 5) is presented in Fig. 4.4.2.1C and Table 4.4.2.1C. The compound was tested in the following micromolar concentrations: 0.01, 0.1, 0.5, 1, 5, 7.8, 10, 50, 100 and 250 μM.

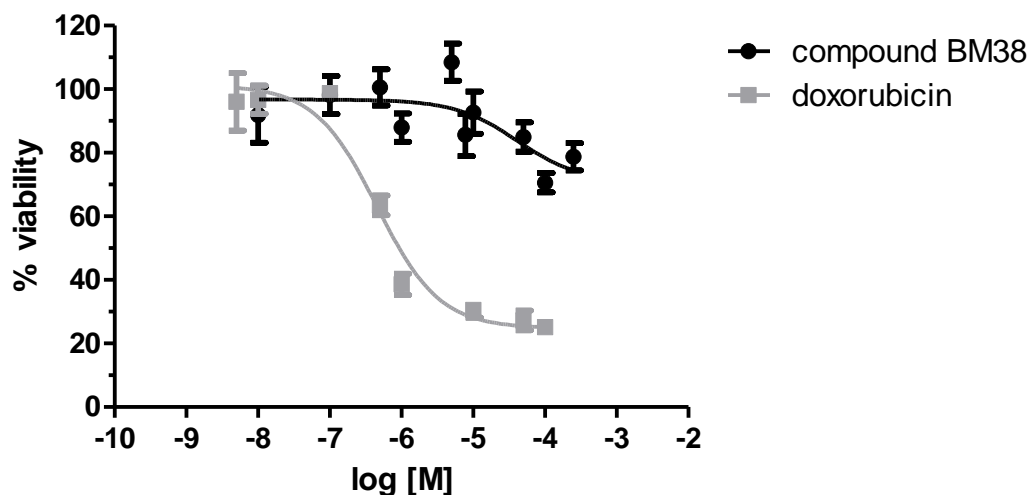


**Figure 4.4.2.1C.** Anti-proliferative effect of compound BM38

**Table 4.4.2.1C** Anti-proliferative effect of compound BM38

BM38 concentration [ $\mu$ M]	BM38 concentration [M]	log [M]	% viability	
			mean	SD
0.01	0.00000001	-8	91.89	8.77
0.1	0.0000001	-7	98.15	5.97
0.5	0.0000005	-6.3	100.54	5.70
1	0.000001	-6	87.92	4.44
5	0.000005	-5.3	108.46	5.85
10	0.00001	-5	85.60	6.61
50	0.00005	-4.3	92.60	6.61
100	0.0001	-4	84.96	4.60
125	0.000125	-3.9	70.58	3.03
250	0.00025	-3.6	78.75	4.35

The compound was active against MRSA in a quite low concentration (7.8  $\mu$ M). At this concentration, the viability of the cells was 85.6%  $\pm$  6.6% (versus 25.5% for doxorubicin; IC50 of doxorubicin: 0.458  $\mu$ M). It is also worth noting that at higher concentrations compound BM38 was much less toxic than doxorubicin too.

#### 4.4.2.2. Anti-proliferative properties of N-1 arylpiperazine derivatives of 5-phenylhydantoin

The anti-proliferative effect of compound BG1 (8-fold oxacillin activity gain against *S. aureus* HEMSA 5) is presented in Fig. 4.4.2.2A and Table 4.4.2.2A below. The compound was tested in the following micromolar concentrations: 0.01, 0.1, 0.5, 1, 5, 10, 50, 100, 125 and 250  $\mu\text{M}$ .

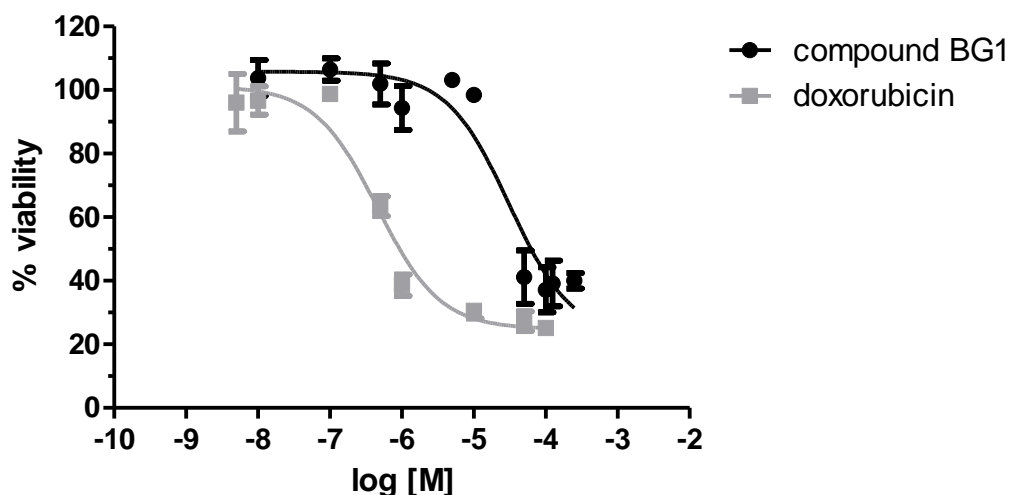


Figure 4.4.2.2A. Anti-proliferative effect of compound BG1

Table 4.4.2.2A Anti-proliferative effect of compound BG1

BG1 concentration [ $\mu\text{M}$ ]	BG1 concentration [M]	log [M]	% viability	
			mean	SD
0.01	0.00000001	-8	103.79	5.61
0.1	0.0000001	-7	106.46	3.46
0.5	0.0000005	-6.3	101.91	6.42
1	0.000001	-6	94.32	6.88
5	0.000005	-5.3	103.12	0.39
10	0.00001	-5	98.40	2.15
50	0.00005	-4.3	41.17	8.42
100	0.0001	-4	37.15	7.11
125	0.000125	-3.9	39.14	7.23
250	0.00025	-3.6	40.00	2.45

Compound BG1 proved to be quite toxic: the viability of the cells exposed to its 125  $\mu\text{M}$  concentration (active against MRSA) was  $39\% \pm 7.23\%$  (versus 25.5% for doxorubicin). The  $\text{IC}_{50}$  of BG1 is 31.24  $\mu\text{M}$  versus 0.458  $\mu\text{M}$  for doxorubicin.

# 5. Structure activity relationship – summary

---

The aim of this PhD dissertation was to test selected compounds synthesized in the Department of Technology and Biotechnology of Drugs of the Jagiellonian University Medical College against bacteria and cancer cells.

As far as bacteria are concerned, my research aimed to:

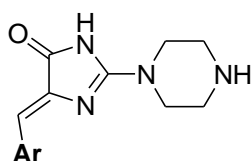
- determine direct antibacterial activity of selected hydantoin derivatives synthesized in the Department of Technology and Biotechnology of Drugs against *S. aureus* and *E. coli* strains
- determine ability of the compounds to increase/restore efficacy of selected antibiotics

For the active compounds, the research aimed to:

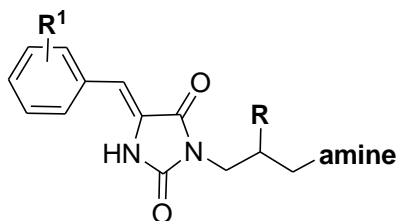
- determine their mechanism of action
- check their toxicity

Hydantoin derivatives selected for testing belonged to four groups:

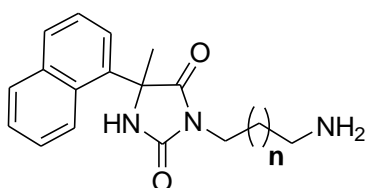
- 2-piperazine derivatives of 5-arylideneimidazolone



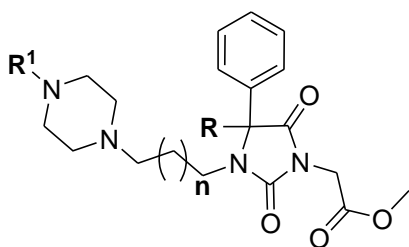
- amine derivatives of 5-arylidenehydantoin



- amine derivatives of 5-naphthalen-5-methylhydantoin



- N-1 arylpiperazine derivatives of 5-phenylhydantoin



As far as **2-piperazine derivatives of 5-arylideneimidazolone** are concerned (structures presented on page 36), only two compounds with relatively large substituents compared to other compounds in this group were active. The most active compound was **BM36** with the 2-naphthalene substituent. It increased cloxacillin activity 256-fold and oxacillin activity 128-fold. The other active compound in this group was **DS9** with the anthracene substituent which increased oxacillin efficacy 64-fold and cloxacillin efficacy 8-fold (results and structures presented in Tables 4.2.2.1A and 4.2.3.1A).

**BM38** with the 2-fluorene substituent caused an 8-fold increase in cloxacillin activity, but had no effect on oxacillin activity (Tables 4.2.2.1A and 4.2.3.1A). **DS11** with a phenanthrene substituent had no effect on the efficacy of none of the tested antibiotics. Likewise, compounds with smaller substituents such as p-chlorophenyl, 2-thiophenyl, 3-thiophenyl (**BM7b**, **BM33**, **BM34**, respectively) did not have any effect on the efficacy of the tested antibiotics either (Table 4.2.7).

Based on molecular modeling studies, it seems that both **BM36** (a naphthalene derivative) and **DS9** (an anthracene derivative) do not interact with residues from the binding site of PBP2a, and therefore the mechanism of their action through this protein is less probable than interaction with MecR1. Docking shows that oxacillin and cloxacillin are very likely to interact with Ser391 of MecR1 (Fig. 4.3.1.2), which has also been proven experimentally previously by other authors [179] and which in turn supports the reliability of docking results. The comparison of the binding modes of **DS9** (an anthracene derivative) and **DS11** (a phenanthrene derivative) reveals differences in their interaction with MecR1. Compound **DS9** (an anthracene derivative) is more likely to bind in the region of entrance to the binding site, while **DS11** (a phenanthrene derivative) locates in the upper part of the cavity, leaving free space in the binding pocket and allowing oxacillin to bind. This may be the reason why **DS9** (an anthracene derivative) is more effective, as it completely blocks the entrance to binding site for oxacillin. This hypothesis of the steric effect being the reason of activity of **BM36** (a naphthalene derivative) and **DS9** (an anthracene derivative) was also supported by molecular

dynamic simulations - **BM36** and **DS9** stay in the entrance to the binding cavity during the whole simulation, preventing oxacillin or cloxacillin from coming into the close proximity of Ser391 and activating MecR1 (Fig. 4.3.2.1A, Fig. 4.3.2.2A). On the other hand, compound **DS11** (a phenanthrene derivative) moves from its initial position and leaves space for oxacillin to interact with the active site of this protein and thus induce the synthesis of PBP2a with lowered affinity to  $\beta$ -lactam antibiotics (when simulations taking the pose with the lowest docking score were carried out) or flips in a way that aromatic rings are no longer preventing oxacillin from interaction with the active site (which was proved in simulations started from the pose of **DS11** (a phenanthrene derivative) analogous to **DS9** (an anthracene derivative)) (Fig. 4.3.2.1B, Fig. 4.3.2.1C).

**DS9** did not exert any significant anti-proliferative effect against HEK-293 cell line which makes it a drug-like candidate (Fig.4.4.2.1).

In case of **amine derivatives of 5-arylidenehydantoin** (structures presented on page 37), compound **A2** with the methoxy group in the para position at the benzene ring, methylpiperazinepropylamine and unbranched propyl chain between hydantoin and amine turned out to be active against cloxacillin (8-fold reduction of the MIC of cloxacillin against the resistant *S. aureus* MRSA HEMSA 5 strain) (Table 4.2.3.1B). Neither **A2** nor **A18** with two chlorine atoms at the benzene ring, piperazine and 2-hydroxypropyl chain had any effect on oxacillin activity (Table 4.2.7).

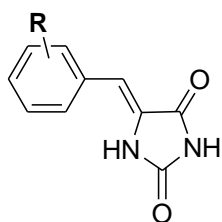
In the group of **amine derivatives of 5-naphthalen-5-methylhydantoin** (structures presented on page 38), 5-aryl substituent was naphthalene. The compounds differed with the length of the linker between hydantoin and amine. The effect of three types of linkers propyl, butyl, pentyl on the activity of the compounds was tested. Microbiological studies showed that no compound had any activity as 2-fold MIC reduction observed for **JM3** fits in the method's inaccuracy range (Table 4.2.7).

In the group of **N-1 arylpiperazine derivatives of 5-phenylhydantoin** (structures presented on page 39), the only compound that had any effect against the resistant strain was **BG1**. It reduced the MIC of oxacillin against *S. aureus* MRSA HEMSA 5 8-fold (Table 4.2.2.1D). The compound is a phenylpiperazine derivative of 5,5-diphenylhydantoin with a hexyl linker. Compound **GG4a**, which is a phenylpiperazine derivative of 5,5-diphenylhydantoin with a shorter 4-carbon linker, reduced the MIC of oxacillin of the reference *S. aureus* ATCC 25923

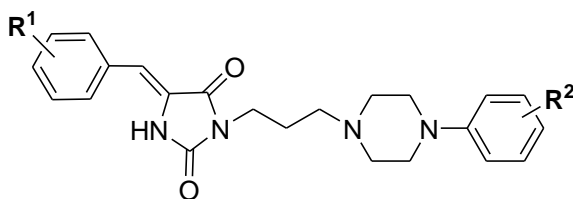
strain 8-fold (Table 4.2.2.2D). These two findings may suggest that phenylpiperazine moiety and butyl (**GG4**) or hexyl (**BG1**) linkers are more favorable for activity than methylpiperazine moiety and propyl linkers found in other compounds from this group. Efflux pumps inhibitors are recommended to have amphiphilic properties because they facilitate membrane transport. This may explain why **BG1** with a hexyl linker was more effective against the resistant *S. aureus* MRSA HEMSA 5 strain in combination with oxacillin than the compounds with shorter linkers. The results for **BG6** which proved to be ineffective do not confirm this hypothesis, but octyl linker in **BG6** may in turn be too long: it may make the compound roll up and prevent it from interacting with its target.

As far as cancer cells are concerned, my research aimed to test the ability of the hydantoin derivatives synthesized in our Department to inhibit an efflux pump, P-glycoprotein, in mouse lymphoma cells using EB accumulation assay. Hydantoin derivatives selected for testing belonged to four groups:

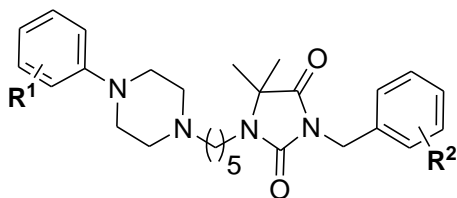
- arylidene hydantoin (N-unsubstituted)



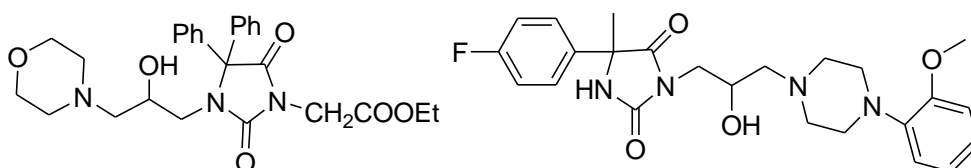
- arylidene hydantoin (N-3 phenylpiperazine derivatives)



- dimethylhydantoin (N-1 phenylpiperazine derivatives)



- other hydantoin derivatives



Arylidene hydantoins, especially phenylpiperazine derivatives, were the groups that showed the highest activity (Fig. 4.1.2).

As far as arylidene hydantoins (N-3 phenylpiperazine derivatives) (structures presented on page 42) are concerned, the compounds shared two common fragments: a benzylidene moiety linked with hydantoin and a phenylpiperazine moiety linked with hydantoin on the other side by means of a propyl linker. When it comes to R<sup>1</sup> substituent, the compounds differed in the location of chlorine either in *meta* or *para* position at the benzylidene moiety. R<sup>2</sup> substituent at the benzene ring of the phenylpiperazine moiety was either fluorine, chlorine or two chlorine atoms in different positions. The compounds from this group had comparable activity. However, the most active compounds (**R3** and **R5**) (Fig. 4.1.2, Table 4.1B) were the compounds with chlorine in the *para* position (R<sup>1</sup> substituent) and two chlorine atoms at the benzene ring of the phenylpiperazine moiety (R<sup>2</sup> substituent). This can be explained by slightly higher hydrophobic properties (recommended for P-gp inhibitors) of both aromatic ends within their structure. The compound **R2** (chlorine in *meta* position as R<sup>1</sup> substituent and two chlorine atoms as R<sup>2</sup> substituent) was slightly more active than **R6** (chlorine in *para* position as R<sup>1</sup> substituent and one chlorine atom as R<sup>2</sup> substituent). Compounds with fluorine as R<sup>2</sup> substituent (compounds **R1** and **R4**) had the lowest activity irrespective of the fact whether chlorine at the benzene ring of the benzylidene moiety (R<sup>1</sup> substituent) was located in the *para* or *meta* position (Fig. 4.2.7, Table 4.1B).

As far as **N-unsubstituted arylidene hydantoins** are concerned (structures presented on page 41), all the tested compounds shared a common fragment: a benzyloxy moiety linked with a benzylidene moiety that was in turn linked with hydantoin. The compounds differed with the number and location of the benzyloxy moiety in the *para/meta* position as well as presence/absence of chlorine atom(s) at the benzene ring of the benzyloxy group. It is worth emphasizing that the compound with two benzyloxy moieties (**HY115**) was distinctly more potent which may be due to its high hydrophobic properties. The fact whether benzyloxy moiety was located in the *para* or *meta* position did not make any difference in terms of activity as both **HY84** and **HY112** were equally active. Out of the compounds from this group, compounds with chlorine at the benzyloxy moiety (**HY83**, **HY111**, **HY110**; order of descending activity) had the lowest activity. The compound **HY83** was slightly less active than **HY84**, which suggests that not only does introduction of chlorine at the benzyloxy moiety not improve activity but even makes it worse. The least active compound was **HY110** with a chlorine atom in the *para* position of the benzyloxy moiety. It was less active than

**HY111** with two chlorine atoms at the benzyloxy moiety (Fig. 4.2.7, Table 4.1A). It is evident that chlorine has unfavorable impact, but it is difficult to determine its role based on these results.

**Dimethylhydantoins** (structures presented on page 42) shared two common fragments: a benzyl moiety and a phenylpiperazine moiety linked with dimethylhydantoin by means of a pentyl linker. R<sup>1</sup> substituent located at the phenyl group of the phenylpiperazine moiety was either a hydrogen atom, a methoxy group (in different positions), fluorine atom(s) in different positions or chlorine atom(s) in different positions.

The most active compounds were **PI2A** and **PI7A**. **PI2A** has methoxy group in *ortho* position at the benzene ring of the phenylpiperazine moiety. It may be assumed that this group is favorable for activity as **PI1A** without this group was less active. *Ortho* position of this group is more favourable for activity than *meta* position (compound **PI3A** with methoxy group in *ortho* position was less active) (Table 4.1C, Fig. 4.1.2).

The other most active compound was **PI7A** which has two fluorine atoms at the benzene ring of the phenylpiperazine moiety and a fluorine atom at the benzyl group. It seems that the location of fluorine in the *ortho* position is crucial for activity: the compounds **PI4A** with fluorine in the *ortho* position and hydrogen as substituent at the benzyl moiety as well as **PI6A** (two fluorine atoms in the *ortho* and *para* position at the benzene ring of the phenylpiperazine moiety and hydrogen as substituent at the benzyl moiety) also showed high activity. In contrast, **PI5A** with fluorine in the *para* position and hydrogen as substituent in the benzyl moiety as well as **PI8A** with fluorine in the *para* position and fluorine as substituent in the benzyl moiety were less active (Table 4.1C, Fig. 4.1.2). All the compounds with chlorine from this group (**PI9A**, **PI10A**, **PI11A**) had two chlorine atoms at the benzyl moiety. They differed with the number of chlorine atoms (1 or 2) and their positions at the benzene ring of the phenylpiperazine moiety. The compounds **PI9A** and **PI10A** with two chlorine atoms at the benzene ring of the phenylpiperazine moiety were the least active compounds in the whole group of dimethylhydantoins (Table 4.1C, Fig. 4.1.2).

Compounds from the group ‘other hydantoin derivatives’ (structures presented on page 43) were not active (Table 4.1D, Fig. 4.1.2).

The analysis of the results for P-gp reveals that the presence of chlorine is significant. However, its role is unclear: in some cases its impact is beneficial (arylidene hydantoins (N-3 phenylpiperazine derivatives)) and in others unfavorable (arylidene hydantoins N-unsubstituted).

# References

---

- [1] World Economic Forum 2013, Global Risks 2013, Eighth Edition
- [2] L.L. Silver, Challenges of Antibacterial Discovery, *Clin. Microbiol. Rev.* 24 (2011) 71–109.
- [3] S.S. Costa, M. Viveiros, L. Amaral, I. Couto, Multidrug efflux pumps in *Staphylococcus aureus*: an update., *Open Microbiol. J.* 7 (2013) 59–71.
- [4] M.A. Cooper, M.T. Fiorini, C. Abell, D.H. Williams, Binding of vancomycin group antibiotics to D-alanine and D-lactate presenting self-assembled monolayers., *Bioorg. Med. Chem.* 8 (2000) 2609–2616. <http://www.ncbi.nlm.nih.gov/pubmed/11092546> (accessed February 5, 2018).
- [5] G. Wright, Bacterial resistance to antibiotics: enzymatic degradation and modification, *Adv. Drug Deliv. Rev.* 57 (2005) 1451–1470.
- [6] K. Poole, Resistance to  $\beta$ -lactam antibiotics, *Cell. Mol. Life Sci.* 61 (2004) 2200–2223.
- [7] S. Garneau-Tsodikova, K.J. Labby, Mechanisms of resistance to aminoglycoside antibiotics: overview and perspectives., *Medchemcomm.* 7 (2016) 11–27.
- [8] M. Ceccarelli, P. Ruggerone, Physical insights into permeation of and resistance to antibiotics in bacteria, *Curr. Drug Targets.* 9 (2008) 779–788. <http://www.ncbi.nlm.nih.gov/pubmed/18781923> (accessed March 10, 2019).
- [9] T. Köhler, J.C. Pechère, P. Plésiat, Bacterial antibiotic efflux systems of medical importance., *Cell. Mol. Life Sci.* 56 (1999) 771–778. <http://www.ncbi.nlm.nih.gov/pubmed/11212337> (accessed March 12, 2019).
- [10] L. Amaral, A. Martins, G. Spengler, J. Molnar, Efflux pumps of Gram-negative bacteria: what they do, how they do it, with what and how to deal with them., *Front. Pharmacol.* 4 (2014) 168.
- [11] X.-Z. Li, H. Nikaido, Efflux-mediated drug resistance in bacteria: an update, *Drugs.* 69 (2009) 1555.
- [12] A. Jarmula, E. Oblak, D. Wawrzycka, J. Gutowicz, Efflux-mediated antimicrobial multidrug resistance, *Postepy Hig. Med. Dosw.* 65 (2011) 216–227.
- [13] A.M. Buckley, M.A. Webber, S. Cooles, L.P. Randall, R.M. La Ragione, M.J. Woodward, et al., The AcrAB-TolC efflux system of *Salmonella enterica* serovar *Typhimurium* plays a role in pathogenesis, *Cell. Microbiol.* 8 (2006) 847–856.
- [14] A. V Polkade, S.S. Mantri, U.J. Patwekar, K. Jangid, Quorum Sensing: An under-

- explored phenomenon in the phylum actinobacteria., *Front. Microbiol.* 7 (2016) 131.
- [15] J. Sun, Z. Deng, A. Yan, Bacterial multidrug efflux pumps: mechanisms, physiology and pharmacological exploitations, *Biochem. Biophys. Res. Commun.* 453 (2014) 254–267.
- [16] M. Kvist, V. Hancock, P. Klemm, Inactivation of efflux pumps abolishes bacterial biofilm formation., *Appl. Environ. Microbiol.* 74 (2008) 7376–7382.
- [17] S. Baugh, A.S. Ekanayaka, L.J. V. Piddock, M.A. Webber, Loss of or inhibition of all multidrug resistance efflux pumps of *Salmonella enterica* serovar *Typhimurium* results in impaired ability to form a biofilm, *J. Antimicrob. Chemother.* 67 (2012) 2409–2417.
- [18] E. Padilla, E. Llobet, A. Doménech-Sánchez, L. Martínez-Martínez, J.A. Bengoechea, S. Albertí, Klebsiella pneumoniae AcrAB efflux pump contributes to antimicrobial resistance and virulence., *Antimicrob. Agents Chemother.* 54 (2010) 177–183.
- [19] A. Pérez, M. Poza, A. Fernández, M. del C. Fernández, S. Mallo, M. Merino, et al., Involvement of the AcrAB-TolC efflux pump in the resistance, fitness, and virulence of *Enterobacter cloacae*., *Antimicrob. Agents Chemother.* 56 (2012) 2084–2090.
- [20] Y. Hirakata, R. Srikumar, K. Poole, N. Gotoh, T. Suematsu, S. Kohno, et al., Multidrug efflux systems play an important role in the invasiveness of *Pseudomonas aeruginosa*., *J. Exp. Med.* 196 (2002) 109–118. (accessed March 22, 2019).
- [21] B. Alberts, A. Johnson, J. Lewis, M. Raff, K. Roberts, P. Walter, Carrier proteins and active membrane transport, (2002). <https://www.ncbi.nlm.nih.gov/books/NBK26896/> (accessed March 12, 2019).
- [22] X. Li, Efflux-mediated drug resistance in bacteria, *Drugs.* (2004) 159–204.
- [23] M.I. Borges-Walmsley, K.S. McKeegan, A.R. Walmsley, Structure and function of efflux pumps that confer resistance to drugs, *Biochem. J.* 376 (2003) 313–338.
- [24] M.I. Borges-Walmsley, A.R. Walmsley, The structure and function of drug pumps, *Trends Microbiol.* (2001) 71–79.
- [25] M. Saidijam, G. Benedetti, Q. Ren, Z. Xu, C.J. Hoyle, S.L. Palmer, et al., Microbial drug efflux proteins of the major facilitator superfamily, *Curr. Drug Targets.* 7 (2006) 793–811.
- [26] P.N. Markham, A.A. Neyfakh, Efflux-mediated drug resistance in Gram-positive bacteria, *Curr. Opin. Microbiol.* 4 (2001) 509–514.
- [27] H. Omote, M. Hiasa, T. Matsumoto, M. Otsuka, Y. Moriyama, The MATE proteins as fundamental transporters of metabolic and xenobiotic organic cations, *Trends Pharmacol. Sci.* 27 (2006) 587–593.

- [28] C. Quiblier, A.S. Zinkernagel, R.A. Schuepbach, B. Berger-Bächi, M.M. Senn, Contribution of SecDF to *Staphylococcus aureus* resistance and expression of virulence factors., *BMC Microbiol.* 11 (2011) 72.
- [29] B.D. Schindler, G.W. Kaatz, Multidrug efflux pumps of Gram-positive bacteria, *Drug Resist. Updat.* 27 (2016) 1–13.
- [30] L. Yang, S. Lu, J. Belardinelli, E. Huc-Claustre, V. Jones, M. Jackson, et al., RND transporters protect *Corynebacterium glutamicum* from antibiotics by assembling the outer membrane., *Microbiologyopen.* 3 (2014) 484–496.
- [31] K. Poole, Efflux-mediated multiresistance in Gram-negative bacteria., *Clin. Microbiol. Infect.* 10 (2004) 12–26. <http://www.ncbi.nlm.nih.gov/pubmed/14706082> (accessed March 19, 2019).
- [32] F. Van Bambeke, E. Balzi, P.M. Tulkens, Antibiotic efflux pumps, *Biochem. Pharmacol.* 60 (2000) 457–470.
- [33] J. Lubelski, W.N. Konings, A.J. Driessen, Distribution and physiology of ABC-type transporters contributing to multidrug resistance in bacteria, *Microbiol. Mol. Biol. Rev.* 71 (2007) 463–476.
- [34] H.I. Zgurskaya, H. Nikaido, Multidrug resistance mechanisms: drug efflux across two membranes, *Mol. Microbiol.* 37 (2000) 219–225.
- [35] A. Moussatova, C. Kandt, M.L. O'Mara, D.P. Tieleman, ATP-binding cassette transporters in *Escherichia coli*, *Biochim. Biophys. Acta - Biomembr.* 1778 (2008) 1757–1771.
- [36] R. Edgar, E. Bibi, MdfA, an *Escherichia coli* multidrug resistance protein with an extraordinarily broad spectrum of drug recognition., *J. Bacteriol.* 179 (1997) 2274–2280. <http://www.ncbi.nlm.nih.gov/pubmed/9079913> (accessed March 25, 2019).
- [37] S. Mandal, S. Sarkar, A. Bhattacharyya, YnfA, An SMR family efflux pump is abundant in *Escherichia coli* isolates from urinary infection, *Indian J. Med. Microbiol.* 33 (2015) 139.
- [38] J.R. Guelfo, A. Rodríguez-Rojas, I. Matic, J. Blázquez, A MATE-family efflux pump rescues the *Escherichia coli* 8-oxoguanine-repair-deficient mutator phenotype and protects against H<sub>2</sub>O<sub>2</sub> killing., *PLoS Genet.* 6 (2010) e1000931.
- [39] D. Du, Z. Wang, N.R. James, J.E. Voss, E. Klimont, T. Ohene-Agyei, et al., Structure of the AcrAB-TolC multidrug efflux pump., *Nature.* 509 (2014) 512–515.
- [40] M. Shepherd, The CydDC ABC transporter of *Escherichia coli*: new roles for a reductant efflux pump, *Biochem. Soc. Trans.* 43 (2015) 908–912.

- [41] Z. Wang, G. Fan, C.F. Hryc, J.N. Blaza, I.I. Serysheva, M.F. Schmid, et al., An allosteric transport mechanism for the AcrAB-TolC multidrug efflux pump, *Elife*. 6 (2017).
- [42] E.C. Hobbs, X. Yin, B.J. Paul, J.L. Astarita, G. Storz, Conserved small protein associates with the multidrug efflux pump AcrB and differentially affects antibiotic resistance, *Proc. Natl. Acad. Sci.* 109 (2012) 16696–16701.
- [43] H. Okusu, D. Ma, H. Nikaido, AcrAB efflux pump plays a major role in the antibiotic resistance phenotype of *Escherichia coli* multiple-antibiotic-resistance (Mar) mutants., *J. Bacteriol.* 178 (1996) 306–308. <http://www.ncbi.nlm.nih.gov/pubmed/8550435> (accessed March 3, 2019).
- [44] M.A. Seeger, K. Diederichs, T. Eicher, L. Brandstätter, A. Schiefner, F. Verrey, et al., The AcrB efflux pump: conformational cycling and peristalsis lead to multidrug resistance., *Curr. Drug Targets.* 9 (2008) 729–749. <http://www.ncbi.nlm.nih.gov/pubmed/18781920> (accessed March 1, 2019).
- [45] S. Murakami, R. Nakashima, E. Yamashita, A. Yamaguchi, Crystal structure of bacterial multidrug efflux transporter AcrB, *Nature*. 419 (2002) 587–593.
- [46] Y. Takatsuka, C. Chen, H. Nikaido, Mechanism of recognition of compounds of diverse structures by the multidrug efflux pump AcrB of *Escherichia coli*, *Proc. Natl. Acad. Sci.* 107 (2010) 6559–6565.
- [47] N. Tsukagoshi, R. Aono, Entry into and release of solvents by *Escherichia coli* in an organic-aqueous two-liquid-phase system and substrate specificity of the AcrAB-TolC solvent-extruding pump., *J. Bacteriol.* 182 (2000) 4803–4810. <http://www.ncbi.nlm.nih.gov/pubmed/10940021> (accessed March 15, 2019).
- [48] Z. Pietras, V.N. Bavro, N. Furnham, M. Pellegrini-Calace, E.J. Milner-White, B.F. Luisi, Structure and mechanism of drug efflux machinery in Gram negative bacteria., *Curr. Drug Targets.* 9 (2008) 719–728. <http://www.ncbi.nlm.nih.gov/pubmed/18781919> (accessed March 3, 2019).
- [49] K.M. Pos, A. Schiefner, M.A. Seeger, K. Diederichs, Crystallographic analysis of AcrB, *FEBS Lett.* 564 (2004) 333–339.
- [50] K.M. Pos, Drug transport mechanism of the AcrB efflux pump, *Biochim. Biophys. Acta - Proteins Proteomics.* 1794 (2009) 782–793.
- [51] J.A. Bohnert, S. Schuster, E. Fährnich, R. Trittler, W. V Kern, Altered spectrum of multidrug resistance associated with a single point mutation in the *Escherichia coli* RND-type MDR efflux pump YhiV (MdtF)., *J. Antimicrob. Chemother.* 59 (2007)

- 1216–1222.
- [52] C.A. Elkins, H. Nikaido, Substrate specificity of the RND-type multidrug efflux pumps AcrB and AcrD of *Escherichia coli* is determined predominantly by two large periplasmic loops., *J. Bacteriol.* 184 (2002) 6490–6498.  
<http://www.ncbi.nlm.nih.gov/pubmed/12426336> (accessed March 3, 2019).
- [53] S. Murakami, R. Nakashima, E. Yamashita, T. Matsumoto, A. Yamaguchi, Crystal structures of a multidrug transporter reveal a functionally rotating mechanism., *Nature.* 443 (2006) 173–179.
- [54] J.A. Bohnert, S. Schuster, M.A. Seeger, E. Fahrnich, K.M. Pos, W. V. Kern, Site-directed mutagenesis reveals putative substrate binding residues in the *Escherichia coli* RND efflux pump AcrB, *J. Bacteriol.* 190 (2008) 8225–8229.
- [55] V. Koronakis, A. Sharff, E. Koronakis, B. Luisi, C. Hughes, Crystal structure of the bacterial membrane protein TolC central to multidrug efflux and protein export, *Nature.* 405 (2000) 914–919.
- [56] C. Andersen, C. Hughes, V. Koronakis, Protein export and drug efflux through bacterial channel-tunnels., *Curr. Opin. Cell Biol.* 13 (2001) 412–416.  
<http://www.ncbi.nlm.nih.gov/pubmed/11454445> (accessed March 3, 2018).
- [57] V. Koronakis, TolC--the bacterial exit duct for proteins and drugs., *FEBS Lett.* 555 (2003) 66–71. <http://www.ncbi.nlm.nih.gov/pubmed/14630321> (accessed March 3, 2019).
- [58] J.M. Pages, L. Amaral, S. Fanning, An original deal for new molecule: reversal of efflux pump activity, a rational strategy to combat gram-negative resistant bacteria, *Curr. Med. Chem.* 18 (2011) 2969–2980.
- [59] S. Michalet, G. Cartier, B. David, A.M. Mariotte, M.G. Dijoux-franca, G.W. Kaatz, et al., N-caffeoylphenalkylamide derivatives as bacterial efflux pump inhibitors, *Bioorg. Med. Chem. Lett.* 17 (2007) 1755–1758.
- [60] J.J. Vecchione, B. Alexander, J.K. Sello, J.K. Sello, Two distinct major facilitator superfamily drug efflux pumps mediate chloramphenicol resistance in *Streptomyces coelicolor*., *Antimicrob. Agents Chemother.* 53 (2009) 4673–4677.
- [61] O. Lomovskaya, M.S. Warren, A. Lee, J. Galazzo, R. Fronko, M. Lee, et al., Identification and characterization of inhibitors of multidrug resistance efflux pumps in *Pseudomonas aeruginosa*: novel agents for combination therapy., *Antimicrob. Agents Chemother.* 45 (2001) 105–116.
- [62] O. Lomovskaya, H.I. Zgurskaya, M. Totrov, W.J. Watkins, Waltzing transporters and

- “the dance macabre” between humans and bacteria, *Nat. Rev. Discov.* 6 (2007) 56–65.
- [63] T.E. Renau, R. Léger, L. Filonova, E.M. Flamme, M. Wang, R. Yen, et al., Conformationally-restricted analogues of efflux pump inhibitors that potentiate the activity of levofloxacin in *Pseudomonas aeruginosa*., *Bioorg. Med. Chem. Lett.* 13 (2003) 2755–2758. <http://www.ncbi.nlm.nih.gov/pubmed/12873508> (accessed March 16, 2019).
- [64] Mpex, <https://www.fiercebiotech.com/biotech/glaxosmithkline-and-mpex-pharmaceuticals-form-alliance-to-develop-novel-efflux-pump> (accessed March 17, 2019).
- [65] J. Chevalier, S. Atifi, A. Eyraud, A. Mahamoud, J. Barbe, J.M. Pagès, New pyridoquinoline derivatives as potential inhibitors of the fluoroquinolone efflux pump in resistant *Enterobacter aerogenes* strains., *J. Med. Chem.* 44 (2001) 4023–4026. <http://www.ncbi.nlm.nih.gov/pubmed/11689091> (accessed March 17, 2019).
- [66] S. Gallo, J. Chevalier, A. Mahamoud, A. Eyraud, J.-M. Pagès, J. Barbe, 4-alkoxy and 4-thioalkoxyquinoline derivatives as chemosensitizers for the chloramphenicol-resistant clinical *Enterobacter aerogenes* 27 strain., *Int. J. Antimicrob. Agents.* 22 (2003) 270–273. <http://www.ncbi.nlm.nih.gov/pubmed/13678833> (accessed March 17, 2019).
- [67] M. Malléa, A. Mahamoud, J. Chevalier, S. Alibert-Franco, P. Brouant, J. Barbe, *et al.*, Alkylaminoquinolines inhibit the bacterial antibiotic efflux pump in multidrug-resistant clinical isolates, *Biochem. J.* 376 (2003) 801–805.
- [68] J. Chevalier, J. Bredin, A. Mahamoud, M. Malléa, J. Barbe, J.-M. Pagès, Inhibitors of antibiotic efflux in resistant *Enterobacter aerogenes* and *Klebsiella pneumoniae* strains., *Antimicrob. Agents Chemother.* 48 (2004) 1043–1046. <http://www.ncbi.nlm.nih.gov/pubmed/14982806> (accessed March 17, 2019).
- [69] J.A. Bohnert, W. V Kern, Selected arylpiperazines are capable of reversing multidrug resistance in *Escherichia coli* overexpressing RND efflux pumps., *Antimicrob. Agents Chemother.* 49 (2005) 849–852.
- [70] W. V. Kern, P. Steinke, A. Schumacher, S. Schuster, H. von Baum, J.A. Bohnert, Effect of 1-(1-naphthylmethyl)-piperazine, a novel putative efflux pump inhibitor, on antimicrobial drug susceptibility in clinical isolates of *Escherichia coli*, *J. Antimicrob. Chemother.* 57 (2006) 339–343.
- [71] G.W. Kaatz, V. V Moudgal, S.M. Seo, J.B. Hansen, J.E. Kristiansen, Phenylpiperidine selective serotonin reuptake inhibitors interfere with multidrug efflux pump activity in

- Staphylococcus aureus.*, Int. J. Antimicrob. Agents. 22 (2003) 254–261.  
<http://www.ncbi.nlm.nih.gov/pubmed/13678830> (accessed March 17, 2019).
- [72] M. Martins, S.G. Dastidar, S. Fanning, J.E. Kristiansen, J. Molnar, J.M. Pages, et al., Potential role of non-antibiotics (helper compounds) in the treatment of multidrug-resistant Gram-negative infections: mechanisms for their direct and indirect activities, Int. J. Antimicrob. Agents. 31 (2008) 198–208.
- [73] M. Pieroni, D. Machado, E. Azzali, S. Santos Costa, I. Couto, G. Costantino, et al., Rational design and synthesis of thioridazine analogues as enhancers of the antituberculosis therapy, J. Med. Chem. 58 (2015) 5842–5853.
- [74] L. Amaral, M. Martins, M. Viveiros, J. Molnar, J.E. Kristiansen, Promising therapy of XDR-TB/MDR-TB with thioridazine an inhibitor of bacterial efflux pumps., Curr. Drug Targets. 9 (2008) 816–819. <http://www.ncbi.nlm.nih.gov/pubmed/18781927> (accessed March 5, 2019).
- [75] T. Coelho, D. Machado, I. Couto, R. Maschmann, D. Ramos, A. von Groll, et al., Enhancement of antibiotic activity by efflux inhibitors against multidrug resistant *Mycobacterium tuberculosis* clinical isolates from Brazil, Front. Microbiol. 6 (2015) 330.
- [76] I.M. Gould, Antibiotic resistance: the perfect storm, Int. J. Antimicrob. Agents. 34 Suppl 3 (2009) S2-5.
- [77] C.C.S. Fuda, J.F. Fisher, S. Mobashery,  $\beta$ -lactam resistance in *Staphylococcus aureus*: the adaptive resistance of a plastic genome., Cell. Mol. Life Sci. 62 (2005) 2617–2633.
- [78] P. Macheboeuf, C. Contreras-Martel, V. Job, O. Dideberg, A. Dessen, Penicillin binding proteins: key players in bacterial cell cycle and drug resistance processes, FEMS Microbiol. Rev. 30 (2006) 673–691.
- [79] A.C. Shore, D.C. Coleman, Staphylococcal cassette chromosome mec: recent advances and new insights, Int. J. Med. Microbiol. (2013).
- [80] J. Handzlik, A. Matys, K. Kieć-Kononowicz, Recent advances in multi-drug resistance (MDR) efflux pump inhibitors of Gram-positive bacteria *S. aureus*, Antibiotics. 2(1) (2013) 28–45.
- [81] I.A. Cree, P. Charlton, Molecular chess? Hallmarks of anti-cancer drug resistance., BMC Cancer. 17 (2017) 10.
- [82] G. Khamisipour, F. Jadidi-Niaragh, A.S. Jahromi, K. zandi, M. Hojjat-Farsangi, Mechanisms of tumor cell resistance to the current targeted-therapy agents, Tumor Biol. 37 (2016) 10021–10039.

- [83] V. Nogales, W.C. Reinhold, S. Varma, A. Martinez-Cardus, C. Moutinho, S. Moran, et al., Epigenetic inactivation of the putative DNA/RNA helicase SLFN11 in human cancer confers resistance to platinum drugs., *Oncotarget*. 7 (2016) 3084–3097.
- [84] H. Zahreddine, K.L.B. Borden, Mechanisms and insights into drug resistance in cancer, *Front. Pharmacol.* 4 (2013) 28.
- [85] G. Housman, S. Byler, S. Heerboth, K. Lapinska, M. Longacre, N. Snyder, et al., Drug resistance in cancer: an overview, *Cancers (Basel)*. 6 (2014) 1769–1792.
- [86] C.C. Ogu, J.L. Maxa, Drug interactions due to cytochrome P450., *Proc. (Bayl. Univ. Med. Cent)*. 13 (2000) 421–3. <http://www.ncbi.nlm.nih.gov/pubmed/16389357> (accessed March 20, 2019).
- [87] M. Michael, M.M. Doherty, Tumoral drug metabolism: overview and its implications for cancer therapy., *J. Clin. Oncol.* 23 (2005) 205–229.
- [88] K.T. Douglas, Mechanism of action of glutathione-dependent enzymes., *Adv. Enzymol. Relat. Areas Mol. Biol.* 59 (1987) 103–167. <http://www.ncbi.nlm.nih.gov/pubmed/2880477> (accessed July 22, 2017).
- [89] A. Oakley, Glutathione transferases: a structural perspective, *Drug Metab. Rev.* 43 (2011) 138–151.
- [90] M. Li, M.M. Ittmann, D.R. Rowley, A.A. Knowlton, A.K. Vaid, D.E. Epner, Glutathione S-transferase pi is upregulated in the stromal compartment of hormone independent prostate cancer, *Prostate*. 56 (2003) 98–105.
- [91] S.-T. Chuang, P. Chu, J. Sugimura, M.S. Tretiakova, V. Papavero, K. Wang, *et al.*, Overexpression of glutathione S-transferase  $\alpha$  in clear cell renal cell carcinoma, *Am J Clin Pathol.* 123 (2005) 421–429.
- [92] C.C. Chao, Y.T. Huang, C.M. Ma, W.Y. Chou, S. Lin-Chao, Overexpression of glutathione S-transferase and elevation of thiol pools in a multidrug-resistant human colon cancer cell line., *Mol. Pharmacol.* 41 (1992). <http://molpharm.aspetjournals.org/content/41/1/69> (accessed March 26, 2019).
- [93] F. Su, X. Hu, W. Jia, C. Gong, E. Song, P. Hamar, Glutathione S-transferase indicates chemotherapy resistance in breast cancer, doi:10.1016/S0022-4804(03)00200-2.
- [94] S. Elmore, Apoptosis: a review of programmed cell death., *Toxicol. Pathol.* 35 (2007) 495–516.
- [95] C. Holohan, S. Van Schaeybroeck, D.B. Longley, P.G. Johnston, Cancer drug resistance: an evolving paradigm, *Nat. Rev. Cancer*. 13 (2013) 714–726.
- [96] N. Rivlin, R. Brosh, M. Oren, V. Rotter, Mutations in the p53 tumor suppressor gene:

- important milestones at the various steps of tumorigenesis., *Genes Cancer*. 2 (2011) 466–474.
- [97] F. Dietlein, L. Thelen, H.C. Reinhardt, Cancer-specific defects in DNA repair pathways as targets for personalized therapeutic approaches, *Trends Genet*. 30 (2014) 326–339.
- [98] G.L. Fiszman, M.A. Jasnis, Molecular mechanisms of trastuzumab resistance in HER2 overexpressing breast cancer, *Int. J. Breast Cancer*. 2011 (2011) 1–11.
- [99] S.A. Price-Schiavi, S. Jepson, P. Li, M. Arango, P.S. Rudland, L. Yee, et al., Rat Muc4 (sialomucin complex) reduces binding of anti-ErbB2 antibodies to tumor cell surfaces, a potential mechanism for herceptin resistance., *Int. J. Cancer*. 99 (2002) 783–791.
- [100] S. Wilkens, Structure and mechanism of ABC transporters., *F1000Prime Rep*. 7 (2015) 14.
- [101] M.C. Rebecca Feldman, Brian L. Abbott, Sandeep K. Reddy, Drug efflux pump expression in 50,000 molecularly-profiled cancer patients, *J. Clin. Oncol*. 33 (2015) 11108–11108.
- [102] M.M. Gottesman, V. Ling, The molecular basis of multidrug resistance in cancer: The early years of P-glycoprotein research, *FEBS Lett*. 580 (2006) 998–1009.
- [103] B.L. Lum, M.P. Gosland, MDR expression in normal tissues. Pharmacologic implications for the clinical use of P-glycoprotein inhibitors., *Hematol. Oncol. Clin. North Am*. 9 (1995) 319–336. <http://www.ncbi.nlm.nih.gov/pubmed/7642466> (accessed March 14, 2019).
- [104] A.H. Schinkel, J.W. Jonker, Mammalian drug efflux transporters of the ATP binding cassette (ABC) family: an overview, *Adv. Drug Deliv. Rev*. 64 (2012) 138–153.
- [105] S.G. Aller, J. Yu, A. Ward, Y. Weng, S. Chittaboina, R. Zhuo, et al., Structure of P-glycoprotein reveals a molecular basis for poly-specific drug binding., *Science*. 323 (2009) 1718–1722.
- [106] R.B. Kim, Drugs as P-glycoprotein substrates, inhibitors, and inducers, *Drug Metab. Rev*. 34 (2002) 47–54.
- [107] X. Yang, X. Li, Z. Duan, X. Wang, An update on circumventing multidrug resistance in cancer by targeting P-glycoprotein, *Curr. Cancer Drug Targets*. 17 (2017).
- [108] E. Tóthová, A. Elbertová, M. Fricová, A. Kafková, M. Hlebasková, E. Svorcová, et al., P-glycoprotein expression in adult acute myeloid leukemia: correlation with induction treatment outcome., *Neoplasma*. 48 (2001) 393–397. <http://www.ncbi.nlm.nih.gov/pubmed/11845985> (accessed March 10, 2019).

- [109] L. Senent, I. Jarque, G. Martín, A. Sempere, Y. González-García, F. Gomis, et al., P-glycoprotein expression and prognostic value in acute myeloid leukemia., *Haematologica*. 83 (1998) 783–787. <http://www.ncbi.nlm.nih.gov/pubmed/9825574> (accessed March 10, 2019).
- [110] C. Wuchter, K. Leonid, V. Ruppert, M. Schrappe, T. Büchner, C. Schoch, et al., Clinical significance of P-glycoprotein expression and function for response to induction chemotherapy, relapse rate and overall survival in acute leukemia., *Haematologica*. 85 (2000) 711–721. <http://www.ncbi.nlm.nih.gov/pubmed/10897123> (accessed March 10, 2019).
- [111] D. Poeta, R. Stasi, G. Aronica, A. Venditti, M. Cox, A. Bruno, *et al.*, Clinical relevance of P-glycoprotein expression in de novo acute myeloid leukemia, *Blood*. 87 (1996). <http://www.bloodjournal.org/content/87/5/1997?sso-checked=true> (accessed March 10, 2019).
- [112] P. Wood, R. Burgess, A. MacGregor, J.A. Yin, P-glycoprotein expression on acute myeloid leukaemia blast cells at diagnosis predicts response to chemotherapy and survival., *Br. J. Haematol.* 87 (1994) 509–514. <http://www.ncbi.nlm.nih.gov/pubmed/7993790> (accessed March 10, 2019).
- [113] C. Dhooge, B. De Moerloose, Clinical significance of P-glycoprotein (P-gp) expression in childhood acute lymphoblastic leukemia. Results of a 6-year prospective study., *Adv. Exp. Med. Biol.* 457 (1999) 11–19. <http://www.ncbi.nlm.nih.gov/pubmed/10500775> (accessed March 10, 2019).
- [114] F. Casale, V. D’Angelo, R. Addeo, M. Caraglia, S. Crisci, R. Rondelli, et al., P-glycoprotein 170 expression and function as an adverse independent prognostic factor in childhood acute lymphoblastic leukemia., *Oncol. Rep.* 12 (2004) 1201–1207. <http://www.ncbi.nlm.nih.gov/pubmed/15547738> (accessed March 10, 2019).
- [115] S.H. Park, C.-J. Park, D.-Y. Kim, B.-R. Lee, Y.J. Kim, Y.-U. Cho, et al., MRP1 and P-glycoprotein expression assays would be useful in the additional detection of treatment non-responders in CML patients without ABL1 mutation, *Leuk. Res.* 39 (2015) 1109–1116.
- [116] L. En-xiao, L. Rong, Z. Zhen-hua, W. Jian-bo, Clinical significance of P-glycoprotein expression in breast cancer, *Chinese J. Cancer Res.* 11 (1999) 218–220.
- [117] S. Gregorcyk, Y. Kang, D. Brandt, P. Kolm, G. Singer, R.R. Perry, P-glycoprotein expression as a predictor of breast cancer recurrence., *Ann. Surg. Oncol.* 3 (1996) 8–14. <http://www.ncbi.nlm.nih.gov/pubmed/8770296> (accessed March 10, 2019).

- [118] S. Vishnukumar, G. Umamaheswaran, D. Anichavezhi, S. Indumathy, C. Adithan, K. Srinivasan, et al., P-glycoprotein expression as a predictor of response to neoadjuvant chemotherapy in breast cancer, *Indian J. Cancer.* 50 (2013) 195.
- [119] I. Sedláková, J. Laco, K. Caltová, M. Červinka, J. Tošner, A. Řezáč, et al., Clinical significance of the resistance proteins LRP, P-gp, MRP1, MRP3, and MRP5 in epithelial ovarian cancer, *Int. J. Gynecol. Cancer.* 25 (2015) 236–243.
- [120] M.M. Baekelandt, R. Holm, J.M. Nesland, C.G. Tropé, G.B. Kristensen, P-glycoprotein expression is a marker for chemotherapy resistance and prognosis in advanced ovarian cancer., *Anticancer Res.* 20 1061–1067.  
<http://www.ncbi.nlm.nih.gov/pubmed/10810398> (accessed March 10, 2019).
- [121] M. Geng, L. Wang, X. Chen, R. Cao, P. Li, The association between chemosensitivity and P-gp, GST- $\pi$  and Topo II expression in gastric cancer., *Diagn. Pathol.* 8 (2013) 198.
- [122] J.W. Kim, Y. Park, J.-L. Roh, K.-J. Cho, S.-H. Choi, S.Y. Nam, et al., Prognostic value of glucosylceramide synthase and P-glycoprotein expression in oral cavity cancer, *Int. J. Clin. Oncol.* 21 (2016) 883–889.
- [123] G.S. Vlachogeorgos, E.D. Manali, E. Blana, S. Legaki, N. Karagiannidis, V.S. Polychronopoulos, et al., Placental isoform glutathione S-transferase and P-glycoprotein expression in advanced nonsmall cell lung cancer, *Cancer.* 114 (2008) 519–526.
- [124] H.S.L. Chan, G. Haddad, P.S. Thorner, G. DeBoer, Y.P. Lin, N. Ondrusek, et al., P-glycoprotein expression as a predictor of the outcome of therapy for neuroblastoma, *N. Engl. J. Med.* 325 (1991) 1608–1614.
- [125] Q.-J. Ma, Y.-C. Zhang, J.-S. Shi, G.-C. Li, Clinical significance of P-glycoprotein and glutathione S-transferase  $\pi$  expression in gallbladder carcinoma., *Exp. Ther. Med.* 7 (2014) 635–639.
- [126] W. Pranay, V. Kumar Atul, Y. Sanjay, W. Ankita, Role of P-glycoprotein protein, *Int. J. Res. Pharm. Biomed. Sci.* 4 (2013) 709–715.
- [127] F. Vigiúé, P-gp, in: *Atlas Genet. Cytogenet. Oncol. Haematol.*, 1998: pp. 45–46.  
<http://atlasgeneticsoncology.org//Genes/PGY1ID105.html#LINKS>. (accessed 18 March 2019).
- [128] E.M. Leslie, R.G. Deeley, S.P.C. Cole, Multidrug resistance proteins: role of P-glycoprotein, MRP1, MRP2, and BCRP (ABCG2) in tissue defense, *Toxicol. Appl. Pharmacol.* 204 (2005) 216–237.
- [129] A.B. Ward, P. Szewczyk, V. Grimard, C.-W. Lee, L. Martinez, R. Doshi, et al.,

- Structures of P-glycoprotein reveal its conformational flexibility and an epitope on the nucleotide-binding domain, *Proc. Natl. Acad. Sci.* 110 (2013) 13386–13391.
- [130] S. Nobili, I. Landini, B. Giglioni, E. Mini, Pharmacological strategies for overcoming multidrug resistance, *Curr. Drug Targets.* 7 (2006) 861–879.
- [131] E. Solary, L. Mannone, D. Moreau, et al., Phase I study of cinchonine, a multidrug resistance reversing agent, combined with the CHVP regimen in relapsed and refractory lymphoproliferative syndromes, *Leukemia.* 14 (2000) 2085-2094.
- [132] W.R. Friedenberg, M. Rue, E.A. Blood, W.S. Dalton, C. Shustik, R.A. Larson, et al., Phase III study of PSC-833 (valspodar) in combination with vincristine, doxorubicin, and dexamethasone (valspodar/VAD) versus VAD alone in patients with recurring or refractory multiple myeloma (E1A95), *Cancer.* 106 (2006) 830–838.
- [133] L. Gandhi, M.W. Harding, M. Neubauer, C.J. Langer, M. Moore, H.J. Ross, et al., A phase II study of the safety and efficacy of the multidrug resistance inhibitor VX-710 combined with doxorubicin and vincristine in patients with recurrent small cell lung cancer, *Cancer.* 109 (2007) 924–932.
- [134] Database of clinical trials, <https://clinicaltrials.gov/> (accessed March 5, 2019).
- [135] L.D. Cripe, H. Uno, E.M. Paietta, M.R. Litzow, R.P. Ketterling, J.M. Bennett, *et al.*, Zosuquidar, a novel modulator of P-glycoprotein, does not improve the outcome of older patients with newly diagnosed acute myeloid leukemia: a randomized, placebo-controlled trial of the Eastern Cooperative Oncology Group 3999, *Blood.* 116 (2010) 4077–4085.
- [136] N.C. Reynolds Jr, V.S. Murthy, Serum free levels and evaluation anticonvulsant drug interactions, *Wis. Med. J.* 88 (1989) 25–27.
- [137] J.C. Thenmozhiyal, P.T. Wong, W.K. Chui, Anticonvulsant activity of phenylmethylenhydantoins: a structure-activity relationship study, *J. Med. Chem.* 47 (2004) 1527–1535.
- [138] Dantrolene, <https://www.drugs.com/search.php?searchterm=dantrolene> (accessed April 20, 2019).
- [139] A. Elizalde, J. Sánchez-Chapula, Effects of the novel antiarrhythmic compound TR 2985 (ropitoin) on action potentials of different mammalian cardiac tissues., *Naunyn-Schmiedeberg's Arch. Pharmacol.* 337 (1988) 316–322.  
<http://www.ncbi.nlm.nih.gov/pubmed/3393234> (accessed April 2, 2019).
- [140] Nilutamide, <https://www.drugs.com/pro/nilutamide.html> (accessed April 1, 2019).
- [141] K. Kieć-Kononowicz, E. Szymańska, Antimycobacterial activity of 5-arylidene

- derivatives of hydantoin, *Farmaco*. 57 (2002) 909–916.
- [142] K. Kieć-Kononowicz, E. Szymańska, M. Motyl, W. Holzer, A. Białecka, A. Kasprowicz, Synthesis, spectral and antimicrobial properties of 5-chloroarylidene aromatic derivatives of imidazoline-4-one, *Pharmazie*. 53 (1998) 680–684.
- [143] E. Szymańska, K. Kieć-Kononowicz, A. Białecka, A. Kasprowicz, Antimicrobial activity of 5-arylidene aromatic derivatives of hydantoin. Part 2, *Farmaco*. 57 (2002) 39–44.
- [144] E. Szymańska, K. Kieć-Kononowicz, Antimycobacterial activity of 5-arylidene aromatic derivatives of hydantoin, *Farmaco*. 57 (2002) 355–362.
- [145] T. Dyląg, M. Zygmunt, D. Maciąg, J. Handzlik, M. Bednarski, B. Filipek, *et al.*, Synthesis and evaluation of in vivo activity of diphenylhydantoin basic derivatives, *Eur. J. Med. Chem.* 39 (2004) 1013–1027.
- [146] K. Kieć-Kononowicz, H. Byrtus, A. Zejc, B. Filipek, P. Chevallet, Synthesis and antiarrhythmic properties of basic amide derivatives of imidazolidine-2,4-dione and pyrrolidine-2,5-dione II, *Farmaco*. 50 (1995) 355–360.
- [147] K. Kieć-Kononowicz, K. Stadnicka, A. Mitka, E. Pękala, B. Filipek, J. Sapa, *et al.*, Synthesis, structure and antiarrhythmic properties evaluation of new basic derivatives of 5,5-diphenylhydantoin, *Eur. J. Med. Chem.* 38 (2003) 555–566.
- [148] E. Pękala, K. Stadnicka, A. Broda, M. Zygmunt, B. Filipek, K. Kieć-Kononowicz, Synthesis, structure-activity relationship of some new anti-arrhythmic 5-arylidene imidazolidine-2,4-dione derivatives, *Eur. J. Med. Chem.* 40 (2005) 259–269.
- [149] J. Handzlik, E. Szymańska, R. Wójcik, A. Dela, M. Jastrzębska-Więsek, J. Karolak-Wojciechowska, *et al.*, Synthesis and SAR-study for novel arylpiperazine derivatives of 5-arylidenehydantoin with alpha(1)-adrenoceptor antagonistic properties, *Bioorg. Med. Chem.* 20 (2012) 4245–4257.
- [150] J. Handzlik, D. Maciąg, M. Kubacka, S. Mogilski, B. Filipek, K. Stadnicka, *et al.*, Synthesis, alpha 1-adrenoceptor antagonist activity, and SAR study of novel arylpiperazine derivatives of phenytoin, *Bioorg. Med. Chem.* 16 (2008) 5982–5998.
- [151] J. Handzlik, E. Szymańska, K. Nędza, M. Kubacka, A. Siwek, S. Mogilski, *et al.*, Pharmacophore models based studies on the affinity and selectivity toward 5-HT1A with reference to alpha1-adrenergic receptors among arylpiperazine derivatives of phenytoin, *Bioorg. Med. Chem.* 19 (2011) 1349–1360.
- [152] S. Weyand, T. Shimamura, S. Yajima, S. Suzuki, O. Mirza, K. Krusong, *et al.*, Structure and molecular mechanism of a nucleobase-cation-symport-1 family

- transporter, *Science*. 322 (2008) 709–713.
- [153] J.M. Bolla, S. Alibert-Franco, J. Handzlik, J. Chevalier, A. Mahamoud, G. Boyer, *et al.*, Strategies for bypassing the membrane barrier in multidrug resistant Gram-negative bacteria, *FEBS Lett.* 585 (2011) 1682–1690.
- [154] J. Handzlik, E. Szymańska, J. Chevalier, E. Otrębska, K. Kieć-Kononowicz, J.M. Pagés, *et al.*, Amine-alkyl derivatives of hydantoin: new tool to combat resistant bacteria, *Eur. J. Med. Chem.* 46 (2011) 5807–5816.
- [155] Y. Zhu, C. Liu, C. Armstrong, W. Lou, A. Sandher, A.C. Gao, Antiandrogens inhibit ABCB1 efflux and ATPase activity and reverse docetaxel resistance in advanced prostate cancer, *Clin. Cancer Res.* 21 (2015) 4133–4142.
- [156] C. Carmi, A. Cavazzoni, V. Zuliani, A. Lodola, F. Bordi, P.V. Plazzi, *et al.*, 5-Benzylidene-hydantoins as new EGFR inhibitors with antiproliferative activity, *Bioorg. Med. Chem. Lett.* 16 (2006) 4021–4025.
- [157] V. Zuliani, C. Carmi, M. Rivara, M. Fantini, A. Lodola, F. Vacondio, *et al.*, 5-Benzylidene-hydantoins: synthesis and antiproliferative activity on A549 lung cancer cell line, *Eur. J. Med. Chem.* 44 (2009) 3471–3479.
- [158] A. Cavazzoni, R.R. Alfieri, C. Carmi, V. Zuliani, M. Galetti, C. Fumarola, *et al.*, Dual mechanisms of action of the 5-benzylidene-hydantoin UPR1024 on lung cancer cell lines, *Mol. Cancer Ther.* 7 (2008) 361–370.
- [159] M.A. Khanfar, K.A. El Sayed, Phenylmethylene hydantoins as prostate cancer invasion and migration inhibitors. CoMFA approach and QSAR analysis, *Eur. J. Med. Chem.* 45 (2010) 5397–5405.
- [160] Basappa, C.S. Ananda Kumar, S. Nanjunda Swamy, K. Sugahara, K.S. Rangappa, Anti-tumor and anti-angiogenic activity of novel hydantoin derivatives: inhibition of VEGF secretion in liver metastatic osteosarcoma cells, *Bioorg. Med. Chem.* 17 (2009) 4928–4934.
- [161] M. Viveiros, M. Martins, I. Couto, L. Rodrigues, G. Spengler, A. Martins, *et al.*, New methods for the identification of efflux mediated MDR bacteria, genetic assessment of regulators and efflux pump constituents, characterization of efflux systems and screening for inhibitors of efflux pumps., *Curr. Drug Targets.* 9 (2008) 760–778.  
<http://www.ncbi.nlm.nih.gov/pubmed/18781922> (accessed March 6, 2019).
- [162] S. Gibbons, M. Oluwatuyi, G.W. Kaatz, A novel inhibitor of multidrug efflux pumps in *Staphylococcus aureus.*, *J. Antimicrob. Chemother.* 51 (2003) 13–17.  
<http://www.ncbi.nlm.nih.gov/pubmed/12493782> (accessed March 11, 2019).

- [163] I.A. Khan, Z.M. Mirza, A. Kumar, V. Verma, G.N. Qazi, Piperine, a phytochemical potentiator of ciprofloxacin against *Staphylococcus aureus.*, *Antimicrob. Agents Chemother.* 50 (2006) 810–812.
- [164] C.E. DeMarco, L.A. Cushing, E. Frempong-Manso, S.M. Seo, T.A. Jaravaza, G.W. Kaatz, Efflux-related resistance to norfloxacin, dyes, and biocides in bloodstream isolates of *Staphylococcus aureus*, *Antimicrob. Agents Chemother.* 51 (2007) 3235–3239.
- [165] G. Spengler, M. Viveiros, M. Martins, L. Rodrigues, A. Martins, J. Molnar, *et al.*, Demonstration of the activity of P-glycoprotein by a semi-automated fluorometric method., *Anticancer Res.* 29 (2009) 2173–2177.  
<http://www.ncbi.nlm.nih.gov/pubmed/19528478> (accessed March 9, 2019).
- [166] W. Strober, Trypan blue exclusion test of cell viability., *Curr. Protoc. Immunol.* Appendix 3 (2001) Appendix 3B.
- [167] bioMérieux, Slidex MRSA Detection Package Insert, (2007).
- [168] J.M. Andrews, Determination of minimum inhibitory concentrations, *J. Antimicrob. Chemother.* 48 (2001) 5–16.
- [169] Polfa Tarchomin S.A., Drug Leaflet: Unasyn, (2008).
- [170] M. Martins, M. Viveiros, I. Couto, S.S. Costa, T. Pacheco, S. Fanning, *et al.*, Identification of efflux pump-mediated multidrug-resistant bacteria by the ethidium bromide-agar cartwheel method, *In Vivo (Brooklyn)*. 25 (2011) 171–178.  
<http://www.ncbi.nlm.nih.gov/pubmed/21471531> (accessed March 6, 2019).
- [171] F.C. Bernstein, T.F. Koetzle, G.J. Williams, E.F.J. Meyer, M.D. Brice, J.R. Rodgers, The protein data bank: A computer-based archival file for macromolecular structures., *Arch Biochem Biophys.* 185 (1978) 584–591.
- [172] W.L. Jorgensen, J. Tirado-Rives, The OPLS [optimized potentials for liquid simulations] potential functions for proteins, energy minimizations for crystals of cyclic peptides and crambin., *J Am Chem Soc.* 110 (1988) 1657.
- [173] <http://www.organic-Chemistry.org/prog/peo/tox.html>.
- [174] <http://www.ccohs.ca/products/rtecs/> (accessed March 18, 2019).
- [175] Biomedica, EZ4U. The 4th generation non radioactive cell proliferation and cytotoxicity assay. Product leaflet.
- [176] M. V Berridge, A.S. Tan, Characterization of the cellular reduction of 3-(4,5-dimethylthiazol-2-yl)-2,5-diphenyltetrazolium bromide (MTT): subcellular localization, substrate dependence, and involvement of mitochondrial electron transport in MTT

- reduction, *Arch. Biochem. Biophys.* 303 (1993) 474–482.
- [177] A.H. Cory, T.C. Owen, J.A. Barltrop, J.G. Cory, Use of an aqueous soluble tetrazolium/formazan assay for cell growth assays in culture, *Cancer Commun.* 3 (1991) 207–212.
- [178] The European Committee on Antimicrobial Susceptibility Testing. Breakpoint tables for interpretation of MICs and zone diameters. Version 5.0, 2015.  
<http://www.eucast.org> (accessed March 5, 2019).
- [179] A. Marrero, G. Mallorqui-Fernandez, T. Guevara, R. Garcia-Castellanos, F.X. Gomis-Ruth, Unbound and acylated structures of the MecR1 extracellular antibiotic-sensor domain provide insights into the signal-transduction system that triggers methicillin resistance, *J. Mol. Biol.* 361 (2006) 506–521.

# 6. Annex 1. Equipment and reagents

---

## 6.1. Equipment and reagents used in assessment of the inhibition of P-glycoprotein (EB assay)

### **Equipment:**

- Rotor-Gene™ 3000 thermocycler (Corbett Research)
- HERA Cell 240 incubator (Heraeus)
- 1012 water bath with circulation system (GFL)
- MN120 class II microbiological safety cabinet (NÜVE)
- CKX41 microscope (Olympus)
- Fuchs-Rosenthal counting chamber (Heinz Herenz)
- 2100 autoclave (Prestige Medical)
- analytical balance (Radwag)
- refrigerator with freezer (Mastercook)
- refrigerated MIKRO22R centrifuge (Hettich)
- liquid nitrogen aluminum container (Chart Biomedical)
- MS3 basic vortex (IKA)
- Discovery multi-channel pipettes (HTL; 5-25 µl, 20-200 µl) and sterile tips
- pipettes (Eppendorf; 100-1000 µl, 2-20 µl, 20-200 µl) and sterile tips
- Easypet electronic automatic pipette (Eppendorf) and sterile tips
- 25 cm<sup>2</sup> Nunc™ cell culture flasks (Thermo Scientific)
- sterile 15 ml and 50 ml Falcon tubes (F.L. Medical)
- sterile Nunc™ Petri plates (Thermo Scientific)
- sterile 2.5 ml Eppendorf tubes (Eppendorf)

### **Reagents:**

- colchicine (Sigma-Aldrich)
- McCoy's 5A medium (Sigma-Aldrich)
- 10% heat-inactivated horse serum (Sigma-Aldrich)
- L-glutamine (Sigma-Aldrich)
- penicillin-streptomycin mixture (Sigma-Aldrich)
- phosphate buffered saline (Sigma-Aldrich)

- 5% trypsin EDTA solution (Gibco)
- sterile DMSO suitable for cell culture (Sigma-Aldrich)
- trypan blue (Sigma-Aldrich)
- ethidium bromide (Sigma-Aldrich)
- verapamil (Sigma-Aldrich)
- glucose (Sigma-Aldrich)

## 6.2. Equipment and reagents used in proliferation assay

### **Equipment:**

- HERA Cell 240 incubator (Heraeus)
- 1012 water bath with circulation system (GFL)
- MN120 class II microbiological safety cabinet (NÜVE)
- CKX41 microscope (Olympus)
- Fuchs-Rosenthal counting chamber (Heinz Herenz)
- EnSpire 2300 plate reader (Perkin-Elmer)
- 2100 autoclave (Prestige Medical)
- analytical balance (Radwag)
- refrigerator with freezer (Mastercook)
- refrigerated MIKRO22R centrifuge (Hettich)
- liquid nitrogen aluminum container (Chart Biomedical)
- MS3 basic vortex (IKA)
- Discovery multi-channel pipettes (HTL; 5-25 µl, 20-200 µl) and sterile tips
- pipettes (Eppendorf; 100-1000 µl, 2-20 µl, 20-200 µl) and sterile tips
- Easypet electronic automatic pipette (Eppendorf) and sterile tips
- 25 cm<sup>2</sup> Nunc<sup>™</sup> cell culture flasks (Thermo Scientific)
- sterile 15 ml and 50 ml Falcon tubes (F.L. Medical)
- sterile Nunc<sup>™</sup> Petri plates (Thermo Scientific)
- sterile 2.5 ml Eppendorf tubes (Eppendorf)

### **Reagents:**

- EZ4U BL-5000 proliferation test (Biomedica)

- DMEM/F 12 medium (Gibco)
- antibiotics: penicillin, streptomycin (Polfa Tarchomin)
- phosphate buffered saline (Sigma-Aldrich)
- 100% fetal bovine serum (Gibco)
- 5% trypsin EDTA solution (Gibco)
- 2 mg/ml doxorubicin (Ebewe)
- sterile DMSO suitable for cell culture (Sigma-Aldrich)
- trypan blue (Sigma-Aldrich)

### 6.3. Equipment and reagents used in assessment of restoration of antibiotic efficacy

#### **Equipment:**

- 6131 BioPhotometer (Eppendorf)
- ES-20 shaker incubator (Biosan)
- analytical balance (Radwag)
- 2100 autoclave (Prestige Medical)
- MS3 basic vortex (IKA)
- 96-well microplates (NEST, cat. no. 2014002)
- cuvettes
- sterile 15 ml and 50 ml Falcon tubes (F.L. Medical)
- sterile 2.5 ml Eppendorf tubes (Eppendorf)
- Discovery multi-channel pipettes (HTL; 5-25  $\mu$ l, 20-200  $\mu$ l) and sterile tips
- pipettes (Eppendorf; 100-1000  $\mu$ l, 2-20  $\mu$ l, 20-200  $\mu$ l) and sterile tips

#### **Reagents:**

- Lysogeny broth (LB) (Merck)
- Tryptic Soy Broth (TSB) (Merck)
- Mueller-Hinton Broth (MHB) (Merck)
- antibiotics: oxacillin, ciprofloxacin, cloxacillin, ampicillin (Sigma-Aldrich), neomycin (Fagron)
- sulbactam (Sigma-Aldrich)
- DMSO (POCH)

## Annex 2. Scientific papers published as part of this PhD

---